Geologically Constrained Geophysical Modeling of Magnetics and Gravity – The Baie Verte Peninsula, Newfoundland

By

Bill James Spicer, B.Sc.

A thesis

Submitted to the School of Graduate Studies

In Partial Fulfillment of the Requirements

for the Degree

Master of Science

McMaster University

MASTER OF SCIENCE (2010) McMaster University

(Earth and Environmental Science) Hamilton, Ontario

TITLE:	Geologically Constrained Geophysical Modeling of Magnetics and Gravity – The Baie Verte Peninsula
AUTHOR:	Bill James Spicer, B.Sc. (McMaster University)
SUPERVISOR:	Professor W.A. Morris
NUMBER OF PAGES:	xiii, 166

Abstract

The Baie Verte Peninsula of Northern Newfoundland has a long history of mining and extraction. This area, which plays host to some of the oldest mines in the province, has a geologic setting favorable for Volcanogenic Massive Sulphides and is still considered to be one of the best exploration targets in Newfoundland. As less near-surface discoveries are made the requirement to look for deeper deposits becomes apparent and thus the role of geophysical modeling becomes progressively more important. This thesis examines the task of geologically supported geophysical modeling as a means to predict subsurface geological distributions and structure. Three case studies of modeling on the Baie Verte Peninsula are presented. A fourth study addresses the role of gamma attenuation for rapid density measurements in building physical property databases to be used as modeling constraint.

A case study of the Betts Cove Ophiolite Complex along the western margins of Notre Dame Bay demonstrates the use of magnetic modeling to provide insight into the 3D nature of an area of previously significant ore extraction. While prior models have interpreted this feature to consist of a series of imbricate thrust slices, this new model suggests that the Betts Cove Ophiolite Complex is a doubly plunging syncline segmented by a several normal and high angle reverse faults. On a larger scale, this segmentation comprises a half-graben structure responsible for the morphology of Notre Dame Bay. Supported by petrophysics and a detailed structural dataset 2D forward geophysical models form the basis in the construction of a 3D geologic model of the Betts Cove Ophiolite and its cover series.

An alternative approach to the conventional method of density measurement is presented in chapter three. Modifying an industrial gamma-gamma meter, a portable device has been constructed capable of providing rapid density measurements on bore-core. The device can be calibrated using a suite of metal alloy standards. It is possible to derive secondary empirical calibration based on a one-to-one gamma-gamma to specific gravity technique correlation. This study is one of only a very small fraction implementing this technology in an ocean-floor hard rock geologic setting.

The second modeling case study focuses on the Rambler property in the upper Pacquet Harbour Group of the central Baie Verte Peninsula. The Rambler rhyolite is a felsic dome feature within the upper portions of an incomplete ophiolite. Ore deposits are found in association with contact between the felsic volcanics of the rhyolite and the mafic volcanic cover. 3D magnetic and gravity inversions are performed implementing the University of British Columbia Geophysical Inversion Facility's (UBC-GIF) code. A large physical property database has been constructed and used in the development of a reference model of known geologic distributions. The subsurface distribution of the Rambler rhyolite has been revealed through gravity inversions while additional structural information has been provided from magnetics. The results demonstrate the strengths of including geologic constraint within the inversion process and the ability of geophysical inversions to supplement and support current understanding and exploration techniques.

In the final case study, modeling is performed on a broader perspective in order to provide a regional geologic framework of the Baie Verte Peninsula. 2D forward models of magnetics and gravity profiles are constructed with multiple intersection points in order to enforce continuity in distribution and structure throughout. New geologic maps and a regional physical rock property database have been implemented in modeling while unconstrained 3D magnetic inversions are used as additional support. In addition to addressing such issues as regional basement morphology, the depth extent of the Cape Brule porphyry, and the nature of the Baie Verte Line, several prospective exploration targets have been revealed through this study.

Co-Authorship Statement

This thesis contains four manuscripts which address separate issues of a broader study of the Baie Verte Peninsula. While the content within is principally my own, my thesis supervisor Dr. Bill Morris and McMaster Applied Geophysics and Geographic Imaging Center (MAGGIC) post doctoral fellow Dr. Hernan Ugalde provided editorial assistance with all chapters. The concept for this project and the identification of potential sponsors and contributors was identified by Bill Morris; all of the field and laboratory data acquisition, analysis and thesis writing was executed by myself. All four of the manuscripts have been accepted by, or submitted, for publication within a scholarly journal deemed appropriate by Dr. Bill Morris and myself.

Chapter 2: The Structure of the Betts Cove Ophiolite under the western margin of Notre Dame Bay.

Authors: Bill Spicer, Bill Morris, Hernan Ugale, Heather Slavinski, and Tom Skulski

Accepted within the Canadian Journal of Earth Sciences, December 2nd, 2009, published Feburary 2010.

This chapter focuses on 2D forward modeling and building upon work which began during my undergraduate thesis modeling the Betts Cove Ophiolite. Bill Morris and Hernan Ugalde provided background theory and training in data acquisition techniques, while Heather Slavinski performed as a field assistant collecting data. Tom Skulski imparted geological counsel as well as editorial services.

Chapter 3: Rapid density measurements using a portable gamma-gamma logging device.

Authors: Bill Spicer, Bill Morris, Hernan Ugalde, and Neil Rogers

Submitted to the Journal of Applied Geophysics, January 31, 2010,under review.

This chapter focuses on the execution and acquisition of rapid physical property measurements using a Berthold Technologies LB444 gamma-gamma density gauge. While the fundamental concepts of this chapter have been addressed in the past, I personally assembled, designed and investigated the use of this device in a new and untested environment. Financial support for this project was provided by the Geologic Survey of Canada (GSC) through the TGI3 program. Neil Rogers of the Geological Survey edited and advised on the content of early drafts of the document.

Chapter 4: Structure of the Rambler rhyolite: Geologically constrained inversions using UBC-GIF Grav3D and Mag 3D.

Authors: Bill Spicer, Bill Morris, Hernan Ugalde

Submitted to the Journal of Applied Geophysics, April, 21st, 2010, under review.

The content within this chapter was primarily my own work and research. The computer code and background theory for 3D inversion of magnetic and gravity data sets have been developed by Doug Oldenburg and the University of British Columbia Geophysical Inversion Facility (UBC-GIF). Prior publications have predominantly used unconstrained inversions. In this document I developed a methodology using Modelvision which allowed the introduction of geologic constraints into the standard UBC-GIF inversion modeling. I was solely responsible for developing the data processing stream which introduced the geological constraints into the 3D model. Morris and Ugalde provided guidance on interpretation issues and document revision.

Chapter 5: Regional Modeling of the Baie Verte Peninsula

Authors: Bill Spicer, Bill Morris, Hernan Ugalde, Cees van Staal

To be submitted to the Canadian Journal of Earth Science

This work is primarily my own. Elements of this study are strongly representative of goals outlined in the GSC's Targeted Geoscience Initiative (TGI-3). Geologic council within a complex structural and tectonostratigraphic environment was provided by Bill Morris as well as and Dr. Cees van Staal of the GSC.

Appendix : Data Preparation procedure

Author: Bill Spicer

This is primarily all my work. In this document I provide a step-by-step approach of how to construct a reference (input) mesh from borehole physical property data, and surficial geological maps. I also outline the various processing steps that are needed to introduce the reference model into UBC-GIF, and I discuss the parameters of the observation dataset as it relates to the reference mesh. Finally I discuss the constraints that can be applied in UBC-GIF to optimize the form of the solution (output) model.

Acknowledgements

There are many people who have contributed to the overall outcome of this thesis to whom which I owe a great deal of gratitude.

First and foremost I would like to extend my thanks and appreciation towards my thesis supervisor Dr. Bill Morris. Your guidance and encouragement have played a pivotal role in the outcome of this work and to my overall academic progression. You have constantly been a source of support, providing alternative ideas and approaches to the many problems and roadblocks which arose throughout the development of this thesis. I consider myself extremely lucky having the opportunity to work alongside someone such as yourself with the ability to look past the minor problems and see the bigger picture.

Thanks to Dr. Hernan Ugalde who has also provided much guidance and assistance throughout my time in the McMaster Applied Geophysics and Geographic Imaging Center (MAGGIC), both during my undergraduate and graduate years. Hernan has always been able to stress the 'real world' application of geophysics and justify its relationship to geology. You are quick to explain the many underlying principles of potential fields, making sure I have an understanding of my tools and avoid slipping into the routines of a mere 'button pusher' geophysicist.

Thank you to my committee members Dr. Joe Boyce and Dr. Alan Dickin for your comments and editing. I would like to thank Tom Skulski, Neil Rogers, Cees van Staal and Sebastian Castonguay of the Geologic Survey of Canada for their contributions of knowledge and critique to this work. In addition to geologic advice, Larry Pilgrim and the people of Rambler Metals and Mining PLC. have been very generous supplying property access as well as confidential and proprietary information. Thanks to Ray Whimbleton, Mike Tucker, Ian Ames and Liam for their aid in field work on the Baie Verte Peninsula.

I am in debt to my fellow MAGGIC co-workers, Victoria Tshirhart, Saralise Underhay, Madeline Lee, Lindsey Oldershaw, Heather Slavinski and Peter Tshirhart, whose support in field or lab oriented work has help contribute to the outcome of this thesis. Thanks to John Maclachlan for his help in the field as well.

I would like to thank my friends and family for their support throughout this process. Mom and Dad, Oliver, Erin and Nathan, I am done with this school thing and can finally get that Letterman jacket with the grade 20 on the sleeve.

Finally, thanks to Kaitlyn Aarts whose love and support kept me going throughout this whole thing. Without you I never could have achieved this while still having so much fun. We can finally do the things we want now.....more school maybe?

Table of Contents

Chapter Four – Structure of the Rambler Rhyolite, Baie Verte Peninsula, Newfoundland: Inversions using UBC-GIF Grav3D And Mag3D

Chapter Five – 3D Regional Geophysical Modeling of the Baie Verte Peninsula, Newfoundland

Chapter Six – Conclusions

Appendix: Building reference models for geologic constraint In UBC-GIF Mag3D and Grav3D inversions

List of Figures

Chapter Two

Chapter Three

Chapter Four

Chapter Five

List of Tables

Chapter Two

Chapter Three

Chapter four

Chapter Five

Chapter One - Introduction

Geophysical modeling is a commonly used tool in mineral and hydrocarbon exploration and is increasingly being relied upon in many environmental based enterprises. In the exploration industry, significant financial decisions are made based on a perceived knowledge of subsurface physical properties and geologic distributions. Integration of geophysical and geologic information within the modeling procedure provides an increased understanding and accuracy in depiction of subsurface features, which consequently leads to an overall reduction in the risks involved with exploration. This thesis focuses on the integration of geologic and petrophysical knowledge within the modeling of potential fields; specifically it centers on the concept of geologically constrained inversion of geophysical data.

The Baie Verte Peninsula

The Baie Verte Peninsula (BVP) is located in Northwestern Newfoundland at the northernmost terminus of the Appalachian mountain belt. Divided by the northeast-southwesterly trending Baie Verte Line, the BVP records the closure of the Iapetus Ocean and subsequent accretion of ophiolites along the margin of the ancient Laurentian continental margin. The BVP is also the location of Newfoundland's earliest mines. With a geologic setting associated with an ocean-floor rift and spreading center environment, the ore deposits of the BVP are mainly of volcanogenic origins. Asbestos as well as minor epigenetic and hydrothermal deposits have been mined as well. Alongside the fisheries, volcanogenic massive sulphide (VMS) deposits are the most important socioeconomic purveyor for the BVP. However, as known deposits have either reached, or approach depletion, the requirement to secure reserves for future generations has transpired. Initial deposits were discovered in outcrop or near-surface using traditional low-risk mapping techniques. No discoveries of significance have occurred for many years though. Future discoveries will undoubtedly occur at greater depths, increasing cost and escalating risk.

Recognizing a rich history of ore extraction and the appropriate geologic setting for further reserves, Natural Resources Canada and the Geologic Survey of Canada have included the BVP in their Targeted Geosciences Initiative (TGI-3). TGI-3 is a multidisciplinary approach to mapping, combining geology, geochemistry and geophysics. The goal of this project is to provide a clear geologic framework in order to reduce risk and generate private sector interest in base metal exploration on the BVP. Utilizing high resolution geologic and geophysical data collected by university, government and industry parties, the goal of this thesis is to model the BVP providing a 3D geophysically supported framework, vectoring towards the most prospective sites and structures for base metal potential. Four case studies have been presented regarding such goals in this work:

1) Utilization of high resolution regional magnetics producing geophysical models and a 3D geologic model of the Betts Cove Ophiolite Structure under geological and petrophysical constraint.
2) Implementation of gamma radiation for rapid density measurements of drill core in support of physical rock property database construction.
3) Geologically constrained geophysical inverse modeling of magnetics and gravity to image the 3D structure of a VMS hosting rhyolite body.
4) Regional modeling of the BVP integrating gravity and magnetics with geologic and petrophysical constraints.

Chapter 2 of this thesis is a continuation of work initiated during an undergraduate thesis (Spicer, 2008). A site also studied in previous thesis's (Ricco, 1972; Upadhyay, 1973) then in later government publications (Tremblay et al. 1997, Bédard et al. 2000) the Betts Cove ophiolite (BCO) and its volcano-sedimentary cover series, the Snooks Arm Group, represent an Ordovician seafloor obducted during the closure of the Humber Seaway(van Staal et al. 2007). Host to several significant historic VMS deposits, the BCO has been mapped as one half of a synclinal structure bordering the Atlantic Ocean on the western margin of Notre Dame Bay. Supplementing high resolution airborne magnetics with data from a marine magnetic survey, the full extent of the BCO may be realized. Producing geophysical models with geologic and petrophysical constraints ensures results are more accurate, adhering to previous observations. Geophysically sound models along 2D profiles may then be used as the basis for the generation of a 3D model, providing full insight into the structural characteristics of the subsurface.

Chapter 3 examines the application of gamma radiation for measurements of density on borecore. In the gamma-gamma method, density is acquired as a ratio of ingoing vs. outgoing radiation counts recorded by a sensory device. Borecore is placed in front a beam of gamma radiation emitted by a rod of Cesium-137. Materials with a higher density more greatly impede the flux of gamma particles. Sampling rates are significantly reduced using this approach to acquiring physical rock properties. Including a susceptibility meter, an apparatus can be established permitting complete borecore physical property logging for applications modeling gravity and magnetics. While gamma logging of subsurface holes has been practiced for over 50 years now (Evans, 1965), few studies have tested this method outside of the drill hole and even less have been implemented using fully lithified, or igneous rocks.

In chapter 4 a case study is presented examining the structure of the Rambler rhyolite within the Pacquet Harbour Group (PHG) of the central BVP. The lower PHG represents the upper portions to the typical ophiolite sequence observed on the BVP (Skulski et al. 2010). Cu ± Au VMS deposits are associated with the felsic tuffs, flows and subvolcanic intrusive rocks which together comprise the Rambler rhyolite. Affected by multiphase deformation, cross-folds divide the structure into a series of synforms and antiforms. Mineral deposits throughout the area are elongate ribbon-like features, at or near, the upper rhyolite contact within the hinge zones of folds. Current exploration strategies have followed the contact of the footwall felsics and hanging wall mafic volcanic rocks down plunge. This project implements software and mathematical code developed by the University of British Columbia Geophysical Inversion Facility (UBC-GIF) for 3D geophysical inversions. As a large body of felsic volcanic rocks hosted within an assemblage of primarily pillow basalts, gabbros and mafic volcano sedimentary rocks, the structure of the Rambler rhyolite may be achieved through the inversion of gravity data. A major innovation in this study is the introduction of geological constraints into 3D inversions: Geological constraints were introduced by using a detailed reference model with known geophysical characteristics. The reference model was created using high resolution geologic maps and drillhole information with geology expressed in terms of the petrophysics outlined in the physical rock property database constructed for the Rambler area.

The fifth chapter of this thesis addresses the notion of building a regional 3D framework for the BVP. With allocnthonous ophiolite and island arc rocks of the Dunnage Zone exposed on eastern portions of BVP, an underlying craton margin assemblage of Humber Zone basement, is presumed to be present at depth. Interpretations of subsurface distribution however, are mired by a complex structural history and extensive late stage Silurian intrusions which blanket large portions the BVP. As such, geophysics has played an important role in shaping the geologic understanding of the BVP. Implementation of geophysical modeling on the BVP began in the mid 1970's (Miller and Deusch 1975, Haworth and Miller, 1982). With simple slab models computed to fit extracted geophysical profiles these authors provided important depth estimates for major geologic elements. The 2D nature of the profiles possible at the time these original studies were performed fall short of presenting any appreciable 3D implications. Constructing multiple and intersecting profiles, forward models have more constraint and consistency. Supplemented by 3D inverse modeling this work aims to uncover an improved understanding of subsurface geology on the BVP, specifically the basement morphology and ophiolite distributions beneath intrusive cover.

Modeling

Gravity and Magnetics are two of the most common and widely implemented exploration methods. This stems from the fact that they provide a wealth of information regarding geologic structure, lithological boundaries and, in the case of magnetics, alteration patterns. Information collected within a magnetic survey alludes to the magnetic mineralogy of an area, while gravity data provides knowledge regarding subsurface mass distribution. In comparison to other geophysical methods, these data are easily acquired and considerably less expensive. The two techniques are often employed in regional surveys, or during the early stages of exploration, as they permit a comprehensive understanding of geologic trends within an area. Interpretation of this data usually begins by converting sampled point data into a 2D surface via some gridding algorithm. The resultant geophysical maps may be analyzed as surficial expressions however one would also like to derive some information regarding subsurface contributions to the observed signal. This is achieved through geophysical modeling.

Geophysical modeling can be carried out in multiple dimensions using two specific approaches. Typically, 2D forward modeling of a geophysical signal across profiles has been the conventional approach in the modeling of potential fields. In this case, modeled signal is produced by some physical property distribution based on known or anticipated geology. Deviations in predicted model response from observed geophysical signal are considered the result of discrepancies between the true geology and the physical property array throughout the model. Within inverse modeling however, differences between observed and predicted response are negligible to null. Contrary to forward modeling, the inverse method produces an output physical property value and distribution set from an input geophysical signal. This method is based on a mathematical algorithm which results in a physical property distribution which upon subsequent forward modeling, results in a near identical predicted model response when compared to the observed signal. Inverse modeling is becoming increasingly popular and effective as advances in computer technology creates a greater capacity to invert for large datasets. Inverse modeling is also more conducive within a 3D environment as depths are incorporated from a plane rather than profile. This is important when considering that geology is a three dimensional phenomenon. On the other hand, inverse models inherent a significant flaw. While one solution may be mathematically suitable, this does not necessarily imply it will satisfy the true geology.

The ability for a model to be mathematically sound yet conflict with geological observations is the result of the non-unique nature of potential fields. This is demonstrated by the fact that a single anomaly many be reproduced by an unlimited combination of distributions and physical property values. Allowing an infinite range of physical properties values, the observed potential field signal can be reproduced within the thin upper layer of any model. This leads to the realization then that the signal within a geophysical survey contains limited inherent depth information. Non-uniqueness is also imposed within geophysical data when a finite number of observations are sampled in order to explain a continuous phenomenon. Recognition of non-uniqueness thus generates the requirement of some form of model constraint.

There are several ways in which constraint may be included within a geophysical model. Implementation of restrictions is limited to neither forward nor inverse modeling. In the forward procedure this requires that a modeler maintains the integrity of known surficial patterns and consciously adhere to fundamental geologic principles. Inverse modeling, which is mathematically controlled, requires additional equations within its governing algorithm to guide the optimization solution towards a pre-conceived notion of the subsurface morphology. Most commonly, priori constraints involve some method of forcing the solution to have depth extent. More properly constraints for potential field models should result in the generation of acceptable physical property values and expected distributions based on geologic observations. This form of constraint can be achieved by developing a pre-inversion reference models.

Understanding the physical properties within an area is essential if one wishes to produce geologically meaningful results. Models that do not agree with known observations are fundamentally flawed. A physical property database statistically summarizing the values of lithological units and alteration zones is pivotal to the modeling process. A more accurate outcome and a higher degree of confidence are associated with a model adhering to known values. As a population is more accurately depicted when well represented, many samples must be taken. For magnetics and gravity this implies that a large database of magnetic susceptibility and density values for specific geologic units be established. Ideally this should be done during the initial stages of exploration and updated as newly acquired information becomes available. Including these values as a bound within the forward or inverse procedure increases the probability of realistic results and improves the interpretation process.

The ultimate goal of the modeling procedure is to provide an outline of where geologic units and elements of interest such as oil or minerals are located in space. Traditional means for acquiring this information are invasive methods which provide evidence you can 'put your finger on'. The properties recorded at this location are indisputable and represent powerful constraint that should be enforced within the model. This type of information is acquired on the surface during geologic mapping and exploration while subsurface data are generally acquired through borehole drilling. Including known physical properties at proper locations guides the modeling process towards the 'most correct' solution.

The geophysical model is a powerful tool providing a wealth of information in a non-invasive fashion. Information presented from this procedure can vector towards prospective exploration targets, provide regional and local scale geologic frameworks or offer relevant information for environmental based decisions. The results however should be taken in their appropriate context as with any model. The quality of results is governed by preexistent expectations. While geophysical methods are testable and satisfy a sampled signal, the information from these models should be used to supplement rather than replace our geologic understanding of an area.

References

Bédard, J.H. Lauzière, K. Tremblay, A. Sangster, A. Douma S.L., Dec, T. (2000). Betts Cove Ophiolite and Its Cover Rocks, Newfoundland. Natural Resources Canada,Geologic Survey of Canada, Bulletin 550.

Evans, H. B., (1965).GRAPE – a device for continuous determination of material density and porosity. Trans, SPWLA 6th Annu. Logging Symp. Dallas, 2:B1-B25

Haworth, R. T., and Miller, H.G. (1982). The Structure of Paleozoic Oceanic Rocks beneath Notre Dame Bay, Newfoundland: Major Structural Zones and Faults of the Northern Appalachians, Geological Association of Canada, Special Paper 24

Miller, H.G. and Deutsch E.R. (1975). New gravitational evidence for the subsurface extent of oceanic crust in north-central Newfoundland. Canadian Journal of Earth Science, 13: 459-469.

Ricco, L.M. (1972). The Betts Cove Ophiolite, Newfoundland. Unpublished M.Sc. thesis, University of Western Ontario, London, Ontatio, 91 p.

Skulski, T., Castonguay, S., McNicoll, V., Rogers, N., van Staal, C., Morris, W, Ugalde, H., Slavinski, H., Spicer, W., Moussallam, Y., Kerr, I.(2010). Tectonostratigraphy of the Baie Verte Oceanic Tract and its Ophiolite Cover Sequence, Baie Verte Peninsula, Newfoundland and Labrador. *In* Current Research. Newfoundland and Labrador Department of Natural Resources, Geological Survey, Report 10-1, pages 315-335

Spicer, B. (2008). Geophydically suppored geologic modeling of the Betts Cove Ophiolite. Unpublished B.SC. thesis, McMaster University, Hamilton, Ontario, 56 pages.

Tremblay, A., Bédard, J.H., and Laurière, K. (1997). Structural history of the Betts Cove complex and cover rocks, Canadian Appalachians: from obduction to exhumation and folding of an Ordovician oceanic crust. Journal of Geology, v.105, p.701-716.

Upadhyay, H.D. (1973). The Betts Cove ophiolite and related rocks of the Snooks Arm Group, Newfoundland. Unpublished Ph.D thesis. Memorial University of Newfoundland, St. John's, 224 p.

van Staal, C.R., Whalen, J.B., McNicoll, V.J., Pehrsson, S., Lissenberg, C.J., Zagorevski, A., van Breemen, O., Jenner, G.A. 2007. The Notre Dame arc and the Taconic orogeny in Newfoundland. Frame work of Continental Crust: The Geological Society of America, Memoir 200, pp. 511-552.

Chapter Two

Structure of the Betts Cove Ophiolite Complex beneath the western margin of Notre Dame Bay, Newfoundland

B. Spicer[1], B. Morris[1], H. Ugalde[1], H. Slavinski[1] and T. Skulski[2]

1. MAGGIC, School of Geography & Earth Sciences, McMaster University, 1280 Main Street W., Hamilton, ON L8S 4K1. Canada

2. Geological Survey of Canada, 615 Booth Street, Ottawa, ON, K1A 0E9, Canada

Abstract

Ophiolitic rocks emplaced following closure of the Ordovician Iapetus ocean outcrop around the western margins of Notre Dame Bay in western Newfoundland. Previous geological and geophysical models have interpreted the Betts Cove Ophiolite complex as a series of imbricate thrust slices. A new 3D model indicates that locally the Betts Cove Ophiolite complex has the form of a northeast trending doubly plunging syncline which was later segmented by a series of normal and high angle reverse faults. This segmentation is interpreted in terms of a Carboniferous graben structure which is responsible for the current morphology of the Notre Dame Bay. The 3D model incorporates new high resolution aeromagnetic, marine magnetic and topographic imagery. In addition, newly available structural information is used to both constrain the geometry of the geological contacts in the near surface and to map contacts in the subsurface. Calibration of the computed geophysical models was achieved using newly acquired magnetic susceptibility data. The resulting 3D model, which is compatible with all aspects of the geological and geophysical data, provides an explanation for the distribution of Ordovician ophiolites around Notre Dame Bay.

Introduction

The Betts Cove Ophiolite Complex (BCO), located on the eastern shore of the Baie Verte Peninsula (BVP) in North Western Newfoundland, is one of several ophiolite bodies that are found on the west side of Newfoundland (Fig.1). The BCO is an assemblage of ocean floor volcanic rocks forming part of the Notre Dame Subzone located within the Dunage Zone on the eastern shore of the Baie Verte Peninsula. The Dunnage zone exists as a series of tectonically accreted oceanic and continental arc terrains to the east of and overlaying the Laurentian Continental Margin (Humber Zone) (Williams 1979; Hibbard 1983). The oceanic terrains including all the ophiolite suites on the BVP and elsewhere along strike are known as the Baie Verte Oceanic Tract (BVOT) in order to differentiate them from the more voluminous continental arc portions of the Dunnage Zone (van Staal et al. 2007). Emplacement of these ophiolite sequences is believed to have occurred during closure of the Iapetus Ocean in the early Paleozoic when the oceanic floor was obducted over the adjacent continental margin (Tremblay et al. 1997). While the BCO has been included within several previous geophysical studies on the BVP (Grant 1972; Miller and Deutsch 1975, 1976;

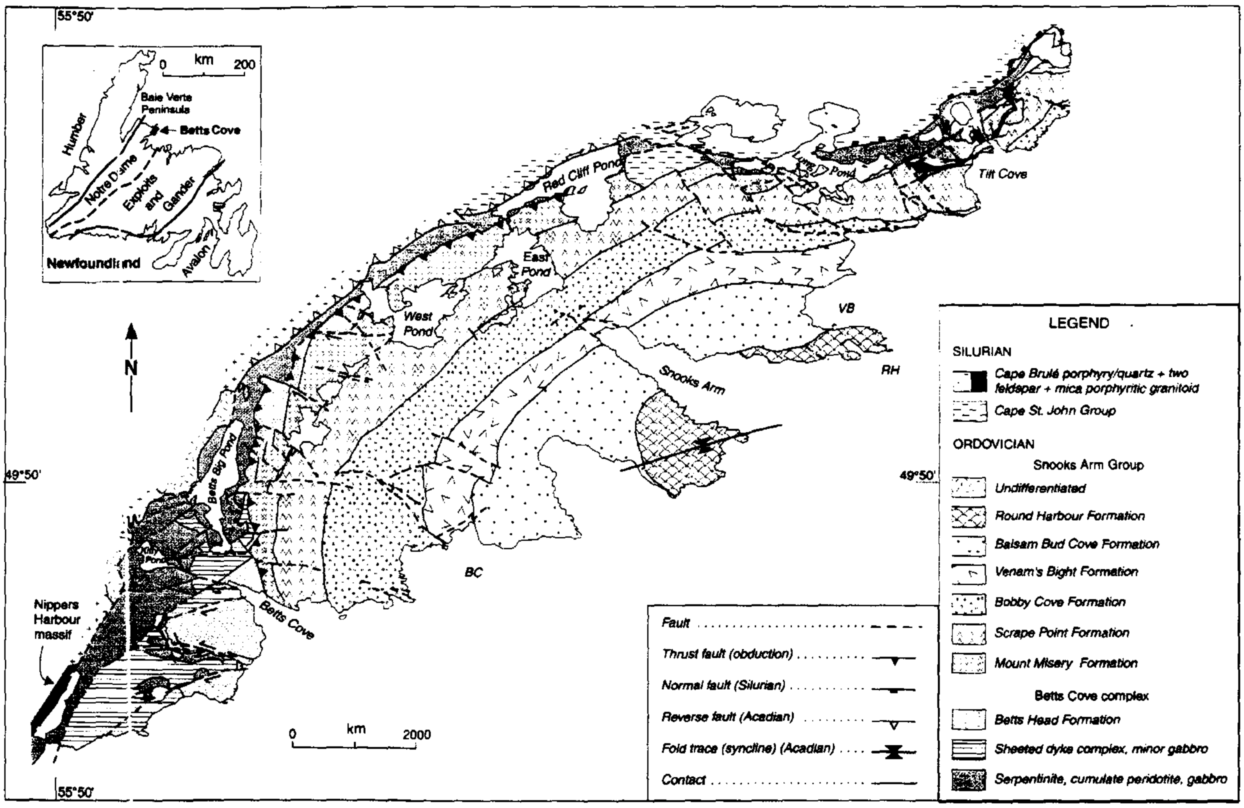
55°50'
0 km 200
Baie Verte Peninsula
Betts Cove
Humber
Notre Dame
Exploits
and
Gander
Avalon
Newfoundland
N
49°50'
Red Cliff Pond
East Pond
West Pond
Tilt Cove
VB
RH
Snooks Arm
Betts Big Pond
BC
Betts Cove
Nippers Harbour massif
0 km 2000
55°50'
49°50'
Fault
Thrust fault (obduction)
Normal fault (Silurian)
Reverse fault (Acadian)
Fold trace (syncline) (Acadian)
Contact
LEGEND
SILURIAN
Cape Brulé porphyry/quartz + two feldspar + mica porphyritic granitoid
Cape St. John Group
ORDOVICIAN
Snooks Arm Group
Undifferentiated
Round Harbour Formation
Balsam Bud Cove Formation
Venam's Bight Formation
Bobby Cove Formation
Scrape Point Formation
Mount Misery Formation
Betts Cove complex
Betts Head Formation
Sheeted dyke complex, minor gabbro
Serpentinite, cumulate peridotite, gabbro

Figure. 2-1 - The Betts Cove Ophiolite. Modified from Bedard, 2000.

Jacobi and Kristoffersen 1976; Haworth and Miller 1978, 1982; Miller and Wiseman 1994) no strong geophysical evidence existed to support any offshore interpretation of its structure or extent.

The direction of the subduction which preserved the BCO had been the subject of previous debate. Using motion indicators derived from geological maps Bird and Dewey (1970) initially proposed a northwestward dipping suture. Church and Stevens (1971) looking at the same rocks interpreted them as indicating a southeastwards dipping suture. Using gravity and magnetic data, Haworth and Miller (1978) also proposed an east dipping subduction zone beneath Northwestern Newfoundland. This is now the generally accepted direction of subduction at Betts Cove, however there have been several Ordovician subduction zone polarity shifts contributing to the formation of the BVP and Notre Dame Bay (van Staal et al. 2007). Bedard et al. (2000a) suggest the BCO was formed in a fore-arc spreading complex located on the margins of the Late Cambrian Iapetus Ocean. This is based on petrological and chemical analyses; specifically the presence of boninitic chemistry seen throughout the cumulates, sheeted dykes and lavas of the BCO (Hickey et al. 1982; Bedard et al. 2000a). van Staal et al. (2007) show though that the BVOT ophiolites, including the BCO, formed upon the inception of a new subduction zone in the ancient Humber seaway (490-481 Ma). The BVOT would later become the basement to the younger oceanic-arc-back-arc complex of the Snooks Arm Group (Bedard et al. 2000a). This being said, a fore-arc origin of the BCO is unlikely as no evidence of any continental arc material is present at the time of its formation.

The Baie Verte-Brompton Line (BBL) is a northeasterly trending suture zone delineating where the oceanic and continental arc assemblages of the Dunnage zone are tectonically juxtaposed next to the continental metasediments of the Humber zone. The BBL is associated with crustal thickening and ophiolite obduction brought about during the Taconian Orogeny (Hibbard 1983). Unlike other ophiolite suites on the Baie Verte Peninsula such as the Point Rousse and Advocate Complexes, which are more proximal to the BBL, the BCO is more distant and has not experienced the same degree of post-obduction deformation that is directly associated with development of the BBL (Hibbard 1983, Tremblay et al. 1997; Bedard et al. 2000a). A direct consequence is that the original formations are well preserved and provide a clear insight into the structure and physical properties of deep-sea oceanic crust (Bedard et al. 2000a).

The BCO is characterized by a high amplitude magnetic anomaly believed to be related to high magnetite content in the ultramafic cumulates (Miller and Deutsch 1976; Miller and Wiseman 1994,). Haworth and Miller (1982) attempting to interpret the geological significance of these anomalies through two-dimensional modeling of magnetic and gravity anomalies recognized that there were some fundamental limitations to their primary data set. First, the mean station spacing for the gravity data was 2.5 km, widely spaced considering the scale of geological units being investigated. Second, they had limited magnetic data with individual survey lines being up to 10 km apart and sampling along lines being approximately 35m. And third, geological constraints were based on the then available mapping provided by Upadhyay and Strong (1973) and DeGrace et al. (1976).

To accommodate the difference in sampling density between the gravity and magnetic data Haworth and Miller (1982) adopted a compromised approach to their potential field modeling. Slabs originally defined by gravity data were divided into zones with varying magnetism in order to replicate surface magnetic anomalies. The resulting 2-D models presented as a series of profiles suggested that the Betts Cove Ophiolite complex comprised a series of imbricate thrust slices. Haworth and Miller (1982) did recognize that there were some distinctive magnetic horizons within the Betts Cove sequence. Unfortunately, the data available at that time did not permit the definition of any geological scale (sub – kilometer) surficial features. Adding to the complexity associated by thrusting, recent geological mapping has suggested that the Betts Cove sequence has been further dismembered by a series of late Paleozoic faults (Bedard et al. 2000b). This information, unavailable to Haworth and Miller's models has a significant influence in our current models.

While the earlier geophysical modeling revealed the regional extent of some anomalous features of the Betts Cove Ophiolite (Haworth and Miller 1982; Miller and Wiseman 1994), in this study we report a model developed using more recently acquired aeromagnetic and marine magnetic data to construct a 3 dimensional subsurface morphology of the Betts Cove Complex. The new aeromagnetic data was collected using NW-SE oriented flight-lines spaced at approximately 250 m. A recent marine magnetic survey extending 10 km offshore of Betts Cove collected data having these same spatial parameters. We also take advantage of the dramatic improvements in potential field modeling that have been achieved since the 1980's. Specifically, we compute an optimum geological model from: a) geologically constrained forward modeling and inversion of the new magnetic data on a series of 2D profiles perpendicular to the geological strike; and b) a full 3D geologic model which integrates known surface geological constraints with the results of the magnetic profile inversions. Both approaches suggest the onshore exposure of the Betts Cove Ophiolite complex and its cover rocks are part of a faulted doubly plunging syncline most of which is present under Notre Dame Bay. Comparison of this feature with seismic reflection profiles suggest that western Notre Dame Bay may be floored by a complex folded sequence of Ordovician oceanic volcanics segmented into a series of horst and graben structures. This implies a transition from a locally ductile deformation regime during the Salinic Orogeny to that of a more brittle and fault related deformation regime later on.

Local Geology

The northern margin of the Betts Cove Ophiolite Complex is marked by units of serpentinites and talc-carbonate schists. These are believed to have originated from ultramafic cumulates and are the most altered units of the ophiolite suite (Hibbard 1983; Tremblay et al. 1997; Bédard et al. 2000a.). It has been suggested that the schists may also be derived from slivers of mantle, yet no firm proof of mantle presence has ever been established at the BCO (Tremblay, et al. 1997). The BCO is the only ophiolite on the Peninsula where no documented mantle exists. In addition to its highly altered nature, a high magnetic signal is uniformly associated with the talc-carbonate schists throughout the BCO (Miller and Deutsch 1976).

To the south-east and stratigraphically above the ultramafics, the sheeted dyke complex is found in outcrop (Fig. 2). Bédard et al. (2000a) described the contact between the cumulate unit and the sheeted dykes to be gradational but recognized also that the contact was locally intruded by gabbro-norite and also sheared in other instances. In reality, the true nature of this contact is hidden by extensive vegetative cover and remains to be fully interpreted. The bonitic pillow lavas of the Betts Head Formation rest above the sheeted dykes. These are highly faulted and define a series of graben structures (Bédard et al. 2000a).

Pillow lavas of the Snooks Arm Group overlie the BCO. The Snooks Arm Group is a volcanic/sedimentary cover sequence which arose from subsequent tectonic and magmatic activity in the generation of an island arc system. Noting the tholeitic nature of the pillow lavas in this group Bédard (1999) introduced the term Mount Misery Pillows to differentiate them from the bonitic pillows of the Betts Head Lavas. Tremblay et al. (1997) also described the Snooks Arm Group as consisting of increasingly tholeitic pillows and sheet flows interbedded with thick units (~300-500m) of volcanoclastic and basaltic sediments, turbidites, pelagites, as well as arc derived rhyolitic to andesitic clastic rocks.

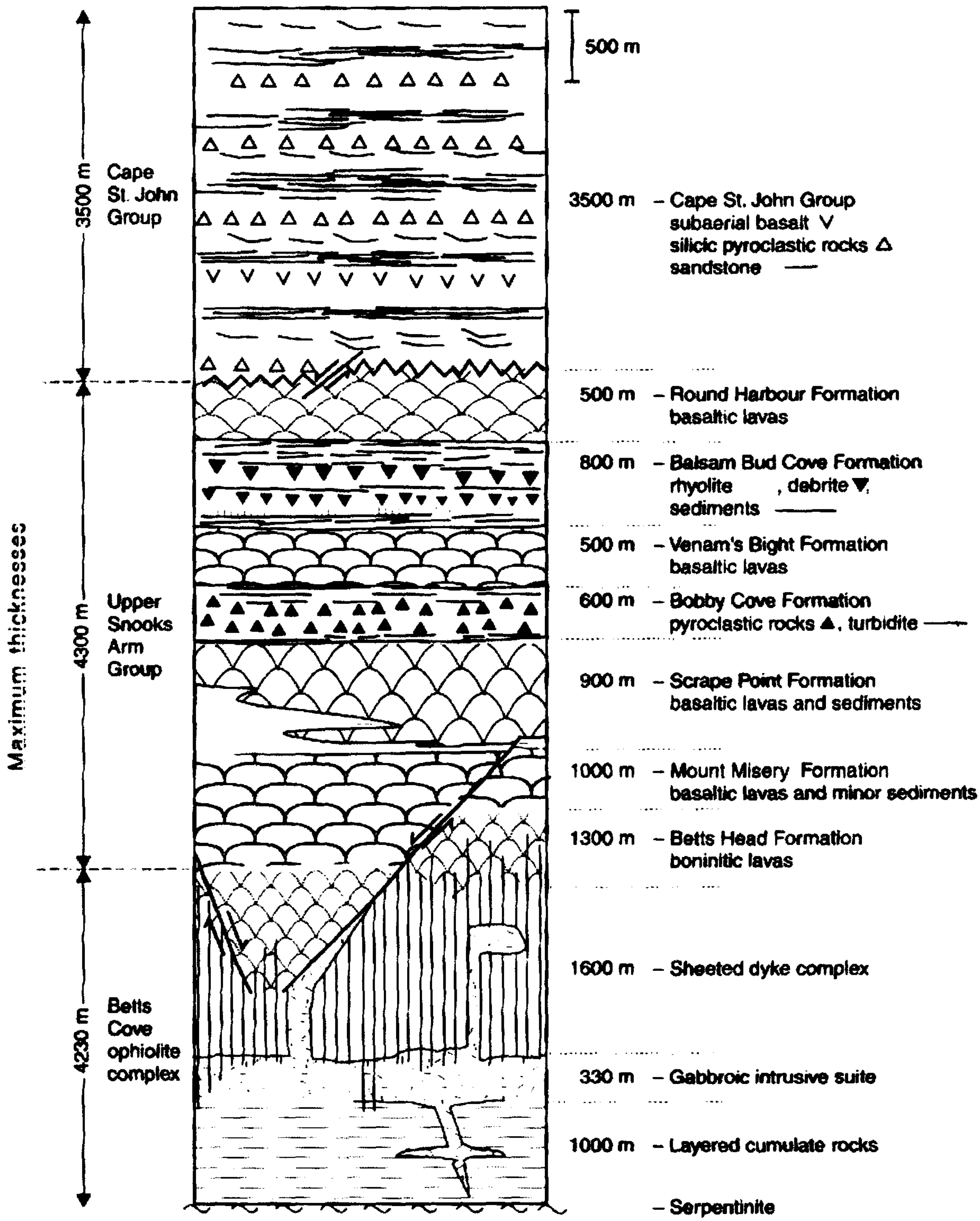
Maximum thicknesses
3500 m
Cape St. John Group
4300 m
Upper Snooks Arm Group
4230 m
Betts Cove ophiolite complex
500 m
3500 m – Cape St. John Group
subaerial basalt V
silicic pyroclastic rocks Δ
sandstone
500 m – Round Harbour Formation
basaltic lavas
800 m – Balsam Bud Cove Formation
rhyolite , debrite ▼,
sediments
500 m – Venam's Bight Formation
basaltic lavas
600 m – Bobby Cove Formation
pyroclastic rocks ▲, turbidite
900 m – Scrape Point Formation
basaltic lavas and sediments
1000 m – Mount Misery Formation
basaltic lavas and minor sediments
1300 m – Betts Head Formation
boninitic lavas
1600 m – Sheeted dyke complex
330 m – Gabbroic intrusive suite
1000 m – Layered cumulate rocks
– Serpentinite

Figure 2-2 - Stratigraphy of the Betts Cove Ophiolite and its cover rocks. Taken from Bedard 2000.

Following the Mount Misery tholeitic pillows is the Scrape Point Formation. At the base of this formation is a thin sedimentary sequence with a characteristically high magnetic susceptibility and associated high anomalous magnetic field. Portions of this unit are recognized by a distinctive jasper-like reddening and for simplicity it is often referred to as an iron formation (Bédard et al. 2000a). A similar iron formation has been reported by Hibbard (1983) in the Point Rouse Complex and is seen in outcrop throughout the Pacquet Harbour Group to the north-west of the BCO. This sedimentary member is found in greater abundance on the eastern portion of the ophiolite near Tilt Cove where extensive faulting and complex geology has exposed it in more locations (Bédard et al. 2000a). On the basis of in-situ susceptibility measurements and an irregular magnetic signature, the magnetic portion of this member appears to be discontinuous. The assessment of remanent magnetization in the sedimentary member may also provide additional insights regarding the magnetic anomalies seen throughout the BCO (see results below). While this "iron formation unit" produces a distinct magnetic anomaly the bulk of the Scrape Point Formation is made of tholeitic pillows and lava flows which are not associated with any high magnetic signal.

The next units in the sequence are the Balsam Bud Cove, Venoms Bight and then Bobby Cove Formations. The Venoms Bight Formation consists of Pillow lavas which are positioned between the volcanoclastic/sedimentary Balsam Bud Cove and Bobby Cove Formations. Overlaying the published geological map on the magnetic anomaly grid indicates that none of these units produce any detectable magnetic anomaly signal. While these formations were observed to possess variable susceptibility across the BCO none of them had a susceptibility of greater than 0.001 cgs.

The Round Harbor Formation which rests at the top of the Snooks Arm Group is composed of pillow lavas and sheet flows. This unit generally displays a strong magnetic signature and is believed to approximate the location of the fold axial plane of the regional synclinal structure that controls the BCO (Bédard et al. 2000b). Scattered throughout the Snooks Arm group, mafic sills intrude along bedding planes and unit interfaces. These are also seen to be structurally controlled at some sites, either moving into brecciated zones or more brittle sheared zones (Bédard et al. 2000a; Sangster 2007). A high magnetic signature is associated with these sills as well.

Field mapping of the orientation of bedding plane surfaces within the Snooks Arm Group show that the dip direction progressively changes from south-southeast to east-northeast along the exposed contact (Tremblay et al. 1997). At the northern limit of these arc pillow basalts of the Round Harbor Formation outline a synclinal fold structure plunging slightly to the southwest. At the southern limit of the same arc the same pillow lavas outline a northeast plunging fold nose (Tremblay et al. 1997; Bédard et al. 2000; Sangster 2007). Taken together these structural elements suggest the BCO has the form of a doubly plunging syncline. Only one half of the complete fold structure outcrops on the Baie Verte Peninsula. In previous maps the full geometry of the fold was never realized.

A simplified tectonic history for the BCO can be described in terms of Taconican obduction followed by Salinic and Acadian shortening (Tremblay et al. 1997; van Staal et al. 2007). Evidence for obduction of the BCO is presented in the form of a north-east trending thrust-fault dipping to the south-east with northwestern shear-sense indicators observed in the hanging wall (Tremblay et al. 1997). Along the eastern margin of the Betts Cove Complex and its northeastern extension, between Betts Cove and Red Cliff Pond, this thrust separates the Betts Head and Mount Misery pillow lavas from the talc-serpentines schists, while just north of Betts Cove the fault splays and offsets layered cumulated and sheeted dyke units next to Mount Misery pillows (Bédard et al. 2000; Sangster 2007). This thrust fault, critical in the interpretation of obduction at the BCO, is found in outcrop at only a few locations. An Acadian reverse fault has been mapped north of this, extending along the northern margin of the BCO. The results of the present study provide a new interpretation of the extent of the reverse fault. Specifically the presence of overturned bedding across the entire northern border of the BCO argues this fault must extend further laterally than the current mapping suggests.

Emplacement of the BCO above the continental margin is inferred to have taken place between 480-469 Ma based on correlations with other ophiolite suites on the Peninsula (Bedard et al. 2000a). In the absence of critical data or observations an absolute lower age limit for northwestern thrusting of the BCO is unknown. The Silurian Cape St. John group unconformably overlying the Snooks Arm Group does however provide the basis for a 430 Ma upper age limit of obduction (Hibbard 1982; Tremblay et al. 1997; Bédard et al. 2000a; Sangster 2007). Recent geologic mapping has revealed bedding of the western portion of the northern fold limb to be overturned (Bédard et al. 2000b). Genesis of this structure is thought to be associated with regional shortening during the Salinic Orogeny. This event was produced by compressional forces caused by accretions of portions of Ganderia to Laurentia from 450-423 Ma (van Staal et al. 2007).

Geophysics

The aeromagnetic data analyzed in this study were collected using three cesium vapor G-822 magnetometers in a 3- axis gradiometer array. This 2006 survey was flown as a drape survey with contract specifications of 100 m terrain clearance and 250 m line separation (Goldak 2007). Information utilized in this study comes from only the tail magnetometer. Future reports implementing the full potential of the magnetic gradiometry covering the whole of the Baie Verte Peninsula including the BCO are in preparation. The marine magnetic data were collected in 2008 using a SeaSpy Overhauser proton precession magnetometer. Like the airborne survey this used 250 m line separation. This marine survey was equivalent to a constant barometric height airborne survey, but in this case with the sensor at a constant elevation just slightly below the ocean surface. In both surveys data were collected along lines oriented NW-SE.

Previous to these two surveys, a lower resolution regional survey was flown for the Geologic Survey of Canada in 1988. Specifications included E-W trending flight lines, 1 km separation, and a mean terrain clearance of 120 m. The new surveys were sampled along NW-SE trending flight lines. Since the local geological strike is approximately NNE – SSW the new survey pattern optimizes the linkage between geology and magnetic signal resolution. In the magnetic images generated from data collected in the earlier 1988 survey it was difficult to differentiate between true geological signal and survey-induced noise effects because flight line orientation was similar to the direction of geological strike. Figure 3 shows the relative location of the 3 surveys (1988EW, 2006 NW-SE and 2008 marine)

The raw magnetic data was leveled and micro-leveled to remove systematic noise and non-geologic signal from the data. This was then gridded at 75 m using a minimum curvature algorithm. While the magnetic signal at any point is predominantly controlled by the magnetic properties of the underlying source rock secondary effects are introduced by topographic effects (Ugalde and Morris 2008) and by variations in the distance between the source and the sensor. A 20m grid cell digital elevation model of the rock surface was computed from a combination of SRTM derived topography and depth-sounding bathymetry. The aeromagnetic survey was flown as a draped surface. The height of each observation above the surface can be estimated from the radar altimeter and GPS data.

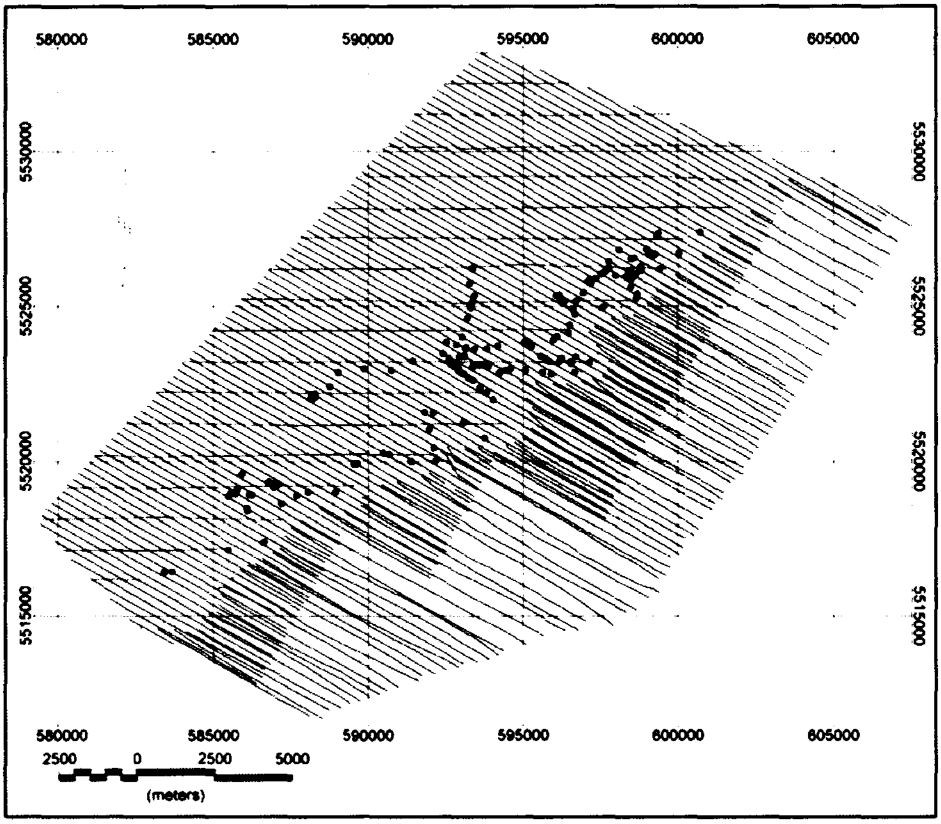
580000
585000
590000
595000
600000
605000
5530000
5525000
5520000
5515000
2500
0
2500
5000
(meters)

Figure 2-3 - Survey layout at the BCO. Northwest trending lines come from the 2006 and 2008 surveys while east-west trending lines represent previous coverage at the BCO. Locations of specimens collected for physical rock property measurements are included (dots).

For the marine magnetic survey the magnetometer was at a constant elevation just below the water surface. Knowing the bathymetry of the area then the height of sensor above the bedrock surface is the difference between sea-level and the bathymetry. Using this sensor height information the magnetic value at each point was reduced to a uniform terrain clearance through application of the 2^{nd} Taylor Series expansion (Pilkington and Roest 1992). This processing step ensures that the amplitudes of the observed magnetic anomalies are normalized to a common terrain clearance and thus the observed anomalies are due to lithological variations rather than flying elevation changes.

The marine and airborne magnetic grids were then combined using the Geosoft grid knitting algorithm. A regional magnetic field trend was computed using a 1000 m upward continuation filter. The residual signal, derived by subtraction of the regional from the micro-leveled dataset, serves to emphasize the magnetic signal produced by surface units and provides the data set for subsequent modeling.

A tilt angle derivative, in which the angle is equivalent to the ratio of the first vertical to total horizontal magnetic gradient, was computed (Miller and Singh 1994). The tilt angle is positive over a magnetic source, is zero near or over a contact, and is negative outside the source. Because the tilt angle is based on a ratio it has the advantage over first or second vertical derivative maps in that it responds well to both shallow and deep sources. The outline of a magnetic source body can be defined by the point where the tilt angle is equal to zero (Salem et al. 2008). An outline of the contacts of the magnetic source bodies within the BCO has been produced by mapping the locus of the zero tilt angle value (Fig. 4). To facilitate the modeling of the magnetic data, a series of sub-parallel profiles oriented perpendicular to the geological strike were extracted from the residual magnetic field grid.

Magnetic anomalies vary based on the size, shape, orientation, and magnetic mineralogy of the causative source body/structure. To interpret magnetic data requires one to understand that signal contributions might arise from two different sources: the induced magnetic field, and the remanent magnetic field. With induced magnetic fields the direction of the applied magnetic vector is derived from estimates of the International Geomagnetic Reference Field (IGRF) at the time of the magnetic data acquisition. The direction of the remanent magnetic vector depends on the time of remanence acquisition, and the magnitude and sense of any post-acquisition tectonic rotation, or tilting (Morris et al. 2007). Especially in iron rich ocean floor rocks the remanent magnetic signal can be dominant. This complicates any tectonic models derived from inversion and/or forward modeling of magnetic data, and underlines the importance of employing geologically constrained modeling procedures.

To assess the observed magnetic signal, physical property measurements (magnetic susceptibility, natural remanent magnetization (NRM) and density) were acquired both in-situ on outcrops and in the laboratory on oriented samples extracted in the field. All susceptibility measurements reported in this study were acquired using a Bartington MS2 susceptibility meter. Induced magnetic field contributions result from the interaction between the present Earth's Magnetic field and the magnetic susceptibility of the rock. The remanent magnetic field contribution is defined by the intrinsic magnetic remanence of each rock unit. In order to measure magnetic remanence it is necessary to have oriented core samples. For this study the cores were extracted from blocks which were oriented in the field using a magnetic compass. Compass readings were performed on the outside edge of a field notebook parallel to the samples to ensure that the measured strike of the block surface was not influenced by the magnetization of the sample. Measurements of the magnetic remanence intensity were obtained using a Schonstedt SSM-1 spinner magnetometer. The presence of remanence for each sample was evaluated using the Koensingsberger or Q-Ratio:

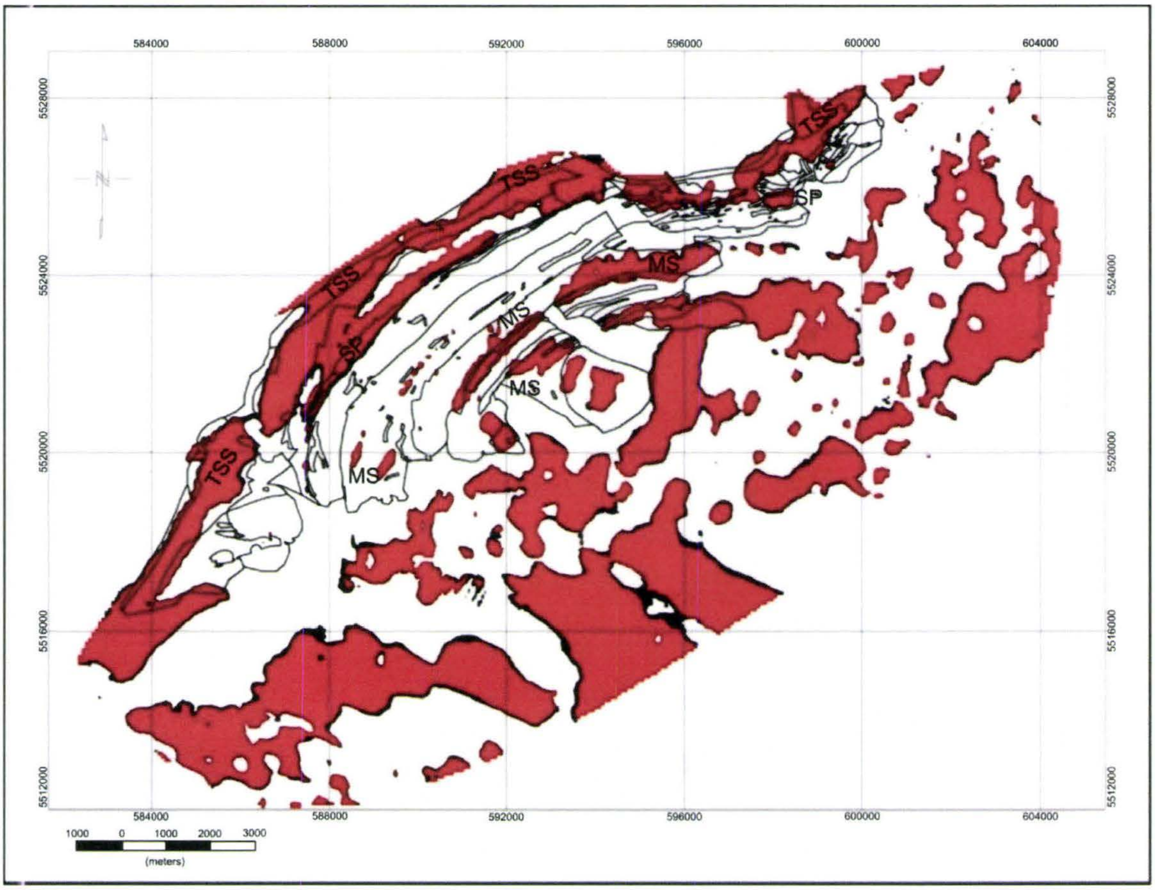
584000
588000
592000
596000
600000
604000
5528000
5524000
5520000
5516000
5512000
TSS
TSS
TSS
TSS
SP
SP
MS
MS
MS
MS
1000 0 1000 2000 3000
(meters)

Figure 2-4. Magnetic Tilt Angle Derivative contours outlining magnetic source bodies with mapped geology overlain. Values have been converted to degrees with red and white representing positive and negative values respectively. The zero degree is shown in black displaying the magnetic boundaries. Highly magnetic units situated along the northern margin of the region exhibit close correlation with geologically mapped units in this area. To the south within the Round Harbor Formation however magnetic boundaries do no coincide with the mapped geology. TSS: Talc-Serpentinite Schist's; SP: Scrape Point Formation; MS: Mafic Sills

$$Q = J/I$$

Where J is defined as the intensity of remanence magnetization in nT and I is the induced component of magnetization. Previous studies (Morris et al. 2007) have shown that there is little change in the orientation of the effective magnetic field direction until the Q-ratio (Koenigsberger ratio) threshold exceeds a value of 0.3 and above. So a remanent magnetic component was introduced for only those units for which Q exceeded 0.3.

Modeling

Five magnetic profiles trending SE-NW were modeled across the ophiolite. 2.5D forward models were produced using GM-SYS software. The objective of each model is to seek an optimum match between a computed signal and the observed magnetic profile. Constraints imposed by surface defined geologic contacts and geometries must be adhered to. Divergence from the known physical properties of each unit was permitted only within an acceptable order of magnitude difference.

The BCO was modeled as a synclinal elongated bowl-like structure resting upon a surface at a depth of approximately 3 km. Magnetic susceptibility values were assigned to each unit based on a calculated unit average from all sampling sites taken of that unit (Table 1). 15 measurements were made of each unit at a given site. The log susceptibility was computed and then averaged for each unit. 140 sites were sampled (Fig. 5; Table 1). To minimize differences between the observed and computed magnetic fields some deviation from the observed magnetic susceptibility estimate was permitted during the modeling experiment. Remember, the magnetic susceptibility measurements are always a small portion of a much larger population. With a limited number of observations there is no way of knowing if the measured value is truly representative of the whole population, or the standard deviation in susceptibility associated with that rock unit. Therefore susceptibility observations only provide a guide line for the value that should be assigned to any unit during modeling. Decreases from the average were interpreted in terms of magnetite degradation as a result of faulting or weathering. Increases may be attributed to deeper less weathered sources of higher susceptibility, unreachable for in-situ measurement.

Geological constraints within each model were derived from the published geological maps and the magnetic data sets. Lithological contacts are based on a 1:20:000 map produced by Bédard et al. (2000b) and zero tilt-angle contours (Fig. 4). The geometry of the bedding contacts in the near surface were extracted from the Bédard et al. (2000b) geological map of the BCO. Since the trend of the magnetic profile was often not truly orthogonal to the local geological strike it was necessary to compute the apparent dip of the units for each section. In the process of seeking the optimum model match it was necessary to slightly adjust the value of unit dips and the position of contacts (see results below).

Three dimensional geological modeling of the Betts Cove Complex was performed using 3D-Geomodeller. In this approach one begins by developing a best fit geometrical model based on the available surficial geological data, and then iteratively includes subsurface geological contacts derived from the magnetic forward models to produce a final best fit geological model. For the purposes of this study the strike and dip measurements of contacts and bedding planes were derived from the GSC structural data set provided by the Bédard et al. (2000b) map of the BCO. The cross sectional profiles computed by the GM-SYS models were imported and used as the structural constraint at depth for the 3D modeling. Geology contact and orientation data were honored.

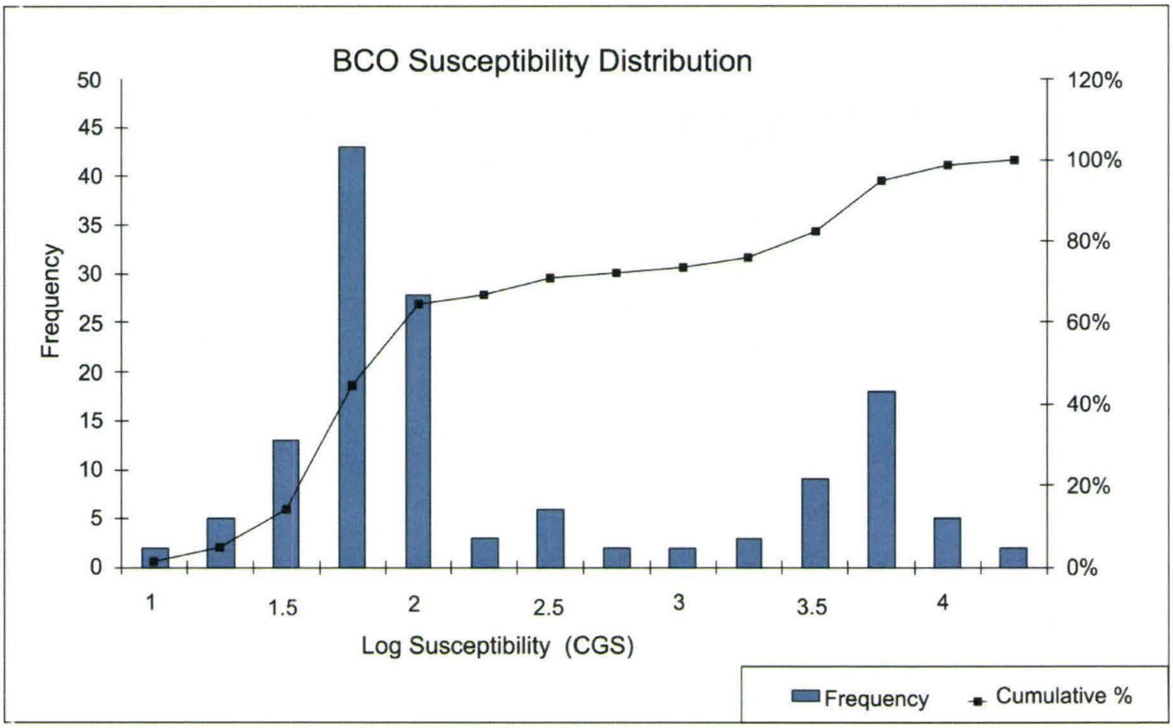
BCO Susceptibility Distribution
Frequency
50
45
40
35
30
25
20
15
10
5
0
120%
100%
80%
60%
40%
20%
0%
1
1.5
2
2.5
3
3.5
4
Log Susceptibility (CGS)
Frequency
Cumulative %

Figure 2-5 - Susceptibility distribution at the BCO. A bimodal distribution highlights the presence of two distinct populations. The low end member population is centered at Log 1.75 cgs^{-1}, the high end member at Log 3.75 cgs^{-1}.

Results and Discussion

Physical Rock Properties

The susceptibility data were organized into interval specific bins and plotted against their frequency of occurrence. Figure 5 reveals that the susceptibility data possesses a bimodal distribution highlighting two unique high susceptibility populations at Betts Cove. The first population is centered on approximately 1.75×10^{-2} cgs. Not surprisingly, these lower susceptibility values were found to be associated with the sedimentary and pyroclastic cover sequences of the Snooks Arm Group. For the purposes of magnetic modeling this would suggest that these units will have little or no impact on the model. The second susceptibility population is centered on 3.75×10^{-2} cgs. These high values are typically associated with the Talc-Carbonate Schists, Serpentinites, the Round Harbor pillows and Mafic Sills. Samples from the Scrape Point Sedimentary Member were heterogeneous; some were strongly magnetic while others were relatively non-magnetic.

Remanent magnetization was a prime concern in this study. It could be crucial for modeling purposes to determine which units possessed any remanent component of magnetization in order to accurately represent their true magnetic nature. Of particular interest was the Scrape Point Sedimentary member. This unit appears as a discontinuous magnetic anomaly across the study site. While a discontinuous induced magnetization may explain this, the presence of remanence could also have an effect and provided insight into the structure of this unit where outcrop is poor. Surprisingly however, it was found that no unit possessed any dominant remanent magnetization (Table 1). In fact, only two sites out of the 140 sampled had a Q-ratio above 0.5. These were sites sampled in the southwest within the ultramafic rocks of the Betts Cove Complex. The talc-carbonate schist and layered cumulates positioned on the south-west portion of the ophiolite have a Q-ratio of 0.9 and 1.4 respectively. Therefore, remanence was ignored across the BCO with the exception of the southwestern most profile, *Sec A* (see discussion below).

Tilt Dip Contacts

Much of the Betts Cove area is vegetated. Often the geological mapping was based on outcrops found in the many near vertical cliff faces. As such the exact locations of geological contacts in many inland locations are poorly constrained. From figure 6a we see how the geological contacts mapped by Bédard et al. (2000b) closely correlate with topographic features: the geology is well exposed in cliff faces but not on the areas in between. In particular the topographic contrasts between the Balsam Bud, Venoms Bight and Bobby Cove Formations stand out. However, when we compare the current geological map with the residual magnetic map we begin to see some incongruities. Especially in areas having less topographic contrast there is less agreement between the magnetics and geological maps. . In particular the mapped contact between the Mount Misery Formation and the Scrape Point Member on the magnetic map is featureless and undefined (Fig. 6b).

Comparing the surface contacts derived from the original geological map to the contacts as outlined by the zero-tilt magnetic response (Fig. 4) serves to highlight a number of items that are relevant to the proposed magnetic modeling. From the physical properties measured it was obvious that the geology of the BCO and its cover rocks has magnetic and non-magnetic populations (Fig 5). The Talc-Serpentinite Schists, the Scrape Point Sedimentary Member and the Mafic Sills stand out as the primary magnetic bodies. Too few samples were collected of the BCO gabbroic intrusive suite. Although it does

Series	Unit	Average Susceptibility (cgs)	Average Density (g/cm^2)	Average Q-Ratio
Cape St. John	Fluviatile Sandstone/Conglomerate	0.000005	2.92	0.08
Snooks Arm Group	Round Harbour Formation	0.000556	2.99	0.12
	Mafic Sills	0.000914	2.93	0.15
	Balsam Bud Rhyolite	0.000016	2.68	0.04
	Balsam Bud Debrite	0.000025	2.81	0.05
	Balsam Bud Basal Member	0.000042	2.92	0.11
	Venoms Bight Formation	0.000113	2.95	0.08
	Bobby Cove Turbidite	0.000021	2.68	0.03
	Bobby Cove Basal Member	0.000013	2.90	0.12
	Scrape Point: Sedimentary Member	0.001069	2.74	0.16
	Scrape Point: Volcanic Member	0.000024	2.89	0.07
	Mount Misery Formation	0.000037	2.86	0.03
Betts Cove Complex	Betts Head Formation	0.000012	2.87	0.38
	Sheeted Dyke Complex	0.000013	2.84	0.38
	Layered Cumulates	0.000020	2.84	1.15
	Talc-Serpentinite Schists	0.001336	2.92	0.33
	Late Intrusive Suite	0.000009	2.98	0.03

Table 2-1 – Physical rock properties averaged for the BCO and its cover rocks.

possess a high magnetic signature the average physical property measurement is much lower than should be. Our model assumed a high susceptibility for this body. Bédard et al. (2000a) described this unit to contain up to 20% Fe-Ti oxide minerals and noted common occurrences of disseminated pyrrhotite. Without sufficient samples however it is difficult to model the distribution of the gabbro with confidence. It may in reality, extend to a deeper level or have an alternative geometry than modeled in some profiles.

The tilt angle contact associated with the Talc-serpentinite Schists can easily be traced across the northern extent of the Ophiolite Complex (Fig. 4). Traced southwestward the anomaly extends for about 2 km along the shoreline to the southwest limit of the survey area. The southwest extension of the anomaly may reflect an offshore continuation of the Gabbroic Intrusive Suite mapped on land, and/or a contribution from the juxtaposed Nippers Harbor Ophiolite Massif to the immediate northwest.

Figure 4 also highlights a geophysical contact issue related to the Round Harbor Formation. Physical rock property measurements indicate that the Round Harbor Formation is more magnetic than any of the other cover series units (Table 1). However this unit was also found to have susceptibilities varying from 0.00004 to 0.004 cgs. The magnetic data define two quite distinct units in an area where geological mapping has recognized only one. In the construction of the magnetic models we have treated the Formation as two separate units.

Discontinuous magnetic highs are found at a number of localities throughout the Betts Cove area (Fig. 4). In some instances where these magnetic highs are found within what are known to be non-magnetic units it is possible to show that these anomalies are associated with the occurrence of the mafic sills. Discontinuous magnetic highs similar to these are found in most of the units through the middle regions of the Betts Cove Ophiolite. Similar scattered mafic sills are postulated to occur offshore of the BCO within Notre Dame Bay, where the presumed associated magnetic anomalies are more circular and less elongate. On profiles within non-magnetic geology where anomalous highs were encountered, mafic sills were often interpreted to satisfy the observed signal. This approach was applied in particular where anomalies were distributed along the apparent offshore extent of non-magnetic units.

Models

Prior to this study onshore mapping of the Betts Cove Ophiolite defined an arc (Upadhay 1973; Bédard et al. 2000b). Limited structural mapping at the south-west tip of the ophiolite suggested that this structure corresponds to a northerly plunging fold nose closure. The newly acquired marine magnetic data when incorporated with the aeromagnetic data confirms that the BCO has the form of a doubly–plunging syncline. The first vertical derivative of the combined magnetic image provides a means to trace continuous geophysically defined units from the onshore known geological environment directly into the offshore unknown marine environment (Fig. 7). On each of the five modeled profiles, the magnetic units identified onshore are encountered in reverse order in the offshore sequence compatible with a synclinal fold structure (Fig. 8). Modeling of the offshore data is permissive of a north-westerly dip direction for the offshore units. However, because of the steep dip of the rock units and the geometrical relationship between the north trending Earth's magnetic field and the north-east strike of the strata a steep south-easterly dip cannot be precluded. The following is a description of the five modeled sections.

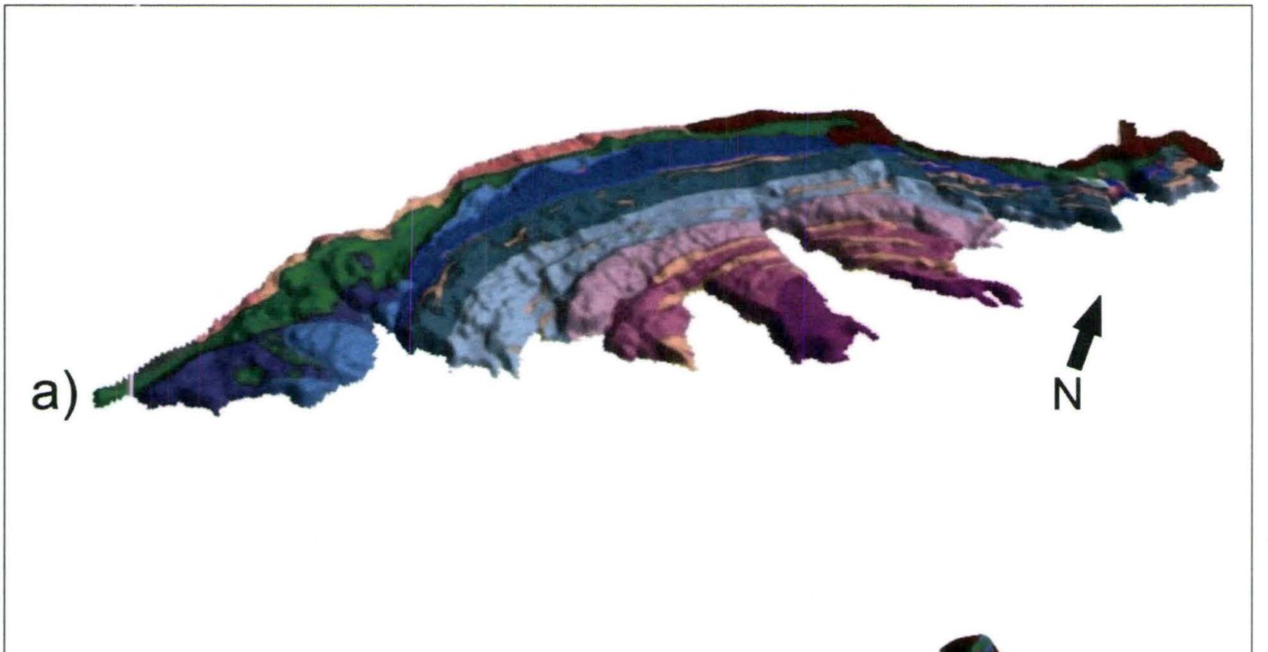
a)
N
b)
N

Figure. 2-6 - Geology of the Betts Cove Ophiolite overlain atop 20m resolution topography (A, above) and geology draped atop magnetic fields (B, below). Geologic boundaries are in agreement with the gently arcuate topographic trends. The magnetic high within the talc-serpentinite schist's (tss) is split into two peaks by a mapped fault. The magnetic anomaly within the round harbor pillows (r) however is not explained by mapping and suggests a revision of the geologic map is necessary. The stretched contact of the Scraper Point volcanics (s) evokes the presence of a gradational contact also not mapped.

Section A

The most westerly of the profiles, section A (Fig. 8), contains ophiolite units exclusively. The first magnetic peak is explained by the presence of the layered cumulates and talc-serpentinite schist. This is a high amplitude and short wavelength anomaly. Offshore the magnetic profile is low amplitude with a long wavelength. The talc-serpentinite schists and layered cumulates were modeled as one unit for the reason that few physical property measurements were taken of the layered cumulates. The susceptibility of the talc-serpentinite schists and layered cumulates were modeled using a susceptibility of 0.003 cgs a value which lies within an acceptable order of magnitude difference from the measured average susceptibility for these units of 0.0013 cgs. Variations in susceptibility within this unit may be attributed to non-uniform alteration of olivine within the ultramafics. When exposed to proper heat/pressure, olivine forms serpentine and magnetite. The sheeted dykes and the pillow lavas were modeled with susceptibilities slightly less than 0.001 cgs.

The shape of the magnetic anomalies in the southwest portion of the study area cannot be explained by varying magnetic susceptibility and/or the geometries of units alone. This being the most exposed area of the BCO, the geological mapping is well constrained so little adjustment to the location of lithological contacts can be permitted. Reversing the dip polarity of the northernmost margin of the BCO did not produce favorable results either. In order for the computed output to match the observed signal an inclusion of remanence effects was required. The physical property measurements indicate that the layered cumulates and the talc-serpentinite schists in this area do have a remanent signature. The results of these measurements are not appropriate for use in the magnetic modeling exercise. Without first completing some sample demagnetization there is no way of knowing if the observed natural remanent magnetization vector is truly representative of the remanence direction, or the vector summation of a viscous magnetic component and the true remanent vector. A better constrained approach to this problem is to use information from the appropriate Apparent Polar Wander Path. The BCO is a well documented example of an early Paleozoic ocean floor relic which was obducted onto the adjacent Grenvillian age foreland (Church and Stevens 1971; Tremblay et al. 1997; Bédard et al. 2000a). As such the actual age of any remanence present in these rocks could have been acquired at any time during the early Paleozoic.

Since Apparent Polar Wander Paths have been confidently established for the early Paleozoic in North America (Van der Voo 2001), knowing the location of the sample site it is possible to compute the orientation of the effective magnetic vector for various times during the Paleozoic. This remanence could have been acquired either before, or after folding. Knowing the current dip and dip direction of the strata it is possible to compute the orientation of the magnetic remanence vector both relative to the present horizontal surface and after untilting to the paleo-horizontal surface. As demonstrated by Cordani and Shukowsky (2009) it is possible to maintain the geometrical constraint imposed by the geology and subsequently vary the remanence direction to determine an optimum match between model and observed data. In this instance a remanence vector with a declination of 155 degrees and an inclination of 40 degrees (compared to the present day field of Dec = -20.5 degrees, Inc = 70 degrees) provided the best solution. This direction coincides with a late Ordovician paleo-pole (455-444 Ma) (Van der Voo 2001) and thus post dates ophiolite emplacement by nearly 20 Ma (Tremblay et al. 1997; Bédard et al. 2000a). Use of a remanence direction referenced to the current horizontal surface suggests this remanence was acquired after folding of the Betts Cove sequence. A likely scenario is that this

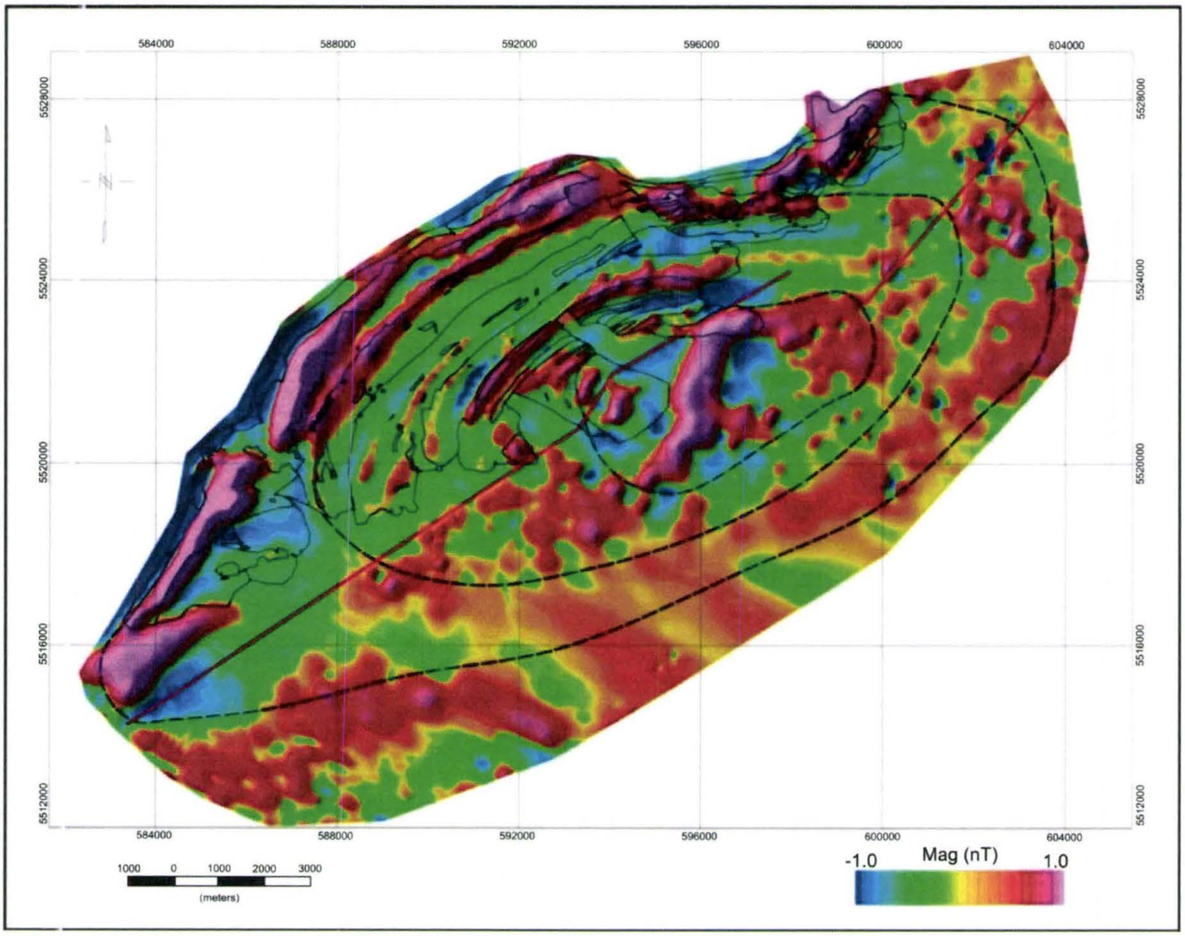
584000
588000
592000
596000
600000
604000
5528000
5524000
5520000
5516000
5512000
1000 0 1000 2000 3000
(meters)
-1.0
Mag (nT)
1.0

Figure 2-7 - Magnetic first vertical derivative with mapped geology overlain. Proposed offshore vicinity of the BCO is represented by the dashed black lines. Thrust fault not in current geologic map, interpreted from the magnetic data is shown as a solid line offshore.

remanence was thermally blocked following exhumation and regional cooling associated with either late Taconic (470-450 Ma) or early Salinic (435-422 Ma) arc-arc deformation events triggered by plate accretionary events along the Red Indian Line on the eastern margin of Notre Dame Bay (Zagorevski et al. 2007; van Staal et al. 2007).

The talc-serpentinite schists and sheeted dykes were modeled with remanence. Even with the introduction of a remanence component to the magnetic signal it was still not possible to achieve a satisfactory match between the observed and computed magnetic fields. To achieve a reasonable match requires that the dip of the talc – serpentinite schists at this point to be overturned with a dip of 65 degrees to the north. While this geometry is not shown on any geological maps of this area it is consistent with the morphology of the BCO at other localities in proximity to the bounding fault A.

Section B

Moving east the next profile is section B. At this location the thickness of the ophiolitic units are decreasing. On this section there is geological evidence that the ophiolites are locally overturned. The sheeted dykes and layered cumulates are no longer present and the Snooks Arm Group, the sedimentary/volcanic cover series, is introduced. Here we again see overturned bedding with a maximum dip of 70 degrees to the north within the talc-serpentinite schists. The shape of the magnetic profile B is similar to that found on profile A, however the magnitude of the northern magnetic high is much greater. The increased anomaly magnitude is attributed to the presence of a late intrusive suite of massive gabbro-gabbronorite that was mapped by Bédard et al. (2000b). This unit which can be seen cross-cutting the stratigraphy of the Ophiolite units as a dyke with branching sillsis described as containing up to 20% Fe-Ti oxide minerals . Accordingly this unit is modeled with a magnetic susceptibility of 0.03cgs.

The susceptibility of the BCO units are higher on profile B than to the west in profile A. Talc-serpentinite schists have susceptibilities of 0.017 cgs while the Betts Head Formation Pillow lavas have a susceptibility of 0.006 cgs. The Scrape Point Volcanic member is quite magnetic in this section of the complex at 0.003 cgs, while the Bobby Cove Basal Member is non magnetic. Intruding the Scrape Point Member are the Mafic Sills. These are more magnetic than most units throughout the BCO and are modeled with variable susceptibilities from 0.007 cgs to 0.014 cgs. These sills intrude along lithological contacts throughout the BCO but are in close association with the highly magnetic sedimentary member within the Scrape Point Formation. The position and thickness of these sills, as indicated on the geologic map, have been revised to better match the magnetic signal observed on profiles. Being mapped as thin bodies to begin with, revision of the thickness of the sills never requires an increase or decrease of more than 100 m in thickness. Using the residual magnetic signal the near surface occurrence of these sills has been well represented, however their nature at depth remains uncertain.

Section C

The shape of the magnetic anomaly in profile C changes relative to that seen in either A or B. The anomaly to the north is still quite large and collectively broader, possessing two peaks. These peaks are interpreted as input from the Talc-serpentinite schists with a susceptibility of 0.005 cgs and a combination of the Scrape Point Sedimentary Member and a Mafic Sill with susceptibilities of 0.005 cgs and 0.003 cgs respectively. The magnetic signal proceeds to decline towards the south before spiking as two peaks again, which are separated from yet another group of two peaks further south by a broad magnetic low. The northern group is modeled as two mafic sills dipping south and the southern group as

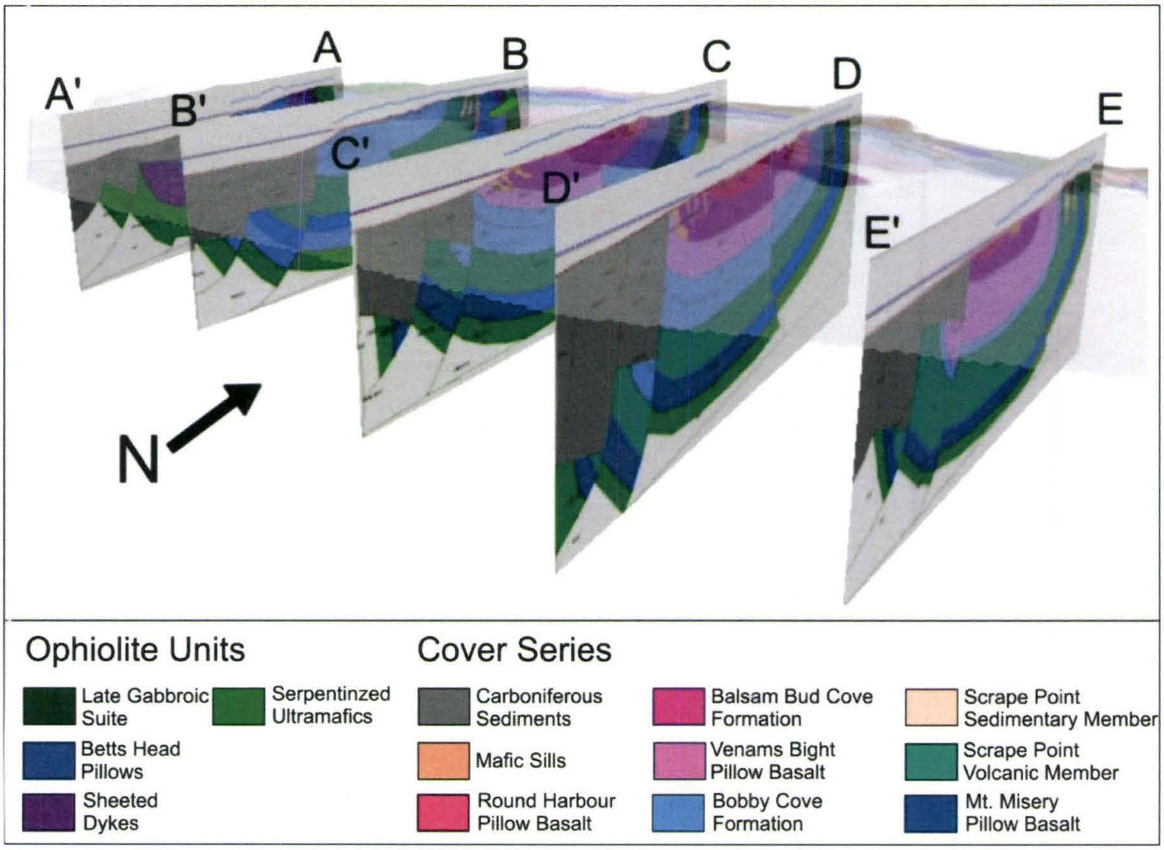
A'
A
B'
B
C'
C
D'
D
E'
E
N
Ophiolite Units
Late Gabbroic Suite
Serpentinzed Ultramafics
Betts Head Pillows
Sheeted Dykes
Cover Series
Carboniferous Sediments
Mafic Sills
Round Harbour Pillow Basalt
Balsam Bud Cove Formation
Venams Bight Pillow Basalt
Bobby Cove Formation
Scrape Point Sedimentary Member
Scrape Point Volcanic Member
Mt. Misery Pillow Basalt

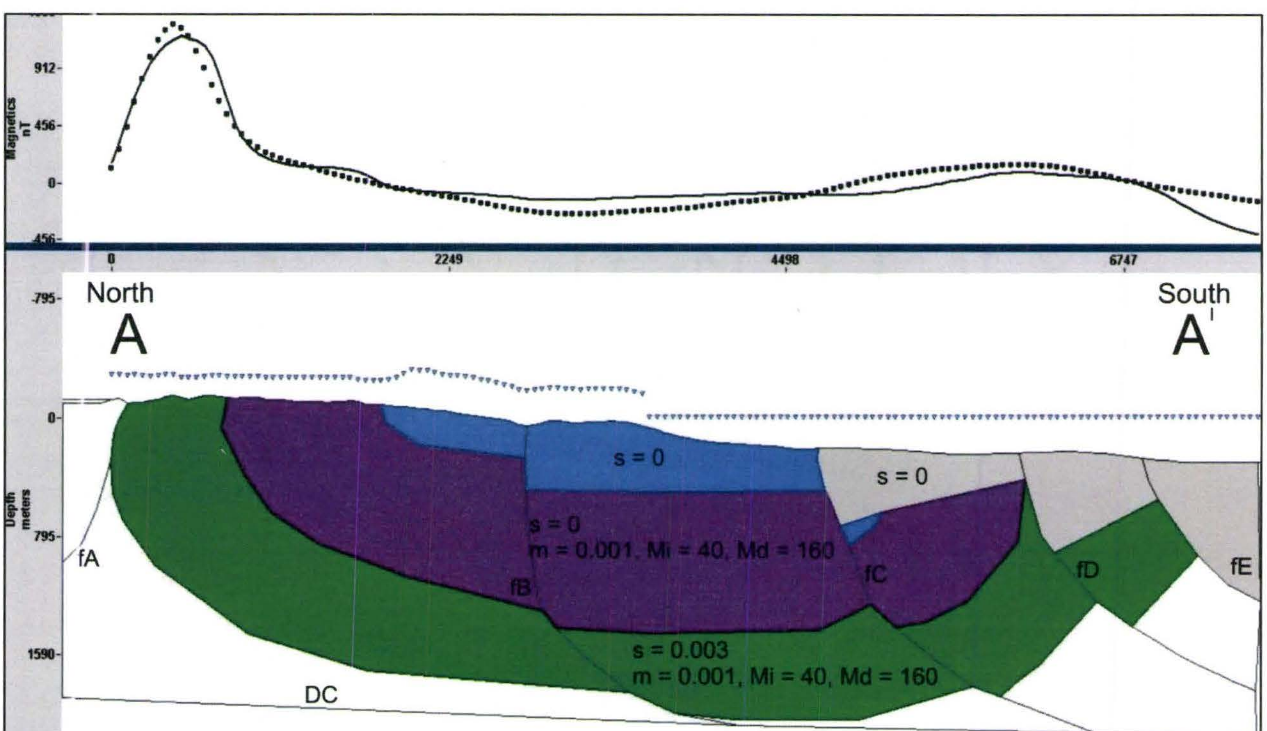
Magnetics nT
912-
456-
0-
-456-
0
2249
4498
6747
-795-
North
A
South
A'
0-
795-
1590-
Depth meters
s = 0
s = 0
s = 0
m = 0.001, Mi = 40, Md = 160
fA
fB
fC
fD
fE
s = 0.003
m = 0.001, Mi = 40, Md = 160
DC

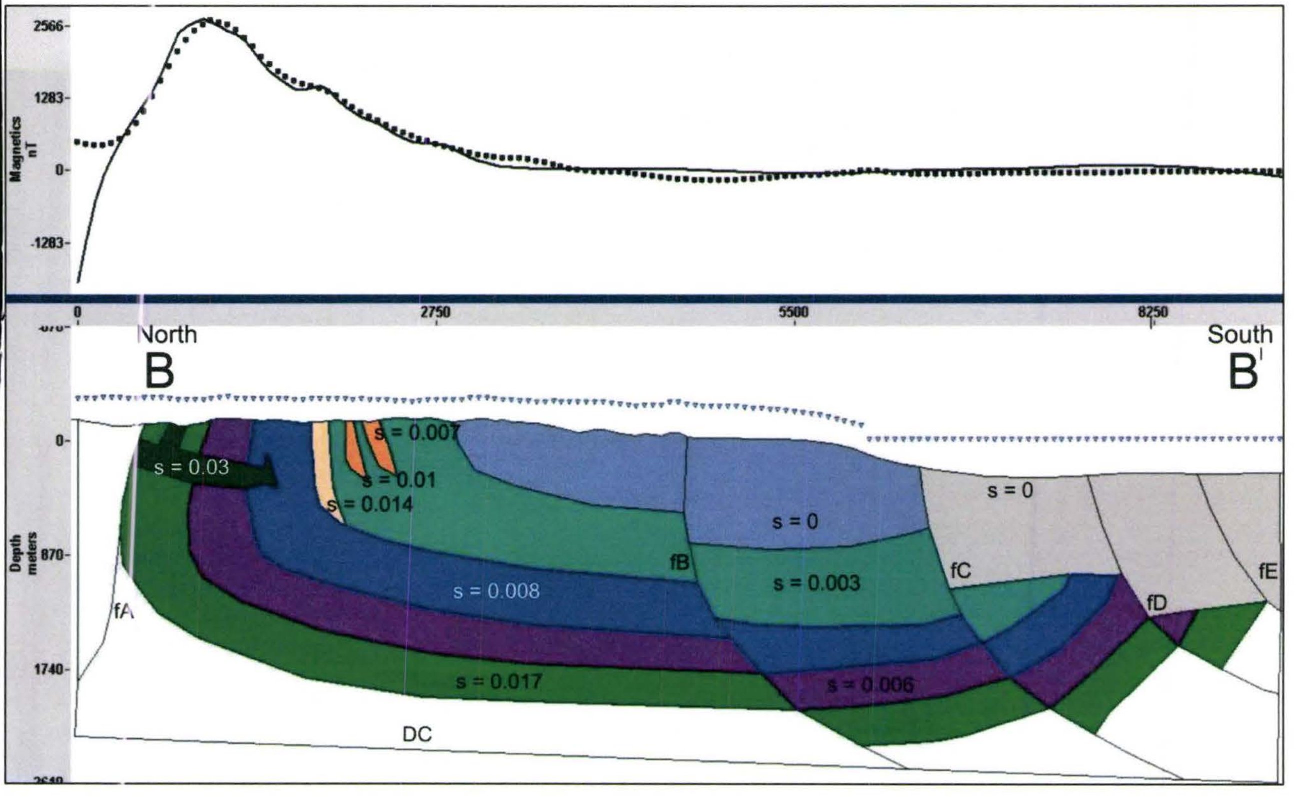
2566-
1283-
0-
-1283-
Magnetics nT
0
2750
5500
8250
North
South
B
B'
0-
870-
1740-
Depth meters
s = 0.03
s = 0.007
s = 0.01
s = 0.014
s = 0
s = 0
s = 0.003
s = 0.008
s = 0.017
s = 0.006
fA
fB
fC
fD
fE
DC

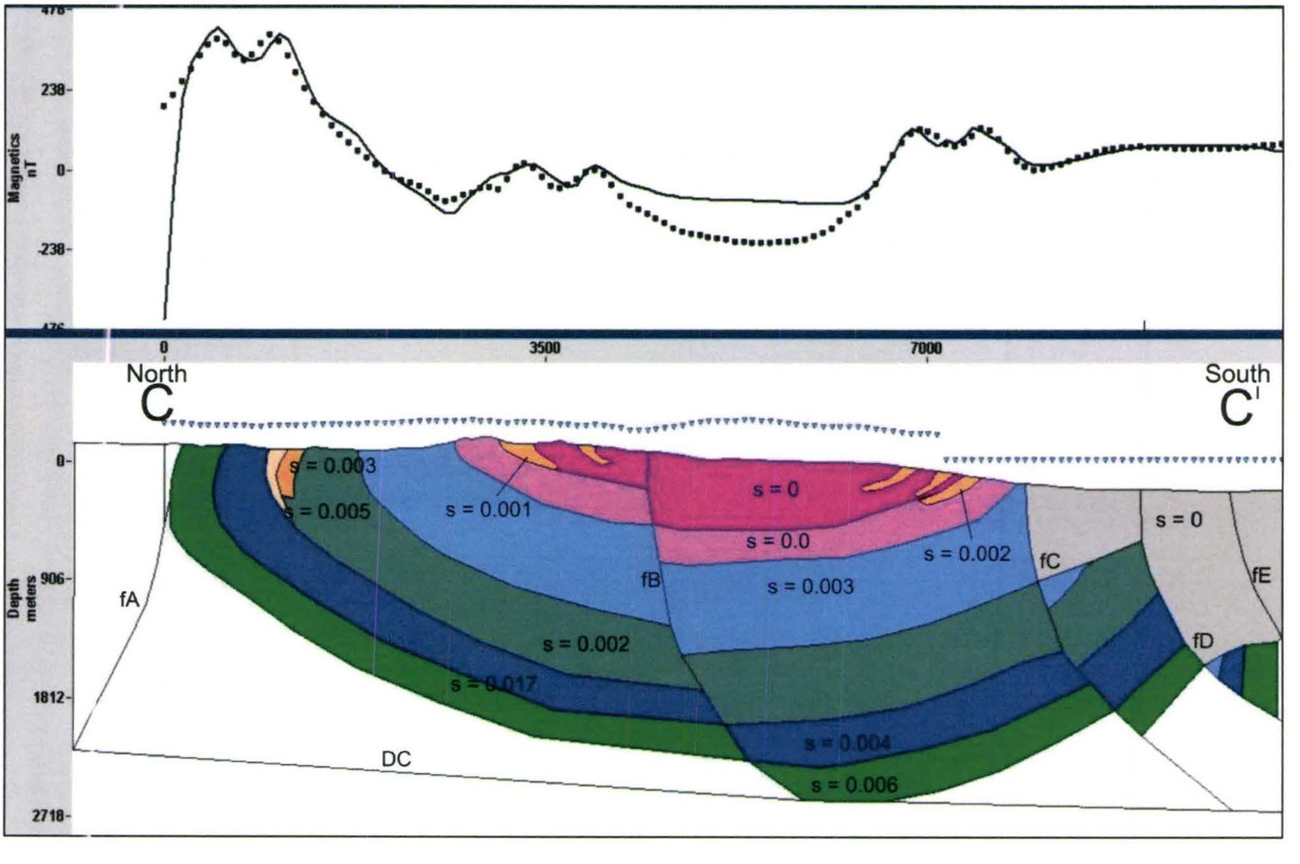
238-
0-
-238-
Magnetics nT
0
3500
7000
North
South
C
C'
0-
906-
1812-
2718-
Depth meters
s = 0.003
s = 0.005
s = 0.001
s = 0
s = 0.0
s = 0.002
s = 0
s = 0.003
s = 0.002
s = 0.017
s = 0.004
s = 0.006
fA
fB
fC
fD
fE
DC

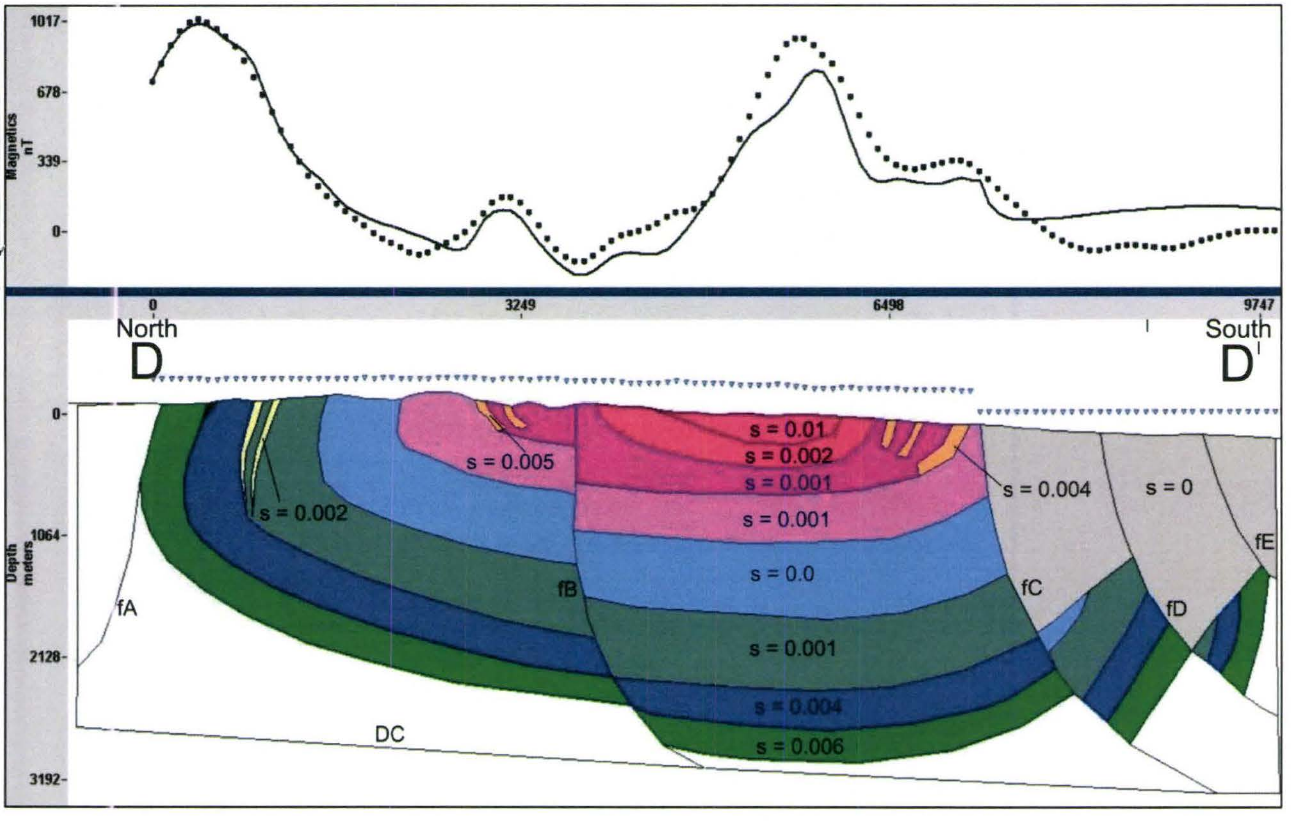
1017
678
339
0
Magnetics nT
0
3249
6498
9747
North
South
D
D'
0
1064
2128
3192
Depth meters
s = 0.01
s = 0.002
s = 0.001
s = 0.005
s = 0.002
s = 0.004
s = 0
s = 0.001
s = 0.0
s = 0.001
s = 0.004
s = 0.006
fA
fB
fC
fD
fE
DC

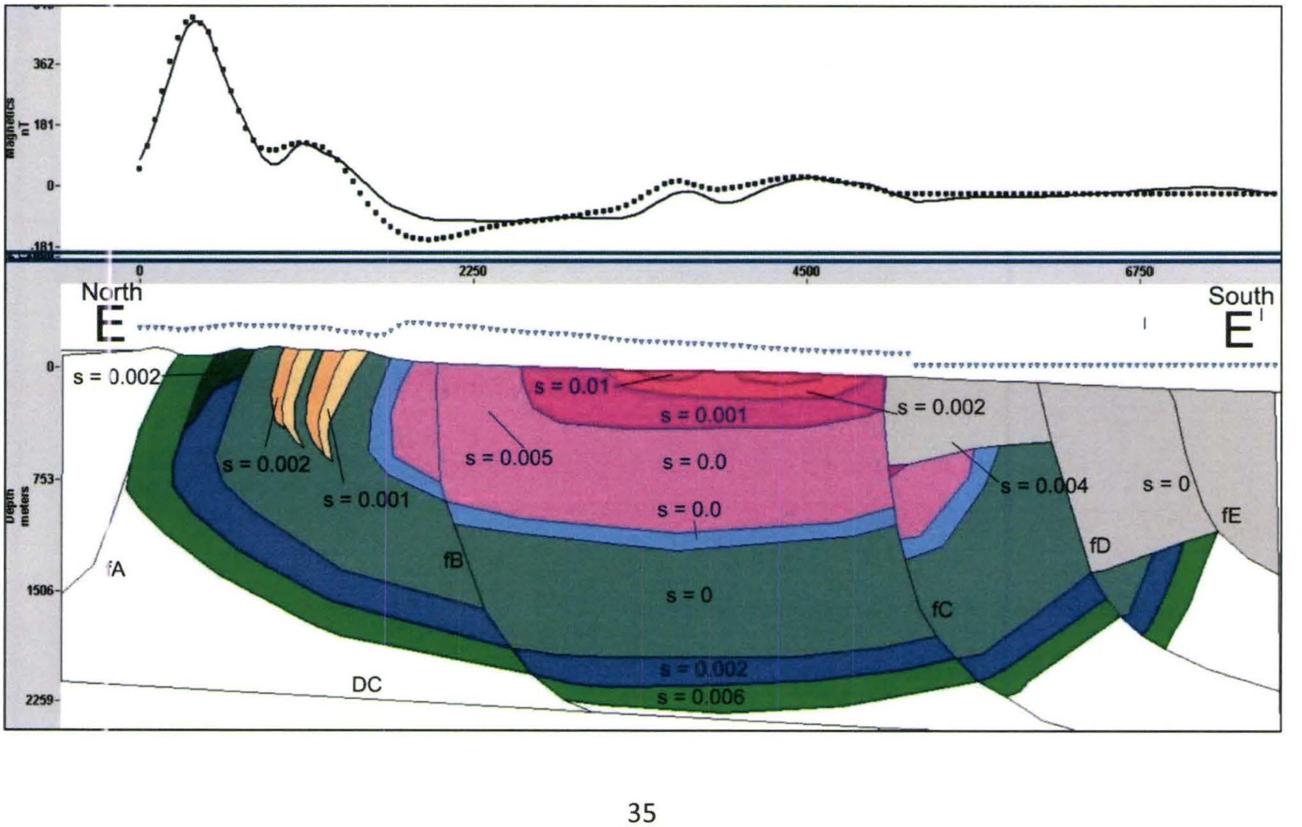
362
181
0
-181
Magnetics nT
0
2250
4500
6750
North
South
E
E'
0
753
1506
2259
Depth meters
s = 0.002
s = 0.01
s = 0.001
s = 0.002
s = 0.002
s = 0.001
s = 0.005
s = 0.0
s = 0.004
s = 0
s = 0.0
s = 0
s = 0.002
s = 0.006
fA
fB
fC
fD
fE
DC

Figure 2-8 - Magnetic Forward Models of cross-sections A through E and their location. Observed signal is displayed as the dotted line, computed signal in black and model error in red (upper panel). The modeled geology with susceptibility information is displayed with a vertical exaggeration of 1(lower panel). Geology is modeled within a floating basement of zero magnetic susceptibility. Section A is the only unit with remenance included.

three sills dipping north. The configuration of these modeled sills is consistent with a synclinal structure. The proposed model along section C differs from information presented on the geologic map. The magnetic data is interpreted with the northernmost Sill being in contact with the Venoms Bight Formation which suggests that the Balsam Bud Basal Member is entirely pinched out. It is hypothesized that this is a fault controlled feature which results in overturned bedding with dips of 75 degrees to the north. However, the match between the observed and computed magnetic anomaly is not completely explained suggesting some other, as yet undefined, anomaly source is present.

Section D

In profile D we again are required to increase the susceptibility of the magnetic units from their measured averages in order to satisfy the observed magnetic data. The talc-serpentinite schists have a susceptibility of 0.006 cgs, the Mount Misery Pillow Lavas have k = 0.004 cgs and Scrape Point ranging from k = 0.001 cgs to k = 0.004 cgs. A dip of 75 degrees to the north has been modeled for the overturned northern section that includes the unit of talc-serpentinite schists and adjacent Mt. Misery Formation. The Scrape Point sedimentary units have been modeled as thin sheets with near-vertical to slightly overturned bedding pinching out at depth. It is unclear whether these units actually pinch out with increasing depth, or if the magnetic signal associated with this thin unit no longer becomes detectable. This section also cuts though a small section of mafic sill with k = 0.007 cgs at the talc-serpentinite/pillow lava contact. Mafic sills are again introduced to explain the adjacent magnetic high to the south, at the mapped lithological contact between the Venom's Bight and Balsam Bud Cove Formations. The model depicts two smaller sills as opposed to the one larger sill displayed on the geological map. While the magnetic anomaly pattern is best explained by two distinct magnetic sources it is quite possible that geologically that this could correspond to a single sill having enhanced magnetic mineral content along its upper and lower surfaces. Further south on this profile the geologic map displays three more sills. However there is no geophysical evidence of their presence, so they have been omitted from the profile.

A high amplitude anomaly exists at the center of profile D which is not observed in any other region of the BCO. This anomalous high can be seen in the middle of the map of the first vertical derivative as a large north-northeast trending curvilinear feature (Fig. 7). The shape and prominent magnetic high of this anomaly remains to be fully understood. For the purposes of modeling this has been treated as a zone of increased susceptibility. There is no geologic information available regarding this feature which is located offshore. The geophysical data indicate the source body has an above average magnetic mineral content and is of limited spatial extent. A speculative option may be the presence of more mafic sills however this anomaly is much larger than others currently found on shore associated with the occurrence of sills.

Section E

The amplitudes of all magnetic anomalies are decreased in profile E relative to all the others. The susceptibilities used for each unit on this profile are much closer to the computed averages based on measurements. This is likely in part to sample biasing. The south western portion which is predominant in the previous sections is accessible by water only. The northeastern side of the ophiolite is road-accessible. This is the area where in-situ susceptibility measurements were made and so it is to be expected that the observed and computed susceptibility values should be in closer agreement (Fig. 3). The talc-serpentinite schists are still represented with a higher than computed average of k = 0.006 cgs on the northeastern portion of the ophiolite.

The bedding modeled in this section is more overturned than in other sections, with some northward dips being as shallow as 60 degrees. This is in agreement with the geologic mapping and produces a signal that matches well the observed magnetics. The gabbro-gabbronorite unit is present again in this area of the ophiolite and has been included in the model with a smaller susceptibility than used to model the gabbro on the west side of the Ophiolite. The gabbro has a susceptibility of k = 0.002 cgs in this section and has the form of a sill rather than a dyke.

The mafic sills and Scrape Point Sedimentary Member are present on the geologic map and required by the model. The geological map suggests the presence of mafic sills intruding again along the contact between the Scrape Point volcanic and sedimentary units. The contact of the Round Harbor Group with the Balsam Bud Cove Group has been positioned based on the geophysical trends from the first vertical derivative (Fig. 7). Again this unit required zones of increased susceptibility in order to satisfy the data. A contrast of 0.001 cgs was modeled between the main body of the Round Harbor Formation and the increased susceptibility zones.

Faults

Structural mapping and interpretation suggests the current morphology of the BCO has been influenced by several significant faults mostly located along the outermost perimeter of the ophiolitic units (Tremblay et al. 1997; Bedard et al. 2000b). These faults are interpreted to include the original obduction surface which is not exposed in outcrop, a normal fault on the western portion of the ophiolite and a high angle Silurian reverse fault thrusting the younger Cape Brule Porphyry above the Talc-serpentinite schists in the area of Tilt Cove. While geologic evidence for these faults is limited incorporating these faults into the geophysical models results in an improved match between the observed and computed magnetic anomaly patterns. .

Models in all of the sections include a decollement (Fault fD) surface which was placed at roughly 3km below the current surface. It is well established that the BCO was obducted over the adjacent Grenvillian continental margin together with the rest of the BVOT. Previous regional scale magnetic modeling reported by Miller and Wiseman (1994) tied to the Lithoprobe seismic reflection data and placed this surface at a depth of greater than 5km. In this more local study of Betts Cove we place the surface at 3km. The actual depth of this surface is poorly constrained by the total field magnetic data. The surface is deep and hence resolution of its position is poor. Further since the surface is for the most part sub-horizontal it would have minimal influence on a magnetic anomaly map. With no borehole constraints available for the BCO at this time, the nature of this surface is the least constrained aspect of the study. High resolution gravity data may aid in constraining the depth to basement in future models.

Each of the profiles includes a high angle northward dipping reverse fault. Fault fA is introduced to satisfy the available geological field mapping. Moving northeast across the ophiolite in the Tilt Cove area the dip polarity of the fault changes from south to north. In the west the younger Cape Brule Group is in fault contact with the older Betts Cove Ophiolite. To bring these two units into contact requires the presence of fault with a north-east dipping thrust surface. Fault fA on the magnetic models provides a possible mechanism to explain the mapped overturned bedding. Evidence for the fault is linked to a northeast trending linear magnetic anomaly (Fig. 7). This fault is positioned, and trends, in the same direction as two inferred faults included in the Bédard et al. (2000b) geologic map.

An anomalous portion of lava flows and pillow basalts north of the ophiolitic units on the western portion of the BCO has been included in the current geological map. Bédard et al. (2000a) classified a series of outcrops by the term "Undifferentiated Snooks Arm Group", noting that these rocks lack the bonitic chemistry commonly found in the ophiolites. Despite the fact these rocks do not posses any of the traditional characteristics of the Snooks Arm Group, Bédard et al. (2000a) explained this sequence as a down dropped block of the Snooks Arm cover series with the mechanism being related to the normal faulting documented further to the east. The geophysical evidence presented in this work however requires overturned bedding to the north of the ophiolite. The mechanism to achieve this has been modeled in the form of a southward directed thrust (fault fA). This thrust may provide another hypothesis as to the origin of the Undifferentiated Snooks Arm Group. This Group was described by Bédard et al. (2000a) as possessing many of the characteristics common to all ophiolitic bodies within the BVOT. It may be that this series of andesitic conglomerates, lapilli tuffs and pillow lavas could be linked to the ophiolitic portions of the Upper Pacquet Harbor Group (Skulski et al. 2007) that have been exhumed by southward thrusting. Similar strata in mapped outcrops of the Upper Pacquet Harbor Group located further to the north of the BCO have been described by Skulski et al. (2007). This alternative interpretation has important economic ramifications since uplift of the ore hosting Upper Pacquet Harbor Group may bring mineralized zones within economically viable depths. Further examination of this hypothesis could be tested through modeling of high resolution gravity data to determine the presence and depth to any zones of high density contrast. This however is not achievable at the moment as insufficient gravity data exists at Betts Cove.

Four normal faults have been modeled based on geophysical evidence. These faults are listric at depth attaching to a regional decollement surface DC approximately 3km deep. As shown by each profile the magnetic modeling is compatible with normal fault displacement of approximately 1 km. In the case of the most northerly of these normal faults fB evidence for of existence is linked to a northeast trending linear magnetic anomaly (Fig. 7). This fault is positioned and trends in the same direction as two inferred faults included in the Bédard et al. (2000b) geologic map. Our fB fault is modeled as a continuous package in the profiles however from it appears this feature may be cut (Fig. 7).

The magnetic anomalies found in the offshore data all have significantly lower amplitude and longer wavelength than those associated with the same units found onshore in the aeromagnetic data. These features in the offshore data are compatible with an increase in depth to the magnetic source, the Ophiolite units. Some of this change though can be attributed to a decrease in magnetic signal resolution linked to an increased source to sensor distance associated with the bathymetry of Notre Dame Bay. An alternative explanation to this phenomenon may be explained in terms of a close proximity of the BCO and its cover rocks to the dextral-transverse Green Bay fault. This fault is shown to outcrop parallel to the Betts Cove shore line roughly 40km to the southwest (Ritcey et al. 1995). It may be possible that offshore portions of the BCO have been offset by this and as such, low offshore anomalies are caused by an absence of ophiolitic units rather than the vertical displacement displayed in these models. The traceability of these units depicted via the first vertical magnetic derivative (Fig. 7) however, provides support for the continuity of the BCO offshore of Betts Cove and as such, validation for the current model.

To make the model compatible with the known bathymetry of Notre Dame Bay it is necessary to introduce an undefined geological unit having very low magnetic susceptibility. This low magnetic unit is modeled as sitting unconformably over the underlying ophiolite sequence. To create the space needed for this unit required the introduction of three normal faults fC, fD and fE suggesting a period of late extensional faulting.

Seismic profiling across Notre Dame Bay provides further support for these proposed normal faults (Grant 1972; Jacobi and Kristofferson 1976). Both of these studies contain evidence for the presence of southward dipping faults within the vicinity of Betts Cove which when combined with northward dipping faults on the other side of the bay define a regional graben structure. Each of the seismic profiles across Notre Dame Bay includes direct evidence for the proposed unconformity surface. Jacobi and Kristofferson (1976) suggest that the minimum age of this unconformity is Lower Cretaceous based on comparisons with an unconformity surface from Grand Banks drill core data. However Grant (1972) proposed a Jurassic age from the more southern Grand Banks drill core data. Grant also notes the possibility of a Carboniferous sediment source based on nearby continental rocks. The size, shape and orientation of this graben feature has many similarities to the Carboniferous age Deer Lake basin which is located to the west of the Baie Verte Peninsula on the Baie Verte – Brompton Line (Cabot 2001). Independent evidence for existence of a Carboniferous fault bound basin within Notre Dame Bay is provided by map compilation of onshore and offshore geology presented by Fader et al. (1989). While the exact bounds of the basin are poorly defined in this regional compilation the map does show that the bounds are faults having an orientation similar to the ones described in this study. As the exact age of this unconformity surface remains indefinite the geophysical models presented within this study provide additional evidence to support normal faulting offshore of the BCO.

3D Model

The end result of this study is a three dimensional model of the BCO and its cover rocks (Fig. 9). The model depicts a doubly plunging syncline resting atop a regional decollement surface. Two high angle reverse faults and three extensional listric faults terminate this decollement at roughly 3km depth. The units included within this model are a simplification of the mapped geology. Here all ophiolitic units are represented as a single formation. This formation is thickest to the southwest (top view) and pinches out to the northeast (bottom view). The core of the fold to this elongate bowl-like structure is hosted within the Round Harbor Formation. From the model we see that the displacement along the extensional faults and the thickness of the sedimentary fill increases towards the northeast. The interpolator of 3D Geomodeller thins the sedimentary fill to the south. As no geophysical data is available here this can neither be confirmed nor denied.

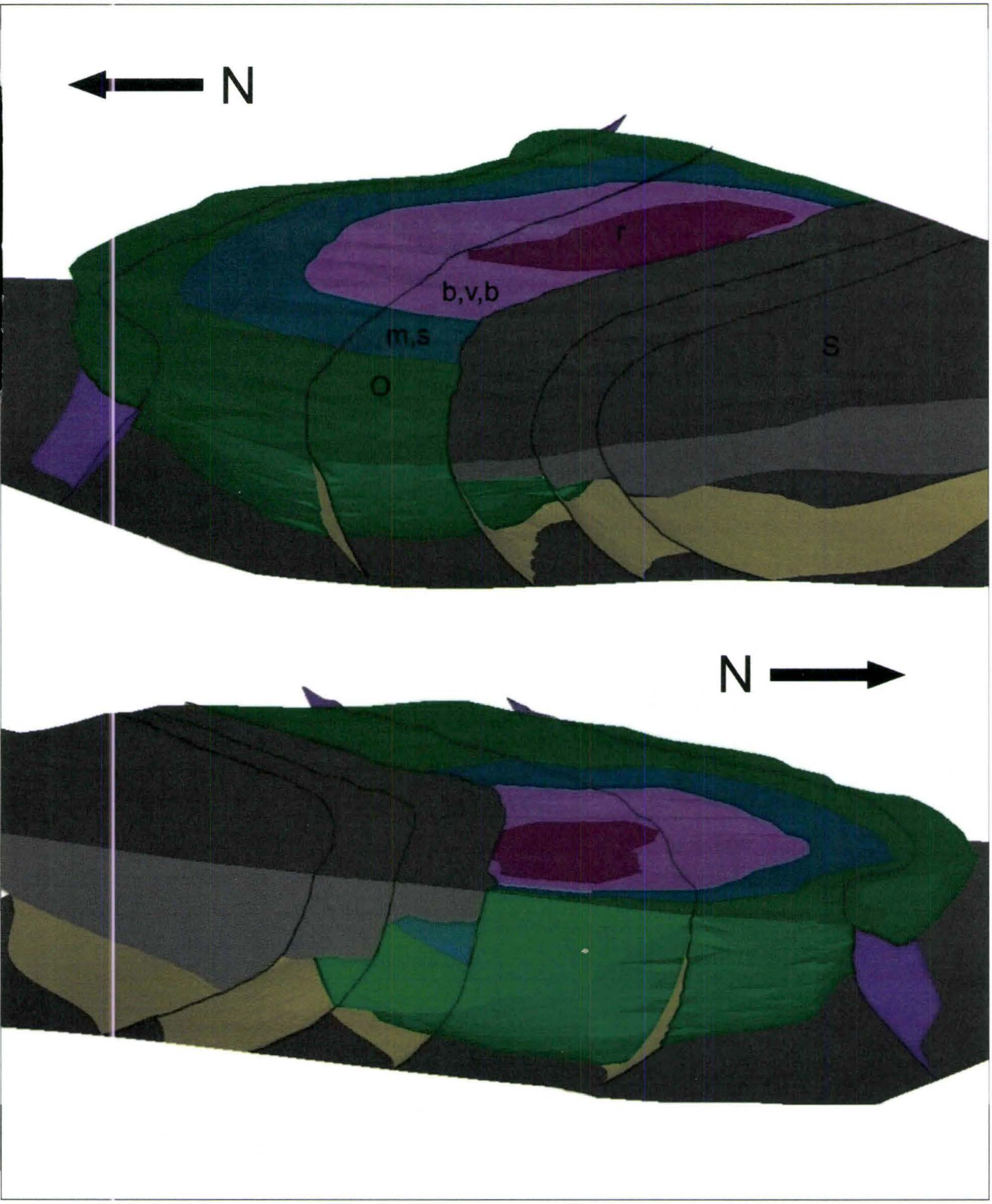
N
r
b,v,b
m,s
o
s
N

Figure 2- 9 - 3D Model of the BCO exhibits an elliptical bowl-like morphology. High angle reverse faults are displayed in purple while normal faults are shown in beige. View 1 (above) looks from the southwest to the northeast with all units displayed. View 2 (below) views from the northeast to the southwest. O: BCO units; m: Mount Misery Formation; s: Scrape Point Formation; b: Bobby Cove Formation; v: Venoms Bight Formation; b_b: Balsam Bud Cove Formation; r: Round Harbour Formation; s: offshore (Carboniferous) sediments.

Conclusions

The Betts Cove Ophiolite is positioned within a significant geologic area of Newfoundland. An extensive literature has been produced describing the surficial geology while geochemical analyses have revealed the significance of these rocks in terms of early Paleozoic ocean dynamics. Previous geophysical work reported for this area is of limited viability for a number of reasons. Earlier workers had access to only regional scale data sets. New magnetic data has documented features that were not detected in previous surveys. Geophysical inversion techniques have made dramatic advances in past 5 years such that previous 2D unconstrained approaches are of limited value.

Using the new high resolution magnetic data the geometry of the magnetic units within the BCO can be better defined. Physical property analysis indicates that magnetization within the BCO is predominantly induced. Remanence effects associated with Late Ordovician thermal overprinting magnetic field are restricted to a few horizons. Geometrically the contacts outlined by this new survey suggest that the northern and southern extremities of the BCO represent fold closures. Combining these boundaries with the structural data suggests the BCO has the form of a doubly plunging regional synclinal structure. Pillow basalts located within the Round Harbor Formation host the core to this fold, plunging slightly to the southwest. This fold hypothesis is supported by geologically and petrophysically constrained 2D forward magnetic inversion models of the observed magnetic field.

The results of this study support the idea that significant faulting has occurred at the BCO. A large scale high angle reverse thrust and four normal listric faults are believed to join at depth in a regional decollement surface. Overturned bedding of the western portion on the northern fold limb documents such a thrust. Further examination of this outermost thrust may reveal more ophiolites in the subsurface north of the BCO. This may in turn reveal new zones of mineralization. Late stage extensional faults, possibly associated with a Carboniferous pull-apart sedimentary basin lead to the current morphology of Notre Dame Bay.

References

Bédard, J.H. (1999). Petrogenesis of boninites from the Betts Cove Ophiolite, Newfoundland, Canada: Identification of subducted source components. Journal of Petrology, **40**: 1853-1889.

Bédard, J.H. Lauzière, K. Tremblay, A. Sangster, A. Tellier, M., Dec, T. (2000a). Betts Cove ophiolitic complex and its cover rocks, Newfoundland. Geological Survey of Canada. Map 1969A, scale 1:20,000.

Bédard, J.H. Lauzière, K. Tremblay, A. Sangster, A. Douma S.L., Dec, T. (2000b). Betts Cove Ophiolite and Its Cover Rocks, Newfoundland. Natural Resources Canada,Geologic Survey of Canada, Bulletin 550.

Bird, J, M. and Dewey, J, F. (1970). Lithosphere plate-continental margin tectonics and the evolution of the Appalachian orogen. Geol Soc. America Bull, **81**: 1031 -1060.

Cabot, M. (2001).Canada's unexplored lands: Deer Lake basin case study. Oil & Gas Journal, **99**: 36-42.

Church, W.R., and Stevens, R.K. (1971). Early Paleozoic Ophiolite Complexes of Newfoundland Appalachians as mantle-oceanic crust sequences. Jour. Geophysics. Research, **76**: 1460-1466.

Codani, R. and Shukowsky, W. (2009). Virtual Pole from Magnetic Anomaly (VPMA): a procedure to estimate the age of a rock from its magnetic anomaly only. Journal of Applied Geophysics, **69**: 96-102

DeGrace, J.R., Kean, B.F., Hsu, E. and Green, T. (1976). Geology of the Nippers Harbor Map Area (2E/13). Newfoundland: Newfoundland Department of Mines and Energy, Mineral Development Division, Report 76-3.

Fader, G.B., Cameron, G.D.M., Best, M,A. (1989). Geology of the Continental Margin of Eastern Canada. Geological Survey of Canada. Map 1705A, scale 1: 5 000 000.

Grant, A.C. (1972). The continental margin off the coast of Labrador and Newfoundland - Morphology and geology. Can. J. Earth Sci, **9**: 1394-1430.

Goldak Airborne Surveys. (2007). Technical report on a fixed wing aeromagnetic survey. Baie Verte, Newfoundland and Larbrador. Solicitation no. 23240-07TG23/A. 28p.

Haworth, R. T., and Miller, H.G. 1978. Geophysical Evidence for an east dipping Appalachian subduction zone beneath Newfouundland. Geology, **6**: 522-526.

Haworth, R. T., and Miller, H.G. (1982). The Structure of Paleozoic Oceanic Rocks beneath Notre Dame Bay, Newfoundland: Major Structural Zones and Faults of the Northern Appalachians, Geological Association of Canada, Special Paper 24.

Hibbard, J.P. (1983). Geology of the Baie Verte Peninsula, Newfoundland. Newfoundland Department of Mines and Energy. Memoir 2, 279p.

Jacobi, R., and Kristoffersen, Y. (1976). Geophysical and Geological Trends on the Continental shelf off northeastern Newfoundland. Canada Jour. Earth Sci, **13**: 1560-1570.

Miller, H.G. and Deutsch E.R. (1975). New gravitational evidence for the subsurface extent of oceanic crust in north-central Newfoundland. Canadian Journal of Earth Science, **13**: 459-469.

Miller, H.G. and Deutsch E.R. (1976). A Gravity Survey of Eastern Notre Dame Bay, Newfoundland. Earth Science Symposium on Offshore Eastern Canada: Geol. Survey Canada Paper 71-23. pp.495-499.

Miller, H.G. and Singh, V. (1994). Potential field tilt – a new concept for location of potential field sources. Journal of Applied Geophysics, **32**: 213-217.

Miller, H.G. and Wiseman, R. (1994). Potential field interpretation of the Baie Verte Peninsula, Newfoundland, utilizing constraints from Lithoprobe East seismic line 89-13. Atlantic Geology. **30**: 25-36.

Morris, W.A., Ugalde, H., and Thomson, V. (2007). Magnetic Remanence Constraints on Magnetic Inversion Models. The Leading Edge, **26**: 960-964.

Pilkington, M. and Roest, W.R. (1992). Draping aeromagnetic data in areas of rugged topography; Journal of Applied Geophysics, **29**: 135-142.

Ritcey, D.H., Wilson, M.R., Dunning, G.R. (1995). Gold mineralization in the Paleozoic Appalachian Orogen; constraints from geologic U/Pb, and stable isotope studies of the Hammer Down Prospect, Newfoundland. Economic Geology and the Bulletin of the Society of Economic Geologist, **90**: 1955-1965.

Salem, A., Williams, S., Fairhead, D., Smith, R., Ravat, D. (2008). Interpretation of magnetic data using tilt-angle derivatives. Geophysics, **73**: L1-L10.

Sangster, A. (2007). Mineral Occurrences of the Betts Cove Complex Baie Verte Peninsula, Newfoundland. Geologic Survey of Canada. Consolidation and Synthesis of Mineral Deposits Knowledge, pp.12.

Skulski, T., Castonguay, S., van Staal, C.R., McNicoll, V.J., Piercey, S., Slavinski, H. (2007). Geology of the Baie Verte Peninsula revisited; stratigraphy and structure of the Pacquet Harbour Group. Proceedings, Geological Society of America, Northeastern Section, 42nd annual meeting, Durham, New Hampshire., pp. 49-50.

Tremblay, A., Bédard, J.H., and Lauzière, K. (1997). Taconian Obduction and Silurian Exhumation of the Betts Cove Ohiolite, Canadian Appalachians. Journal of Geology, **105**: 701-716.

Ugalde, H. and Morris, W.A. (2008). An assessment of topographic effects on airborne and ground magnetic data. The Leading Edge, **27**: 76-79.

Upadhyay, H.D. (1973). The Betts Cove ophiolite and related rocks of the Snooks Arm Group, Newfoundland. Ph.D. Thesis, Memorial University of Newfoundland, St. John's, Newfoundland.

Upadhyday and Strong. (1973). Geologic setting of the Betts Cove copper deposits, Newfoundland: an example of ophiolite sulfide mineralization. Economic Geology, **68**: 161-167.

Van der Voo, R. (2001). Reliability of Palaeozoic palaeomagnetic poles and APWP of Gondwanaland. Tectonophysics, **184**: 87-100.

van Staal, C.R., Whalen, J.B., McNicoll, V.J., Pehrsson, S., Lissenberg, C.J., Zagorevski, A., van Breemen, O., Jenner, G.A. (2007). The Notre Dame arc and the Taconic orogeny in Newfoundland. Frame work of Continental Crust: The Geological Society of America, Memoir 200, pp. 511-552.

Williams, H. (1979). The Appalachians Orogen in Canada. Canadian Journal of Earth Sciences, **16**: 792-807.

Zagorevski, A., van Staal, C.R., McNicoll, V.J. (2007). Distinct Taconic, Salinic, and Acadian deformation along the Iapetus suture zone, Newfoundland Appalachians. Canada Jour. Earth Sci, **44**: 1567-1585.

Chapter Three

Density measurements on bore core with a portable gamma-gamma logging tool

B. Spicer[1], B. Morris[1], H. Ugalde[1], and N. Rogers[2]

1. MAGGIC, School of Geography & Earth Sciences, McMaster University, 1280 Main Street W., Hamilton, ON L8S 4K1. Canada
2. Geological Survey of Canada, 615 Booth Street, Ottawa, ON, K1A 0E9, Canada

Abstract

A portable gamma-gamma logging tool initially intended for industrial purposes has been modified for operation within the realm of hard-rock geology. Exploiting the principles of gamma attenuation, rapid density measurements of bore-hole drillcore is possible. Calibration of the density tool is achieved using a suite of metal alloy standards ranging in density from 2.52-3.48 g/cm^3. Taking a one-to- one measurement approach each value obtained by the logging tool has been supplemented with a standard SG density value. A second empirical calibration has been devised based on a linear correlation between the two density values. Deviations from densities reported by the separate methods can be explained in terms of core diameter variations. The system has been applied within ocean-floor and island-arc volcanics of the Pacquet Harbour Group on the Baie Verte Peninsula, Newfoundland. Upon reductions, results reported by the LB444 device obtain a one-to-one correlation with values of the SG method within +/- 0.2 g/cm^3.

Introduction

Estimation of the bulk density of rocks and sediments using Gamma Ray Attenuation (GRA) has been used mainly by oil companies since the mid 1960's (Evans 1965). The bulk density of any rock is controlled by the mineral composition and packing of the individual grains that form the lithology (Daly 1935). Since sedimentary rocks exhibit little compositional variation the primary interest in developing the GRA based density method was as a means for rapidly estimating the spatial variation of porosity (Evans 1965). GRA is commonly measured with one gamma source and one gamma detector; hence the term gamma-gamma is often applied in describing this array. Gamma – gamma density measurements acquired by a borehole logging tool have now become standard practice in the oil exploration industry. Within a borehole, the gamma – gamma probe comprises a radioactive source with known energy output and two, or more detectors at fixed distances from the source. With the probe held against the borehole wall energy from the radioactive source must interact with the surrounding bore wall in passing to the detectors (Faul and Tittle 1951). An estimate of sediment porosity (density) is derived from the ratio of known gamma radiation activity at the source to the observed value at the detector.

In hard rock geology bulk density measurements have been used primarily to discriminate between lithologies (Killeen et al. 1997, MacMahon 2003). However, recent advances in the development of potential field inversion modeling (Li and Oldenburg 1996, 1998) has established an increased demand for physical property measurements which in-turn are used to validate model outputs, or help provide geological constraints for model inputs (Williams 2008). While there are a number of instruments available for making rapid magnetic susceptibility measurements on core samples, there are few tools capable of providing equivalent density information. With the increased availability of airborne gravity surveys, having access to more density information entails that any inversion models derived from such data will have a higher probability of more accurately reflecting the true subsurface geology. In this study we look at a possible method for increasing the availability of useful density information.

Physical property measurements can be acquired either by a down-hole logging system, or by direct measurement on core retrieved from the borehole. The use of a down-hole logging system is advantageous when performing measurements on sediments, as measurement of the physical properties in-situ is almost certainly a better representation of the true value. However, most rock density measurement systems involve a radioactive source which is a concern for transportation and when used in an open-hole environment. In the event that a probe is lost or non-retrievable, depending on local regulations the probe must either be recovered, or the entire hole must be sealed closed. This is a costly as well as time consuming dilemma. Because of such issues, the development of gamma – gamma density devices for logging sediment cores has become more common. This system, now simply known by the acronym GRAPE, has been successfully implemented on many legs of the Ocean Drilling Program (Rutledge *et al.* 1995, Gunn and Best 1998). Devices used to implement the GRA method range from a wide array of multifunctional marine sediment core loggers (MSCL) produced by GEOTEK Ltd. to standalone gamma core sampling systems (Maucec and Denijs 2009). Ideally for the practical application in a mineral exploration setting the gamma-gamma tool should be fully portable with minimal shipping restrictions (Vatandoost et al. 2008).

This study examines the possibility of using a Berthold Technologies LB 444 Density Meter for hard rock core density logging. Like other gamma devices the LB 444 derives density estimates from the attenuation of gamma radiation passing through the substance of interest. Originally intended as an industrial tool designed for the measurement of liquids, suspensions and pulps, the LB 444 has been utilized in this study to obtain density measurements on borehole drill core. Herein we report some preliminary results obtained using this sensor and discuss some of the issues involved in deriving meaningful density values.

Principle of Operation

Gamma – Gamma based density measurements are in essence provided through the ratio between attenuated to source level radiation. There are several factors involved in the attenuation of the primary radiation energy which revolves around the electron density of the material being measured. The transmission of gamma energy is related to electron density by the equation (Blum 1997):

$$I = I_0 * e^{-nsd} \qquad (1)$$

In this equation *I* is the measured radiation flux in counts per second (cps) after passing through the material of interest, while I_0 is the original source radiation flux. The electron density *n* is understood as the number of scatters per unit volume and *d* is the thickness of the material through which the gamma ray passes. The Compton cross sectional area, *s, is* a term describing the amount of energy scatter and is measured in square centimeters per electron. It has been noted that bulk density *p* is related to electron density *n* by (Blum 1997):

$$n = pN_{Av}\left(\frac{Z}{A}\right) \qquad (2)$$

From this we see that the electron density is a function based on Avogadro's number N_{Av}, bulk density *p*, and the ratio between the atomic number *Z*, and the atomic mass *A*, of any given material. In order to determine bulk density using gamma ray attenuation we must have a consistent ratio between the atomic number and mass of our material.

The more common approach to address GRA however is through consideration of the mass attenuation coefficient μ, which is a value that represents the ability of a material to absorb photon energy. This number is associated with the interaction between the photons of applied radiation with electrons of the atoms comprising the materials subject to the transient gamma energy. The mass attenuation coefficient can be described as:

$$\mu = \left(\frac{Z}{A}\right) N_{Av} * s \qquad (3)\ (\text{Blum 1997})$$

Where Z, A and s are the same as in equations 1 and 2. Depending on the energy level of the radiation source, processes which contribute to the mass attenuation coefficient include Compton and elastic scattering or also the atomic photoelectric effect (Wiedenbeck 1962). With Compton (incoherent) scattering the energy of the incoming photons is dispersed as it interacts with individual atomic electrons, resulting in a significant decline in gamma energy. Elastic (coherent) scattering on the other hand does not impede the photons to such a degree as the energy is withdrawn by the entire atom. With the photoelectric effect all of the incoming photon energy is absorbed by the electron. In this instance incoming energy of a photon is used to break the electron from its bond to an atom. Excess energy is input and then carried away in the electron (Hubbell 2006). The process proceeding is reliant on source radiation levels and the response characteristics of the specific mineral phase. When dealing with medium-energy gamma rays (0.1-1MeV) the primary mode of photon-electron interaction for most elements will be in the form of Compton scattering (Blum 1997). With higher density elements the effect of Compton scattering is reduced (Mwenifumbo et al. 2005). Re-arranging the equations above we see that GRA can be redefined in the more commonly expressed form as:

$$I = I_0 * e^{-p\mu d} \qquad (4)\ (\text{Rutledge } et\ al.\ 1995)$$

This can then be manipulated to isolate for bulk density:

$$p = \frac{1}{\mu d}\ln\left(\frac{I_0}{I}\right) \qquad (5)\ (\text{Rutledge } et\ al.\ 1995)$$

The re-arranged equation above illustrates the effect of two factors in determining bulk density with a gamma – gamma device. Firstly, the degree of signal attenuation varies as a function of the thickness of the material, *d*. By measuring gamma transmission through a number of samples of the same material with varying thickness it is possible to derive an estimate of the material specific Z/A ratio.

The second factor, the absorption coefficient is dependent on both the material and the attenuation process at the energy level of the radioactive source. The mass attenuation coefficient has been well documented for many elements. Using data from the National Institute of Standard Technologies (Hubbell and Seltzer 1996) online data repository website supports Blum's (1997) suggestion that variations in Z/A ratios of many common rocks forming minerals are negligible (Table 1). When the primary mineral in a rock is a silicate or carbonate, as in most sedimentary units, the Z/A ratio will be constant. Applying the same methodology to the wider range of rock types found in a mineral exploration setting could introduce some variability in the Z/A ratio. For example, in rocks with higher potassic, or sodic feldspar content (granites, granophyres) or higher ferromagnesian mineral content (basalts, gabbros) the Z/A ratio will be less than 0.5 (Table 1). Including only the main rock forming elements (carbon to iron, Table 1) produces a poorly defined least squares line fit between density and Z/A ratio with a R^2 value of 0.6183 (Fig. 1). Including other elements which might form mineral deposits in this compilation results in a least squares line fit with similar parameters and a slightly improved R^2 value of 0.6658 (Fig. 1). Noticeable exceptions to this relationship are the two elements barium and lead which plot well below the best fit line. Removing these points from the plot produces a line of best fit with a R^2 of 0.9048. Examining the relationship between attenuation coefficient μ, and density p, reveals a similar, yet inverse relationship. In this instance the main silicate rock forming elements define a near perfect linear relationship with R^2 being 0.9992 while inclusion of ore forming minerals produces a weakened relationship with a decreased R^2 value of 0.9256 (Fig. 2).

All rocks are mixtures of the elements listed in Table 1 with the relative concentration of elements varying from lithology to lithology. While mass attenuation coefficients have been established for most elements, μ values for composite materials such as rocks and minerals has been addressed by few. Han *et al.* (2009) have established theoretical and experimental μ values for several quartz and orthoclase matrices, gypsum, pyrite and pyroxene measured at photon energies of 22.1, 25.0, 59.5 and 88.0 keV. While this study exploited primarily x-rays and weak gamma energies it confirmed that similar to their constituent elements, these minerals possessed decreasing μ values with increasing energy as well as lower μ values to that of the individual comprising elements. This is not the first analysis to show the mass attenuation coefficient to vary over a range of composite materials. Using a borehole gamma-gamma tool Mwenifumbo et al. (2005) demonstrated that there is a near linear relationship between core density and gamma ray attenuation for rocks with densities up to approximately 3.2 gm/cc. Core samples with densities greater than 3.6 gm/cc however, do not exhibit the same linear relationship between attenuation and density (Fig. 5 of Mwenifumbo et al. 2005,). For the purposes of this study we are focusing on silicate and carbonate rocks which have densities in the range 2.4 to 3.5 gm/cc for which there appears to be a near linear relationship between density and attenuation (Fig. 2).

Sensor configuration

The LB 444 operates on the basic physics of gamma attenuation described above. The measurements taken are in effect a ratio between the attenuated *I*, and source radiation value, I_0. The radiation energy implemented in this device is derived from a Cs-137 source. Cesium -137 is the most commonly used isotope employed for density measurements. This stems from the facts that in comparison to other gamma emitting isotopes such as Co-60, Cs-137 is a source is that has a relatively

	Density (p)	Atomic Number (Z)	Atomic Weight (A)	Z/A Ratio	µ/p Ratio	Absorption Coefficient µ
Carbon	2.26	6	12	0.5	0.8	0.18
Sodium	0.97	11	23	0.48	0.8	0.07
Magnesium	1.74	12	24.3	0.49	0.8	0.14
Aluminum	2.7	13	27	0.48	0.8	0.21
Silicon	2.33	14	28.1	0.5	0.8	0.19
Sulfur	2.07	16	32.1	0.5	0.8	0.17
Potassium	0.86	19	39.1	0.49	0.8	0.07
Calcium	1.55	20	40.1	0.5	0.8	0.13
Manganese	7.43	25	54.9	0.46	0.8	0.56
Iron	7.87	26	55.8	0.47	0.8	0.61
Nickel	8.9	28	58.7	0.48	0.8	0.71
Copper	8.96	29	63.5	0.46	0.8	0.68
Zinc	7.13	30	65.4	0.46	0.8	0.55
Siler	10.5	47	107.9	0.44	0.8	0.86
Barium	3.59	56	137.3	0.41	0.8	0.3
Gold	19.32	79	197	0.4	0.12	2.3
Lead	11.35	82	207.2	0.4	0.13	1.42
Uranium	18.95	92	238.3	0.39	0.15	2.82

Table 3- 1 - Physical properties of common rock and ore forming elements. Mass attenuation coefficient's used in calculations have been presented as experimentally determined at an energy level of 600 keV. LB444 operates at 662 KeV.

low energy output (662 keV) requiring lower shielding costs. The physical half-life for ^{137}Cs is 30.22 years and a heavy lead shielding of at least 0.65cm is required for safety.

The LB444 is composed primarily of two components, a shielded ^{137}Cs source and a scintillation counter implemented as a detector. The shield used to contain the ^{137}Cs has a cast iron outer shell lined with an inner shell of lead. Gamma radiation is released through an exit port blocked by a lead filled shutter. The shutter is connected to handle outside of the casing via a secure lead-lined shaft. The lead cup comprising the shutter has a hole in one site. Moving the outside handle into the specified position exposes the ^{137}Cs to this hole, releasing the gamma radiation.

When closed, the source emits radiation at a rate of 0.1 micro Siemens per hour (μSv/h); however, behind an external lead shield the operator is exposed to only 0.01μSv/h. Upon its opening the level of radiation an operator is exposed to remains relatively low at 0.3μSv/h. As incoming gamma energy is introduced to the scintillation counter, ionizing radiation produces a series of florescence within NaI crystals. An electronic amplifier connected to a photomultiplier tube converts this fluorescence into a series of electrical signals. The count rate supplied by a scintillation counter is proportional to the radiation intensity it receives. Automatic drift compensation corrects for temperature and aging effects in order to ensure quality measurements.

In Canada the annual radiation dose limits for people working with or around radioactive substances have been outlined under the Nuclear Safety and Control Act. For an individual falling into the category of 'non-nuclear energy worker' a radiation dose limit of 1mSv per year is permitted (Canadian Nuclear Safety Commission 2009). However after an individual has qualified as a 'nuclear energy worker' they may be subject to 50mSv in one year or as much as 100mSv over five years.

Density Standards / Calibration

The LB444 measures total gamma counts. To convert from counts to density requires a calibration curve for which one must have density standards. To ensure a consistent thickness of the absorbing material (see above equation 5) the standards should all have the same dimensions. The ODP approach to sensor calibration used a cylindrical aluminum rod having an incrementally increasing diameter central hole that was filled with water. With this arrangement varying density levels were created by different proportions of water and aluminum (Blum 1997, Best and Gunn 1999). This type of set-up is ideal for the ODP style cores where the sediments contain significant water content. The value of μ for water is approximately 10% less than that of quartz (Blum 1997). After this calibration tool was introduced ODP reported a revision of the density calibration curve for their Grape logging system.

A water filled standard is not appropriate for hard rock drill core logging since in most cases the cores are dry when they are measured, or have very low porosity levels. For the purpose of this work standards were crafted from a series of plastics and aluminum, copper, magnesium and silicon alloys. The plastics were needed to produce the lower end constraints of the calibration curve. The use of plastics for lower end member constraints is essential as lower density elements such as magnesium (1.738g/cm^3) and silicon (2.33g/cm^3) are easily oxidized when melted. These materials can only be used sparingly to alter the densities of materials such as aluminum (2.70g/cm^3) and copper (8.96g/cm^3) which were the two primary elements used to craft the density standards. The metal alloys were cast with the aid of the McMaster Light Metal Casting Research Centre. Working with a variety of Al, Cu, Si and Mg alloys, 10 metal standards were crafted. For rocks currently under investigation we targeted ophiolite/ocean-floor volcanics, which have densities in the range 2.6 to 3.2 g/cm^3. We constructed

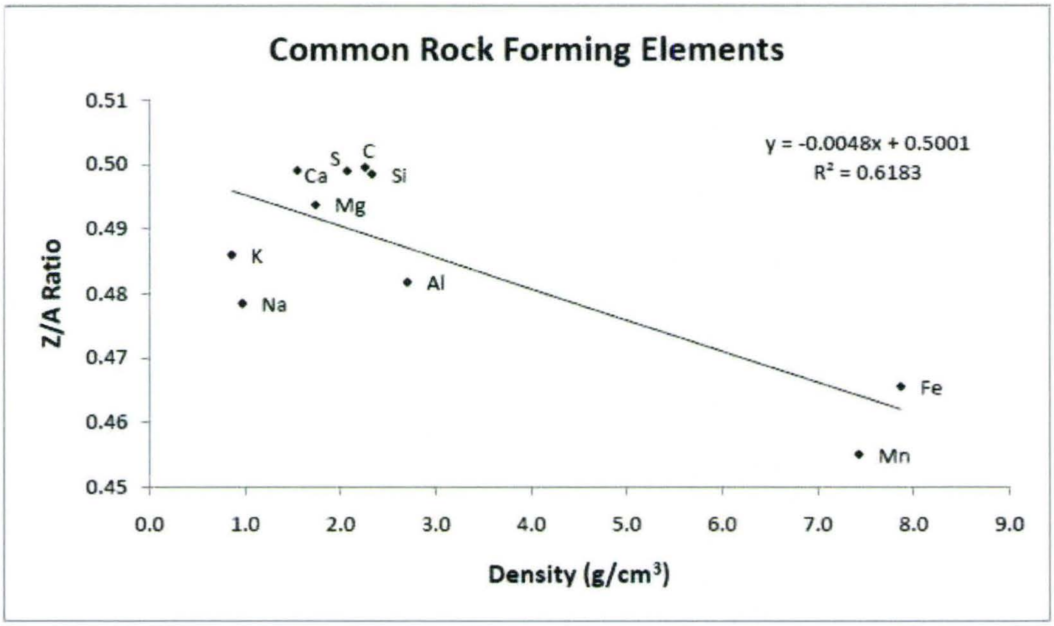
Common Rock Forming Elements
y = -0.0048x + 0.5001
R² = 0.6183
Z/A Ratio
Density (g/cm³)
0.51
0.50
0.49
0.48
0.47
0.46
0.45
0.0
1.0
2.0
3.0
4.0
5.0
6.0
7.0
8.0
9.0
Ca
S
C
Si
Mg
K
Na
Al
Fe
Mn

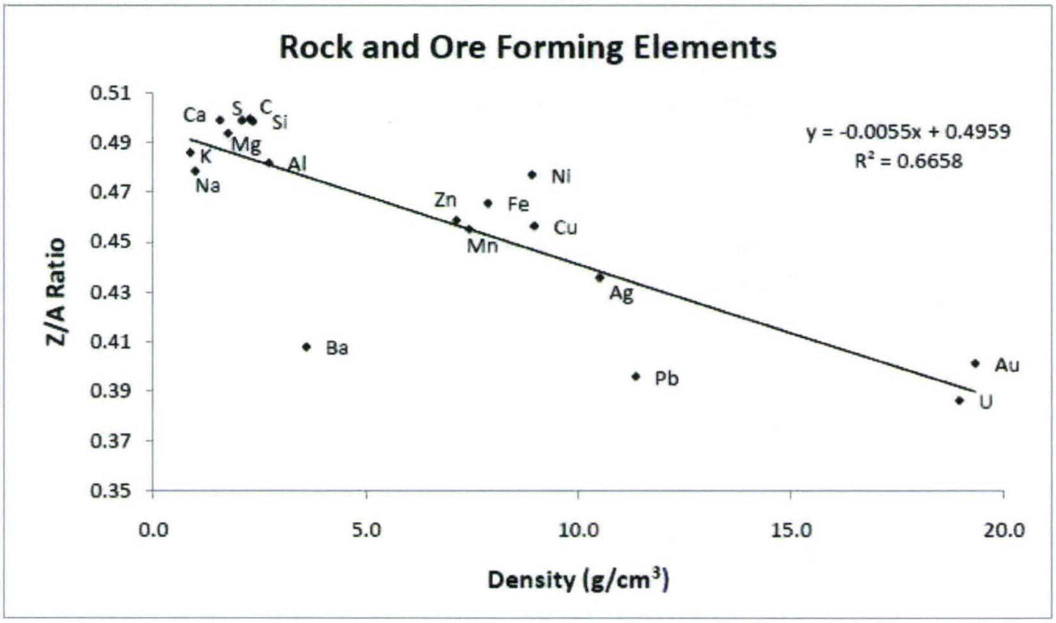
Rock and Ore Forming Elements
y = -0.0055x + 0.4959
R² = 0.6658
Z/A Ratio
Density (g/cm³)
0.51
0.49
0.47
0.45
0.43
0.41
0.39
0.37
0.35
0.0
5.0
10.0
15.0
20.0
Ca
S
C
Si
Mg
K
Na
Al
Zn
Fe
Ni
Cu
Mn
Ag
Ba
Pb
Au
U

Figure 3-1 - Ratio of atomic mass to atomic number for common rock and ore forming elements plotted against density. A relatively linear relationship can be observed for most common rock and ore forming elements. Barium and Lead appear as an exception to this trend.

standards with densities ranging from 2.52 g/cm^3 to 3.48g/cm^3. All of the 10 standards were constructed with the same dimensions of 5cm diameter and 10cm long. The 5cm diameter was chosen to be compatible with NQ sized bore-core.

The LB444 tool contains a built-in facility for generating a calibration curve from input value pairs (count rate and density). A number of possible curve fitting functions (one-point, linear, square or cubic) are provided. More calibration points will provide better constraint on the calibration curve. The quality of the calibration curve can be assessed via the least squares error. The lower this value the better the curve fit and thus the more accurate measured values will be. An ideal error of zero would indicate an exact correlation between the input and output parameters. The standard error for the calibration curve produced using the density standards above varies depending on which points are used and which curve fitting function is selected. Using a least square fitting with all of the standards produces a poor curve reflected by a square error of 0.022. However, using only the standards from 2.52g/cm^3 to 2.79g/cm^3, a third order polynomial yields a least squares error of 0.009. While quicker measurements correspond to increased efficiency, to obtain this level of accuracy each sample is averaged over a period of 20 seconds. This is still much faster and more efficient than traditional standard gravity based measurements.

The internal calibration procedure makes no direct assumption regarding uniformity of the mass attenuation coefficient between the ten reference standards. As demonstrated above we know that the degree of signal attenuation will vary as a function of the mineralogy and hence density of the rock unit. In this study we employ a simple empirical approach to overcome this problem by applying a second calibration correction. To derive the parameters of this correction formula we measured the density of core sections for one borehole. The first density estimate was found using the standard Archimedes Principle approach of weighing the sample suspended in air and then suspended in water. The second method uses the apparent density reported by the LB444 which are density values based on the calibration scheme linked to the reference samples. Knowing the actual density and an estimate of the density provided by the LB444 data it should be possible to derive a correlation that defines the relationship between the two density estimates. Using this correlation as a correction we can transform LB444 measured densities to AP equivalent densities.

The second empirical density calibration procedure hypothesized that a simple linear correlation exists between the SG density values and the LB444 reference density values. The parameters of the linear relationship were determined by iteratively seeking minimum values for both the L1 and L2 norms. In this instance the L1 norm represents the difference between the SG and the LB444 density values, while the L2 norm is the square root of the difference of the two density values squared (Table 2). An initial cross-plot of the two density estimates suggests that a linear correlation might be valid but the data are somewhat scattered (Fig. 3). Each of the density measurements is noisy. In this type of situation points furthest from the best fit correlation line can have a large influence on the computed norms. To minimize the effect of these points we applied an iterative correlation approach designed to identify and remove the most deviant points. The procedure involved varying the offset and gain of the correlation calibration until minima for the L2 and L1 norms were found. The next step involved identifying the points most deviant from the best fit line. This was achieved by producing a simple line plot of the difference between the SG density and the corrected density value. After sorting the difference values in increasing value, a least squares line fit to these data served to define the outliers (Fig. 4). Next the correlation calibration was recalculated upon deletion of the outliers identified. This

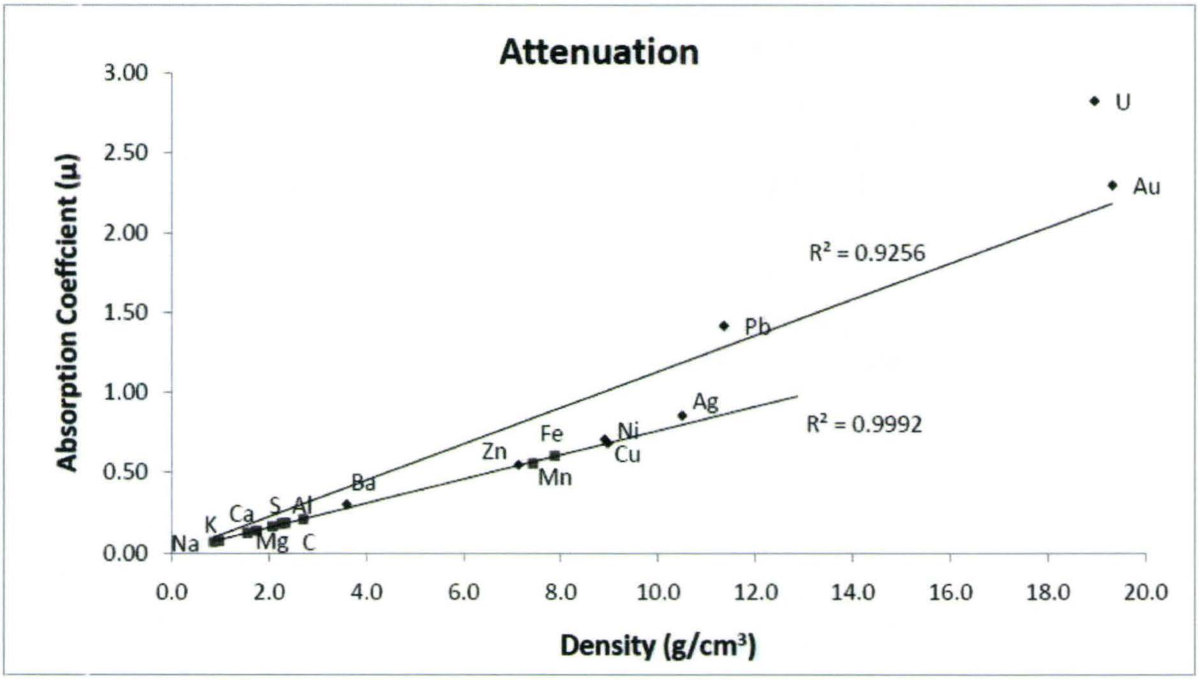
Attenuation
3.00
2.50
2.00
1.50
1.00
0.50
0.00
Absorption Coeffcient (µ)
U
Au
$R^2 = 0.9256$
Pb
Ag
$R^2 = 0.9992$
Ni
Cu
Fe
Zn
Mn
Ba
K
Ca
S
Al
Na
Mg
C
0.0
2.0
4.0
6.0
8.0
10.0
12.0
14.0
16.0
18.0
20.0
Density (g/cm³)

Figure 3-2 - Relationship between the mass attenuation coefficient and density of common rock and ore forming elements. A linear relationship is observed with the rock forming elements (grey squares). Inclusion of ore elements (black diamonds) reduces this trend. The primary elements responsible for this include: gold, uranium and lead.

Hole	Core	Gain	Offfset
MW-89-48	NQ	0.47	1.56
MZ 88-25	BQ	0.22	2.35
HB-88-12	BQ	0.22	2.35
RN-90-6	BQ	0.21	2.25
Average BQ		0.213	2.317

Table 3-2 - Gain and offset values obtained for each core based on empirical minima for the L2 and L1 norms.

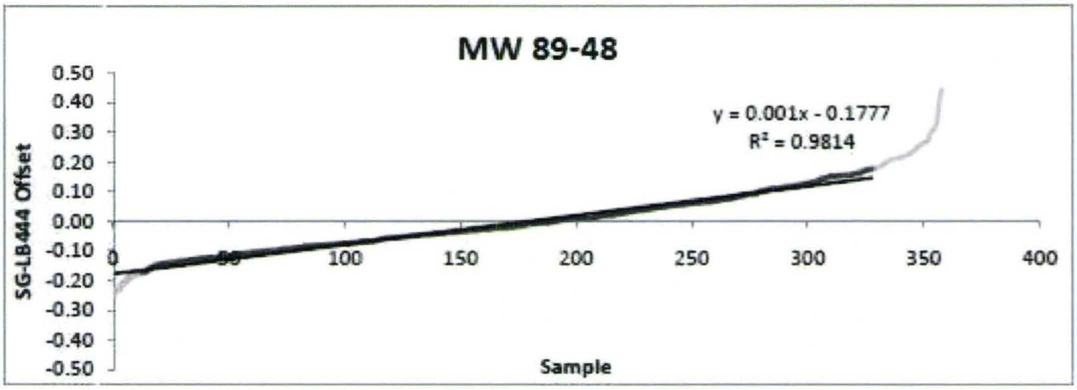
MW 89-48
SG-LB444 Offset
Sample
y = 0.001x - 0.1777
R² = 0.9814

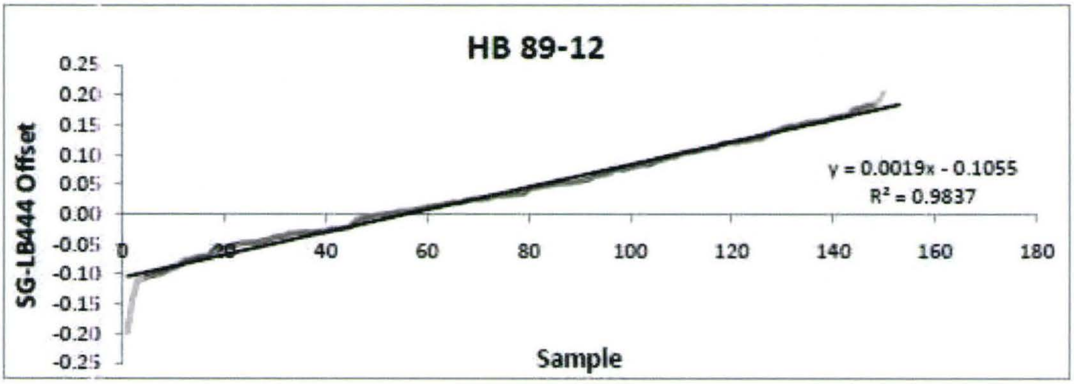
HB 89-12
SG-LB444 Offset
Sample
y = 0.0019x - 0.1055
R² = 0.9837

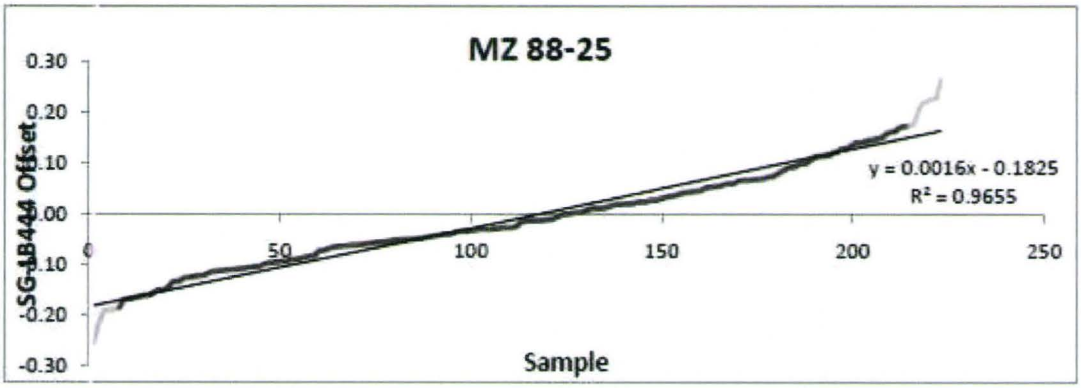
MZ 88-25
SG-LB444 Offset
Sample
y = 0.0016x - 0.1825
R² = 0.9655

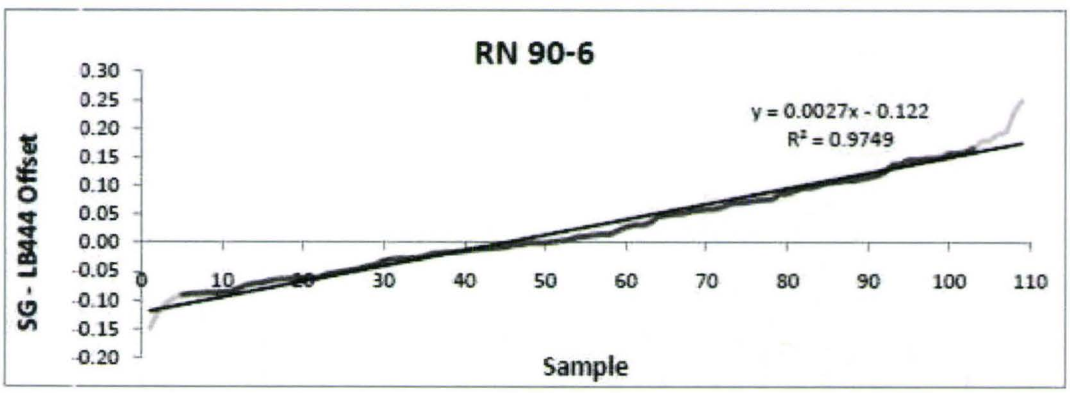
RN 90-6
SG - LB444 Offset
Sample
y = 0.0027x - 0.122
R² = 0.9749

Figure 3-4 - Difference in density measurements between SG and LB444 methods upon empirical calibration. A linear relationship is defined throughout. Outliers were removed based on their correlation with a least squares line of best fit (black). Acceptable data is displayed as dark grey while the light grey tails represent the removed outliers. These outliers may represent SG samples locations not directly coinciding with LB444 beam location or incidents where core diameters varied.

procedure was repeated until all deviant points were removed and there was no change in the value of the parameters of the calibration correlation. In most instances this required at most three iteration steps and over 95% of the original data points were retained (Fig. 5).

Results

Core examined in this study are from the Rambler Mine located in Baie Verte, Newfoundland. The Rambler Mine is an early Paleozoic volcanogenic massive sulphide deposit, with the mineralization being related to ocean floor volcanism. The strata sampled are from the Upper Pacquet Harbor Group which comprises primarily mixed mafic and felsic volcanics and lapilli tuffs/flows, tuff/flow breccias, quartz +/- chlorite sericite schist's and a late gabbroic intrusive suite. Core from four boreholes was logged using the standard SG method and the LB444 instrument. Average distance between observation points was 1.5m but varied from 0.8m up to 5m. The same section of core was measured with both methods. None of the density values were made on any sections of sulphide rich core. Density values ranged between 2.5 and 3.5 gm/cc. Three of the holes, HB 89-12, MZ 88-25 and RN 90-06 are BQ holes with the resulting core having an average diameter of 3.5cm. The fourth hole, MW 89-48 is a NQ hole giving cores with an average diameter of 5.2cm.

An estimate of the optimum correlation calibration was independently computed for each of the four cores. As shown in Table 2 the parameters of the calibration correction for the three BQ cores are very similar but quite different from the NQ core. The gain correction for the NQ core is greater than for the BQ core. This is appropriate since the cross-sectional area of the NQ core is 2.21 times that of the BQ core. The calibration gain for the NQ core is approximately 2.29 times that of the BQ core.

Bore Hole MW 89-48 was the longest core sampled in this study. An initial comparison between the LB444 density values and the SG density values reveals a number of interesting features. The variance of the LB444 apparent density is significantly higher than that shown by the SG density values. From the cross-plot of the two density values (Fig. 3) a broad linear correlation exists, but there is a significant amount of dispersion about a best fit line. Comparing the difference between the two density estimates versus the LB444 apparent density value reveals a linear relationship (Fig. 4). The two methods agree for density value of 3.00 gm/cc. Applying a calibration correction using the method outlined above leads to a reduction in the variance of the LB444 density values. The corrected LB444 density log has many similarities but is not identical to that measured using the SG method (Fig. 6). Locally the SG method gives a density value greater, or lower than the corrected LB444 method (Fig. 4). A cross-plot of the corrected LB444 density and the SG density now shows a near 1:1 (45 degree slope) relationship (Fig. 5). The fit is not ideal, there are still a number of points which show a larger than desired lateral spread.

The three BQ holes reveal a similar type of pattern. In all cases the variance of the raw LB444 density value is much larger than the density variance measured using the SG method (Fig. 3). It should be noted that the variance exhibited by the BQ core is significantly greater than for the NQ core. The gain relationship for these three BQ cores is the same, but the offset value appears to be slightly lower for core RN 90-6 (Table 2). This may be real or an artifact of a limited number of observations which have a wide dispersion. Applying a linear calibration correction to the LB444 density values produces a dramatic improvement in the similarity between the two density values (Fig. 5). Like MW 89-48 there are localized areas where the corrected LB444 density value is systematically above, or below the SG

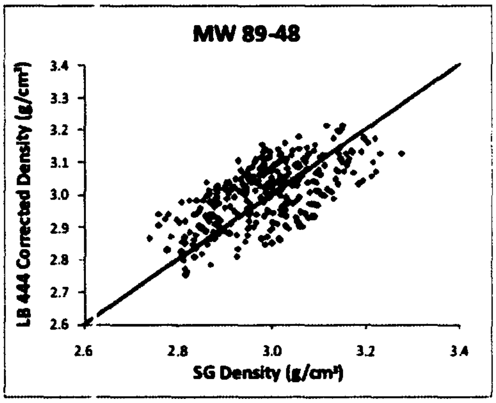
MW 89-48
LB 444 Corrected Density (g/cm^3)
3.4
3.3
3.2
3.1
3.0
2.9
2.8
2.7
2.6
2.6
2.8
3.0
3.2
3.4
SG Density (g/cm^3)

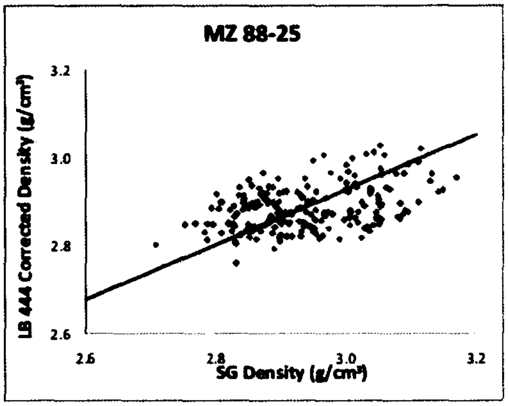
MZ 88-25
LB 444 Corrected Density (g/cm^3)
3.2
3.0
2.8
2.6
2.6
2.8
3.0
3.2
SG Density (g/cm^3)

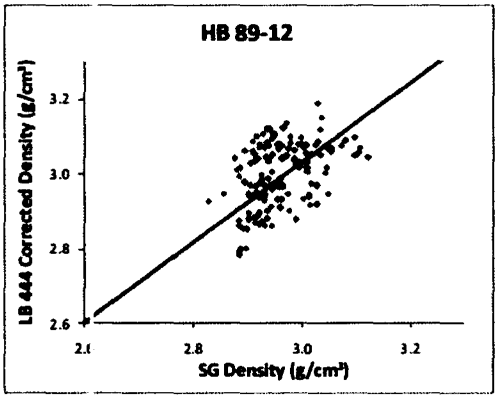
HB 89-12
LB 444 Corrected Density (g/cm^3)
3.2
3.0
2.8
2.6
2.8
3.0
3.2
SG Density (g/cm^3)

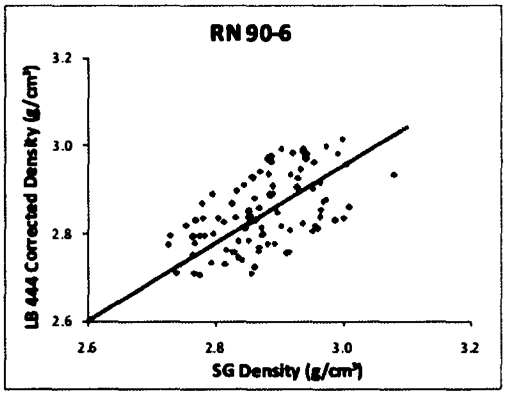
RN 90-6
LB 444 Corrected Density (g/cm^3)
3.2
3.0
2.8
2.6
2.6
2.8
3.0
3.2
SG Density (g/cm^3)

Figure 3-5- Cross-plot of density values obtained along core following empirical corrections and removal of outliers as defined by figure 4. Lines of best are now approaching 45 degrees for all cores, impending towards a one to one relationship.

density value (Fig. 5). In this instance, cross-plots of the corrected LB444 density value versus the SG density value show a well-defined 1:1 linear relationship.

Geologically these intersect a range of rock types (Fig. 6). The initial sampling was made at an average interval of 1.5m. The raw SG density plots show a lot of signal variation some of which is certainly associated with inaccurate measurements. Rutledge et al., (1995) smoothed their density logs with a 29 point running average to improve legibility of the plots. Based on our sampling rate, we chose to use a 7 point polynomial filter (Savitzky and Golay 1964). In some instances it is possible to see density changes which directly correspond to lithological boundaries. The diorite units tend to have higher density values and correlate well with the density high peaks, while the lapilli tuffs have lower density and correlate to troughs (Fig 6).

Discussion

The gamma ray attenuation method provides an estimate of rock density on the basis of a measurement of gamma ray signal remaining after partial absorption of a rock sample located between the radioactive source and a gamma detector. As demonstrated above the gamma count rate and hence density value calculated is dependent upon two variables: the attenuation rate of the mineral matrix, and the diameter of the core. When applied in the Ocean Drilling Program setting both of these variables are relatively constant. There is little overall change in the mineralogy of the sediments; most are either silica, or carbonate sands and shales. And since the core is contained in a plastic sleeve the diameter of the core is fairly constant. In a hard rock mineral exploration setting there will be a much wider range of rock types. As each mineral is in fact composed of many different elements and each rock is an aggregate of those minerals it becomes apparent that difficulties associated with μ are unavoidable. Studies by Mwenifumbo et al. (2005) suggest that variations in attenuation coefficient do not impact calculated gamma density values until actual densities exceed 3.5gm/cm^3. For the purposes of this study initial calibration of the LB444 density tool was achieved using 10 metal standards whose varying composition produced a range of density values from 2.52 gm/cc to 3.48 gm/cm^3. By measuring specific gravity / density and LB444 apparent density on the same sequence of cores from the Pacquet Harbour Group it was possible to establish a simple second linear calibration correction. The parameters of this calibration are dependent on the diameter of the core. Independent calibration of the three BQ cores examined in this study yielded very similar response function. The resulting plot of LB444 density versus depth closely approximates the SG density values.

However, in all cases there is not complete agreement between the two logs. Many of the corrected density logs have sections of core where the LB444 density value is systematically above, or below the SG density value. While the additional correction calibration procedure attempts to minimize the effect of any global density variations it cannot address any density errors introduced by changes in core diameter. As noted above core diameter can have a direct impact of the computation of density. Taking a simple relationship where count rate is related to core diameter it is possible to compute the effective core diameter that might result in the observed difference between SG density and LB444 density. Down-hole profiles of core diameter were inverted based on the ratio of SG to LB444 density values (Fig. 7). A theoretical deviation from the true drill collar diameter was established based on this ratio. As demonstrated in figure 7, in an NQ core a deviation of as little as +/- 2mm from the true diameter of 35mm is all that is required to produce the observed range of error reported.

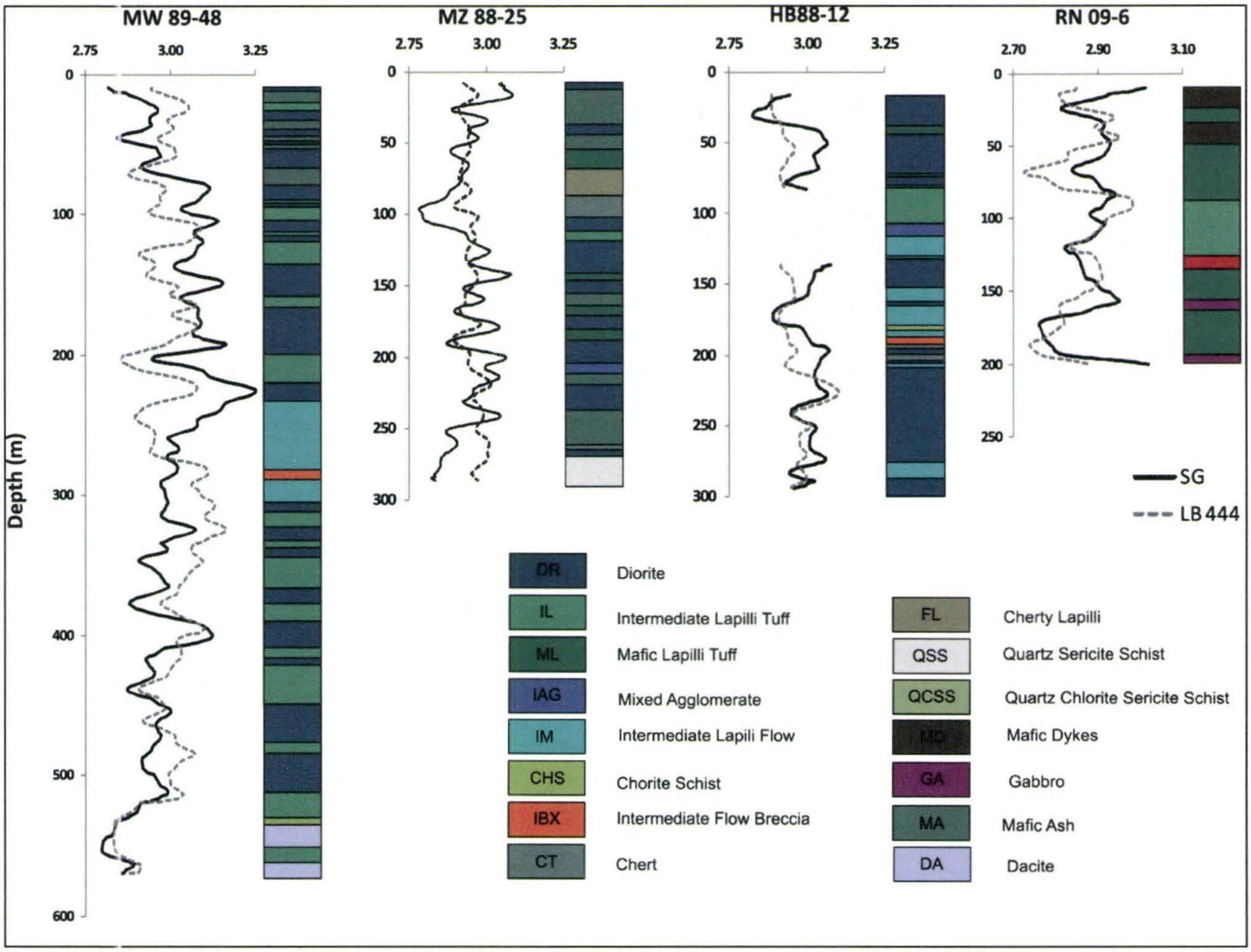
MW 89-48
MZ 88-25
HB88-12
RN 09-6
Depth (m)
SG
LB 444
DR Diorite
IL Intermediate Lapilli Tuff
ML Mafic Lapilli Tuff
IAG Mixed Agglomerate
IM Intermediate Lapili Flow
CHS Chorite Schist
IBX Intermediate Flow Breccia
CT Chert
FL Cherty Lapilli
QSS Quartz Sericite Schist
QCSS Quartz Chlorite Sericite Schist
MD Mafic Dykes
GA Gabbro
MA Mafic Ash
DA Dacite

Figure 3-6 - Density logs and corresponding geologic logs for each of the four holes. Density values from the SG (solid black) and corrected LB444 (dotted gray) have been plotted together. An exact replication of the SG values has not been achieved constantly however the LB444 does match the overall trend of the SG method in most logs.

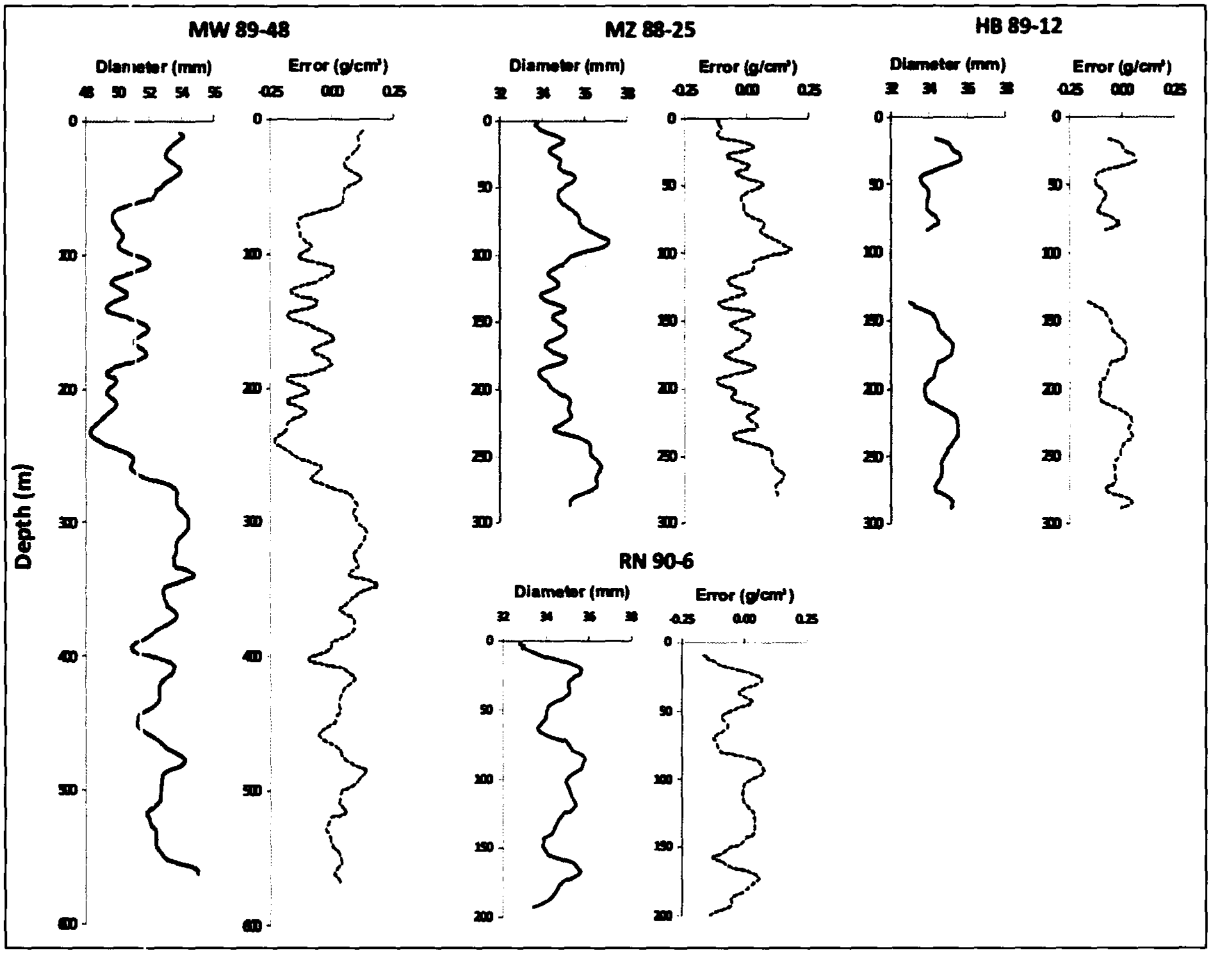
MW 89-48
MZ 88-25
HB 89-12
RN 90-6
Diameter (mm)
Error (g/cm³)
Depth (m)

Figure 3-7 - Differences reported in LB444 values to those of the SG method plotted alongside the hypothetical variations in core diameter. The curves are near identical as the error in this case has been attributed entirely to potential core size variations.

While the development of portable bore-core logging techniques appears to be fairly new there have been many advances in the use of borehole in situ gamma-gamma density logging tools. Both Tchen and Eisler (1992) and Mwenifumbo et al., (2005) advocate the use of spectral gamma-gamma logging methods. That is instead of recording just one energy window the detector records a complete energy spectrum derived from a mono-energetic source. Then by energy response in a number of different windows it is possible to obtain a gamma density estimate which is independent of variations in attenuation coefficient and core diameter variations.

Conclusions

Our initial intent was to find a portable tool which was capable of providing rapid density measurements on bore-core. Ideally we aimed for a tool which could be safely shipped to any core repository, or mineral exploration site. The LB444 was originally designed for measuring the density of sludge in a static set-up. Modification of the system to measure core involved nothing more than a simple track to move the core past the sensor. The system can be packed into a three packing cases and shipped as cargo within Canada.

Individual measurements using the LB444 require only 20 seconds per point. By simultaneously obtaining density values using the standard specific gravity method and the LB444 it is possible to derive a calibration correction. Applying this correction to the raw LB444 density values produces by the density estimates which are comparable to the SG density values. The computed LB444 density values do not fully agree with the SG density values some additional corrections need to be addressed. In future tests with this system we intend to measure the diameter of the core and look at the possibility of acquiring and then interpreting full spectral data.

References

Berthold Technologies, (2003). LB444 density Meter Manual, id no. 32816BA2, April 22nd

Best, A.I., and Gunn, D.E., (1999). Calibration of marine sediment core loggers for quantitative acoustic impedance studies. Marine Geology, 160, 137 – 146.

Blum, P., (1997). Physical Properties Handbook, Chapter 3: Gamma Ray Densiometry. P. 7.

Canadian Nuclear Safety Commission, Government of Canada. (2007). http://www.cnsc-ccsn.gc.ca/eng/lawsregs/index.cfm, July 9th, 2009.

Daly, R. A., (1935). Densities of rocks calculated from their chemical analyses. Proc. N.A.S. 21, 657 – 663.

Evans, H. B., (1965). GRAPE – a device for continuous determination of material density and porosity. Trans, SPWLA 6th Annu. Logging Symp. Dallas, 2:B1-B25

Faul, H., and Tittle, C. W., (1951).Logging of drillholes by the neutron, gamma method and gamma ray scattering. Geophysics, vol. 16, 260-276

GEOTEK, (2000). Documentation for GEOTEK Multi-Sensor Core Logger (MSCL). http://www.geotek.co.uk/ftp/manual.pdf, July 10th, 2009.

Gunn, D., and Best, A., (1998). A new automated nondestructive system for high resolution multi-sensor core logging of open sediment cores. Geo-Marine Letters, 18, 70 – 77.

Han, I., Demir, L., Sahin, M., (2009). Determination of mass attenuation coefficients, effective atomic and electron numbers for some natural minerals. Radiation Physics and Chemistry, 78, 760-764.

Hubbell, J.H., (2006). Review and history of photon cross section calculations. Physics in Medicine and Biology. 51, R245-R262

Hubbell, J.H. and Seltzer, S.M. (1996). Tables of x-ray mass attenuation coefficients and mass energy-absorption coefficients from 1 keV to 20 MeV for elements Z = 1 to 92 and 48 additional substances of dosimetric interest. Ionizing Radiation Division, Physics Labroratoy. National Institute of Standards and Technology. Accessed January 26, 2010. http://physics.nist.gov/PhysRefData/XrayMassCoef/cover.html.

Killeen, P.G., Elliot, B.E., Mwenifumbo, C.J., (1997). Towards prediction of geological drill core logs using geophysical logs in volcanic stratigraphy, Proceedings of the Symposium on the Application of Geophysics to Environmental and Engineering Problems, SAGEEP'97. P. 933-972.

Li, Y. and Oldenburg, D.W., (1996). 3-D inversion of magnetic data. Geophysics, v. 61, p. 394-408.

Li, Y. and Oldenburg, D.W., (1998).3-D inversion of gravity data. Geophysics, v. 63, p. 109-119.

MacMahon, S.E., (2003). Classification and prediction analysis of physical rock property data from downhole geophysical surveys. Ph.D. thesis, McMaster University, Hamilton.

Maucec, M., and Denijs, I., (2009). Development and calibration of a gamma-ray density-meter for sediment-like materials. Applied Radiation and Isotopes, doi: 101016/j.apradiso.2009.06.001.

Mwenifumbo, C.J., Salisbury, M., Elliott, B.E., and Pflug. K.A., (2005). Use of multi-channel Gamma-Gamma logs to improve the accuracy of log derived densities of massive sulfides. Petrophysics, 46(3), 346 – 353.

Rutledge, A. K., Roberts, J.A., Orsi, T.H., Bryant, W.R., Kotilainen, A.T., (1995). Geotechnical properties and consolidation characteristics of north Pacific sediments, sites 881, 883, and 885/886. Proceedings of the Ocean Drilling Programm Scientific Results. 145, 525-546.

Savitzky and Golay. (1964).Smoothing and differentiation of data by simplified least squares procedures. Anal. Chem. V.36 p.1627-1639

Tchen, T., and P.Eisler, (1992). Accurate borehole probe calibration. Exploration Geophysics, 23, 343-352.

Vatandoost, A., Fullagar, P., and Roach, M., (2008). Automated multi-sensor petrophysical core logging. Exploration Geophysics, 39, 181 – 188.

Wiedenbeck, M., (1962). Total X-Ray attenuation coefficients from 40 kev to 412 kev. Physical Review, 126, 1009-1010.

Williams, N., (2008). Geologically constrained UBC-GIF gravity and magnetic inversions with examples from the Agnew-Wiluna greenstone belt, Western Australia. Ph.D. thesis. The University of British Columbia, Vancouver.

Chapter Four

Structure of the Rambler Rhyolite, Baie Verte Peninsula, Newfoundland: Inversions Using UBC-GIF Grav3D and Mag 3D

B. Spicer, B. Morris, H. Ugalde

MAGGIC, School of Geography & Earth Sciences, McMaster University, 1280 Main Street W., Hamilton, ON L8S 4K1. Canada

Abstract

The Rambler rhyolite dome is hosted within the Pacquet Harbour Group (PHG) on the Baie Verte Peninsula of north-central Newfoundland. The lower PHG comprises a fragmented ophiolite including pillowed boninites and felsic volcanic rocks in the south and the larger Rambler rhyolite to the north. The Rambler rhyolite is a 487 Ma structure of felsic tuffs, flows and subvolcanic intrusive rocks. The upper footwall of the rhyolite dome hosts Cu +/- Au volcanogenic massive sulphide deposits (e.g. Rambler and Ming mines). The PHG is affected by multiple phases of deformation, two of which are well displayed in the Rambler area. The earliest phase, D_2, is associated with south-directed thrusting of the Rambler rhyolite onto its cover along the Rambler Brook fault, and thrusting of lower ophiolite crust onto the upper PHG along the Scrape thrust to the north. As a result of this deformation, the Rambler rhyolite and VMS mineralization plunge roughly 35 degrees to the northeast. Broad, northeast plunging upright cross folds (D_4) fold the Rambler rhyolite and its ore. The ore bodies lie in the hinge zone of an F_4 antiform. Geophysical inversions utilizing recently acquired high resolution gravity and magnetic data have been implemented to determine the extent of the dome at depth. A physical property database from drill-holes and surface maps of the Rambler property has been produced for use in reference model development. Employing University of British Columbia Geophysical Inversion Facility software, constrained inversions have been carried out depicting the Rambler rhyolite dome in 3D. The rhyolite is imaged dipping roughly 40 degrees to the northeast as a series of voxels with density values ranging from 2.71-2.75 g/cm^3. While current ore models parallel this structure in the near surface, results from these inversions suggest deeper exploration may be favorable. Magnetic inversion modeling has not provided any insight into dome morphology however outlines the distribution of gabbroic dykes surrounding the dome.

Introduction

The Rambler area, of the Baie Verte Peninsula, has a long history of mineral exploration (Figure 1), dating back to 1903 when local prospector Enos England first discovered the 'England Vein'. Although a low tonnage find, England vectored into the main deposit, eventually discovering the gold bearing 'Rambler Vein' in 1936 only 200m north of the 'England Vein'. The Rambler property would be further explored during the following decades revealing economic deposits of gold, silver, zinc and copper (Hibbard, 1983).

From 1964 to 1982 4,301,532 tonnes of massive sulphide was extracted from four separate deposits (Coates, 1991). The mine was re-opened briefly in the early 1990's but was halted when underground excavation reached a neighbouring property boundary. Recently the newly formed Rambler Metals PLC has gained mineral rights to the neighbouring property and extraction procedures are to begin once again.

The Rambler mineralization is associated with a felsic volcanic structure colloquially termed the Rambler rhyolite which forms part of the Pacquet Harbour Group (PHG) of the Dunnage Zone located on the Baie Verte Peninsula of northwestern Newfoundland. The PHG consists of mixed felsic and mafic volcanic and intrusive rocks that dip steeply to moderately to the north and northeast (Tuach and Kennedy 1978; Hibbard 1983). The PHG is petrographically and stratigraphically linked with the better exposed and less deformed Betts Cove Ophiolite Complex and its cover the Snooks Arm Group that occur on the eastern margin of the Baie Verte Peninsula. The structure of the Rambler rhyolite has been interpreted as an elongate body plunging moderately to the northeast (Tuach and Kennedy 1978; Skulski *et al.* 2008). The true shape and lateral extent of this feature remains unclear though, as poor outcrop combined with the complicated fold interference patterns and faulting in the area have hampered the development of reliable structural interpretations. Recent geophysical surveys, including a high resolution aeromagnetic and ground based gravity surveys have been implemented in order to better understand this important geological feature.

Inversions are applied to geophysical data in order to gain better insight into possible physical property distributions beneath the observation surface. For magnetic data this interpretation relates to magnetic susceptibility or ease of magnetization, whereas gravity inversions reveal information regarding density contrast. The ultimate goal of these inversions is to provide knowledge regarding the subsurface geology of the site. Although practiced since the early 1970's (Oldenburg, 1974) and available in several geophysical software packages, inversions have only recently become to be seen as offering a practical approach to addressing geologic problems through integration of geophysical datasets. Central to this recent adoption of inversion routines is the availability of a graphical user interface linked to a software inversion algorithm supplied by the University of British Columbia's Geophysical Inversion Facility (UBC-GIF). An extensive account on the background and implementation of this software has been produced by Williams (2008). In this study we report results derived using this software on gravity and magnetic grids that cover the spatial extent of the Rambler rhyolite. Results of the inversion process are compatible with prior geological knowledge of the mine property and provide some additional insight into the overall 3D geometry of the local geological structure. While other 3D inversion algorithms have been developed (Zeyen and Pous, 1993; Portniaguine and Zhdanov, 2002; Dias et al. 2009; Fergoso and Gallardo, 2009) the Li and Oldenburg (1996) *smooth and small* inversions are becoming common practice in the mineral exploration industry.

Geology

The Baie Verte Peninsula which plays host to the Rambler rhyolite is divided by a major northeast tending structural zone known as the Baie Verte Line (Figure 1). This tectonic feature juxtaposes continental metasedimentary rocks of the Humber Zone next to ocean-floor volcanic rocks of the Dunnage Zone. The PHG is one of several ophiolitic and arc sequences identified as an encompassing component of the Baie Verte Oceanic Tract (BVOT) of the Baie Verte Belt of the Dunnage Zone (van Staal et al. 2007). Details of the Dunnage Zone stratigraphy of the Baie Verte Peninsula are given in Skulski et al. (2010).

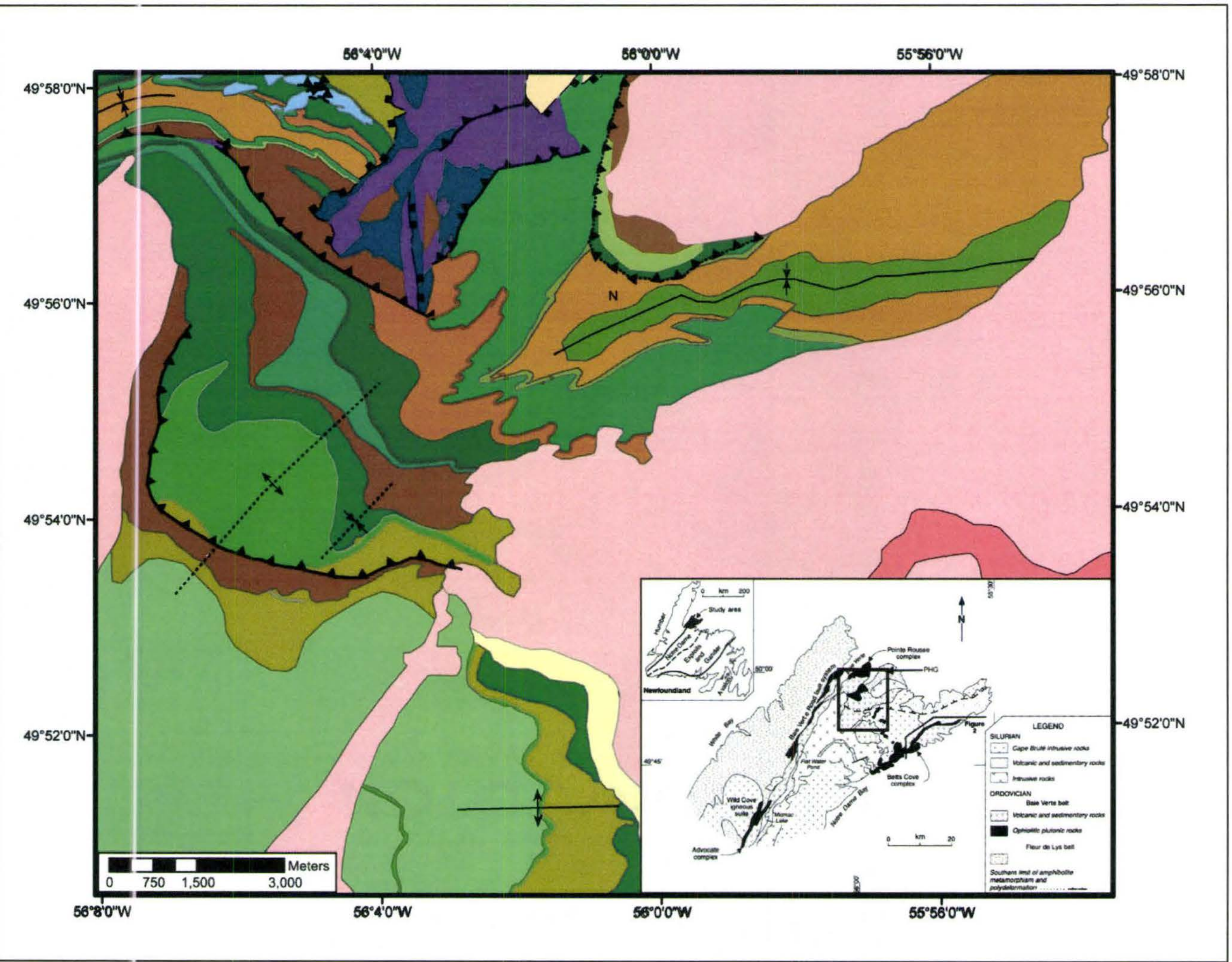
56°4'0"W
56°0'0"W
55°56'0"W
49°58'0"N
49°56'0"N
49°54'0"N
49°52'0"N
N
Meters
0 750 1,500 3,000
56°8'0"W
Study area
Humber
Notre Dame
Exploits
and
Gander
Avalon
Newfoundland
Pointe Rousse complex
PHG
Baie Verte Road fault system
White Bay
Flat Water Pond
Betts Cove complex
Figure 2
Notre Dame Bay
Wild Cove igneous suite
Advocate complex
LEGEND
SILURIAN
Cape Brulé intrusive rocks
Volcanic and sedimentary rocks
Intrusive rocks
ORDOVICIAN
Baie Verte belt
Volcanic and sedimentary rocks
Ophiolitic plutonic rocks
Fleur de Lys belt
Southern limit of amphibolite metamorphism and polydeformation

Figure 4-1 - Geologic Map of the Pacquet Harbour Group within the Baie Verte Peninsula of northwestern Newfoundland (modified from Skulski et al. 2010). Inset from Bédard et al. (2000.)

The Rambler rhyolite was described by Tuach and Kennedy (1978) as a series of silicic volcaniclastics comprised of dacitic, rhyolitic agglomerates with minor rhyolitic tuffs and/or flows. Minor occurrences of mafic tuffs and flows as well as chert and quartz-sericite schists are also present. The rhyolite hosts a series of significant past producing Cu (+/- Au) rich volcanogenic massive sulphide (VMS) deposits such as the Rambler and Ming Mines. Felsic volcanic rocks adjacent to this mineralization have been dated at c. 487 Ma (V. McNicoll, unpublished data, 2008; Skulski *et al.* 2010).

Since the early 1970's numerous authors (e.g., Church, 1971; Gale, 1971, 1973; Tuach, 1976) have attempted to develop a reliable stratigraphic succession for this area. Tuach and Kennedy (1978) produced a stratigraphic succession strictly for the Rambler area of the PHG. They suggested northward continuity within the northernmost units of the Group. This however was subject to much uncertainty as younging indicators were sparse in their study. The occurrence of medium and large scale isoclinal folds added to the confusion as no reliable marker units had been identified at this time. Hibbard (1983) noted extreme layer-parallel transposition suggesting a reliable stratigraphy may never be realized in this area. Piercey (1997) provides a stratigraphy in the southern PHG recognizing at least three phases of volcanic activity based on cross-cutting stratigraphic relationships, however his did not extend to the Rambler rhyolite.

More recent mapping and geological interpretation of the PHG has been presented by Skulski *et al.* (2010). This work suggests the morphology of the Rambler rhyolite comprises a regional syncline refolded by an open northwesterly trending synform. The syncline is open to the south where a lower sequence of submarine boninites and five distinct phases of felsic to intermediate pyroclastic flow deposits are mapped. Skulski *et al.* (2010) propose proximity of this portion of the PHG to a palaeovolcanic vent based on the occurrence of coarse tuff breccias, abundant felsics, a high concentration of gabbro dykes and the presence of hydrothermal alteration. These vent facies sequences are overlain by units of basalt, boninites, turbiditic wacke, siltstone and volcanogenic conglomerate and pyroclastic rocks. Skulski *et al.*(2008, 2010) have suggested the youngest of these units may be a correlative of the Snooks Arm Cover series observed at Betts Cove.

Tuach and Kennedy (1978) recognized at least four distinct phases of regional deformation within the PHG and adjacent Point Rousse Ophiolite Complex. The first phase (D1) consists of an L-S flattening fabric preserved between S2 surfaces. D1, which is thought to be related to obduction of the ophiolite sequence is either poorly preserved or strongly overprinted in the Rambler area (Castonguay et al. 2009). The second phase of deformation (D2), the main tectono-metamorphic event, is recorded by fabrics associated with several southward-directed reverse thrusts (Castonguay *et al.*, 2009). The Rambler rhyolite has been thrust above its cover along the Rambler Brook fault as a result of this southward force. To the north these thrust surfaces terminate on the Scrape Thrust. This thrust is a ductile shear zone that juxtaposes serpentinised mantle of the Point Rousse Group above basalts of the PHG (Hibbard, 1983; Castonguay *et al.* 2009). The intense penetrative D2 fabric also runs parallel to sub-parallel with the local primary layering (Tuach and Kennedy, 1978). To the north schistosity increases with an associated L-fabric. A northeasterly plunging lineation (±035º/35ºNE) is observed within pillows, clasts and minerals. Ore bodies within the PHG, which have all been influenced by D2 run parallel to the lineation while plunging to the northeast as a series of elongate ribbons (Tuach and Kennedy, 1978). D2 is thought to have arisen though crustal thickening and transpression associated with the Late Ordovician to Early Silurian (450-423 Ma) Salinic Orogeny (van Staal, *et al.*, 2007; Castonguay *et al.* 2009). The intensity of this second deformation event decreases towards the southern PHG.

One more main deformation event penetrates the vicinity of the the Rambler rhyolite. Overprinting D2, broad northeast plunging upright cross folds (F3 of Castonguay et al., 2009, F4 of Tuach and Kennedy, 1978) fold the Rambler rhyolite and associated ore. The ore bodies of the Ming Mine lie in the hinge zone to an F3 antiform while other past producing zones (e.g. Rambler Mine) occupied the hinge to an F3 synform along the same stratigraphic horizon(Skuski et al. 2010). A dextral transtensional stress regime has been interpreted for the northerly region of the PHG (Castonguay *et al.* 2009). Here recumbent and shallowly inclined folds terminate onto the Ming's Bight Group. These folds are believed to have been produced by the work of extensional shear zones and the reactivation and inversion of reverse faults. The Ming's Bight Group is a succession of metasedimentary rocks resembling assemblages observed within the Humber zone west of the Baie Verte Line. An anomalous feature surrounded by the mafic and ultramafic bodies of the Dunnage zone, the full nature of this outcropping body of rock has yet to be interpreted (Hibbard, 1983). The current interpretation however is that this is a structural window of continental basement rocks (Anderson 1998; Anderson et al., 2001).

Geological reconstructions of the Rambler property have been limited by extensive vegetative cover. Outcrop exposure estimates range from 0.5% to 5% for the entire property (Cook and Cochrane 2000). Adding to this problem, roughly 2 m of overburden blankets the greater part of the study site. As a result, the lateral extent of many geologic features including the Rambler structure remains unclear. It is because of these problems that the Rambler property has been identified as a suitable candidate for interpretation through geophysical inversion.

Inversions

Inversion is the process whereby a 3D spatial distribution model of physical property variations is derived from a suite of observed geophysical signatures. After applying a series of data corrections, anomalies observed by a gravity survey are imaged as density contrasts in the subsurface. The same logic applies for magnetic data whereby the physical property of interest is primarily controlled by magnetic susceptibility variations. The physical property distributions defined by potential field inversions are not necessarily directly equivalent to geological models since the inversions record density and susceptibility variations that do not necessarily correspond with lithological variations.

A fundamental issue linked with all gravity or magnetic inversions is imposed by the intrinsic non-uniqueness associated with geophysical signatures recorded by potential field data sets (Li and Oldenburg, 1996). An endless array of models, including an infinitely thin zone of density or susceptibility located immediately below the topographic surface, can satisfactorily explain an observed potential field anomaly to some predefined degree of mathematical tolerance. This implies that by themselves, gravity or magnetic data lack any inherent depth information (Li and Oldenburg, 1996). Another problem contributing to non-uniqueness is the fact that geophysical surveys are fragmental and may contain erroneous points. These issues beget the need for some form of constraint to be introduced into the inversion process (Bosch and McGaughey, 2001). Through the imposition of some constraints one aims to limit the derived model solutions to ones that are compatible with limited prior geological knowledge. Such constraints can range from surface geological mapping of a limited number of exposures to depth constraining boreholes with geologic and physical property logs. The most reliable results will come from inversions which are constrained by more information and greater confidence levels in the data. In this study density and susceptibility information from 17 boreholes was included to provide some subsurface constraint on the possible physical property variations in the resulting inversion model. Five of these boreholes were wedged off at depth splitting in as many as 20 different directions for a total of 85 drillholes (Fig 2). A 1:20,000 scaled geologic map produced by Skulski (2010, unpublished) provides the surface control (Fig 1). Additional lithologic boundary constraints were developed from geologic models constructed from borehole lithological observations.

In addition to the problem of non-uniqueness, there are two other issues that impede potential field inversions. These are the problems of instability and non-existence (Williams, 2008). Instability within an inversion refers to major changes in the output model that occur as a result of minor changes in data. This is an important matter to consider as data used within inversions has almost always undergone some form of reduction, leveling and/or filtering. For example, inversions of regions of high potential field gradient may be poorly constrained since different filters may modify the form of the anomaly. Although the inversion process will always provide a solution for the observed signal, the model describing the true subsurface may never actually be realized. This is the concept of non-existence (Williams, 2008). The reasoning behind this stems from the fact that the presence of noise within a dataset is unavoidable. Although correction routines are applied with the intent of removing this noise, a portion of it will always remain. Depending on the magnitude of the actual physical property contrast associated the source body it is quite possible that the inversion will find a source that is associated with the noise rather than real signal.

Within a conventional gravity survey we measure the vertical component of the gravity field. The anomalous field at any site may be the result of a buried object with density ρ. The gravity field, F_z, at the point, r_i, is defined as:

$$F_{z(r_i)} = \gamma \int_v \rho(\boldsymbol{r}) \frac{z-z_i}{|r-r_i|^3} dv \qquad \text{(Li and Oldenburg, 1998)}$$

Here ρ (r) is the distribution of anomalous mass and γ is Newton's gravitational constant. In a UBC-GIF model the study site is represented by a volume of voxels. The geological model is defined by having voxels with uniform density within a lithology and varying density between lithologies. In detail there will always be some limited variation within a lithology bound. The output signal of the inversion process involves computation of the summation of the individual gravity contribution of each voxel to the whole model volume. When performing an inversion within UBC-GIF software, there are two models to consider: a reference (input) model and a recovered (output) model.

The reference model is a generalized pre-inversion model created as a guideline, or constraint, which for areas where the physical properties are known will force these values to be carried through into the recovered model. The reference model is created manually and built using all geological and physical property information available at the time of modeling. The reference model should be updated continually as additional physical property measurements and geologic information become available. Termination of the inversion process and output of the recovered model occurs once the computation has satisfied some criterion defined by a preset model objective function.

The model objective function is the cornerstone of the UBC-GIF inversion process, responsible for each characteristic of the model. The primary purpose of the model objective function is to minimize the difference between the physical properties described within the input reference and output recovered models. The model objective function is made up of terms reflecting the *smallness* and *smoothness* of the desired output and is given as:

$$\begin{aligned}\Phi_{m(\rho)} = {} & \alpha_s \int_v w_s \{w(z)[\rho(\boldsymbol{r}) - \rho_0]\}^2 dv \\ & + \alpha_x \int_v w_x \left\{\frac{\partial(z)[\rho(\boldsymbol{r}) - \rho_0]}{\partial x}\right\}^2 dv \\ & + \alpha_y \int_v w_y \left\{\frac{\partial(z)[\rho(\boldsymbol{r}) - \rho_0]}{\partial y}\right\}^2 dv \quad \text{(Li and Oldenburg 1996)} \\ & + \alpha_z \int_v w_z \left\{\frac{\partial(z)[\rho(\boldsymbol{r}) - \rho_0]}{\partial z}\right\}^2 dv\end{aligned}$$

The first of the four components to this equation measures the smallness (difference) between the reference, m_{ref}, and the recovered model, m. The following three components control the smoothness of the model in x,y,z space. These are included in order to distribute differences between m and m_{ref} throughout the model equally and not simply to individual cells. These terms are all controlled via user input through the Alpha weighting functions α_s, for smallness and α_x, α_y, α_z, for smoothness. These drive the entire inversion within the Li and Oldenburg smooth and small models and can be manipulated to achieve the desired spatial and physical property bounds (Williams, 2008).

As mentioned earlier, potential field data contain no inherent depth information. The weighting function w_z is applied to address the problem of estimating the distribution of anomalous sources versus depth, maintaining a possibility for each cell to contain some source component (Williams, 2008). Without the use of this function, data is most easily solved by the mathematically viable yet geologically unlikely near surface plate (Li and Oldenburg, 1996, 1998). This is the situation where all contributing signal is calculated as the summation of a high density thin slab atop a large body of low density. There are two possible forms of the depth weighting function as supplied by Li and Oldenburg (1998). The true depth weighting function is used to take only the distance below the observation point into account.

$$w_r^2(z_j) = \frac{1}{(z_j+z_0)^\beta} \quad \text{(Williams, 2008)}$$

Here z is the depth to the jth cell. The parameter β is adjusted to best match the kernel's weighting function with depth. In most cases this will be proportional to the signal's exponential decay as a function of distance. For gravity $\beta = 2$ while for magnetics $\beta = 3$. A more robust form of the function should be implemented in situations where significant topography is present or when sporadic or sparse data exists. This function takes into account the lateral and vertical variations in the data. It is computed based on the sensitivity of the potential field data's physical property constraint (density or magnetic susceptibility) at a specific separation interval between source and observation point.

$$w_r^2(r_j) = \sqrt{\sum_{i=1}^{N}\left(\frac{1}{(R_{ij}+R_0)^\beta}\right)^2} \quad \text{(Williams, 2008)}$$

R_{ij} is the distance between cell i and cell j. R_0 is the small stabilizing constant equal to one-quarter the size of the smallest cell. This term ensures the distance weight will be constantly defined.

Data Reduction and Uncertainty

Before any meaningful information can be extracted from a geophysical dataset, proper processing and reduction routines must be applied. In the case of the gravity data used for this study standard processing steps were performed including instrument and tidal drift, latitude, free-air and Bouguer corrections. No terrain corrections were applied as no significant topographic gradients are encountered on the Rambler property. The gravity data set used in this inversion study was collected by the McMaster Applied Geophysics and Geographic Imaging Center (MAGGIC) of McMaster University using two Lacoste and Romberg Gravimeters. Because of the difficulty imposed by vegetation cover the gravity stations were collected in a grid pattern along cut-lines spaced 300 m apart. Positional information was obtained using a two sensor differential GPS set-up. The location of each observation point was computed using a post-processing approach. Additional improvements to the on base-station positions were provided by the Canadian Spatial Reference Systems Precise Point Positioning (CSRS-PPP). The CSRS-PPP is a federal service which provides enhanced positions for observation files using the most precise GPS orbit and clock information available in Canada. Implementing this system all elevation information is orthometrically corrected using the Canadian Geoid Vertical Datum (CGVD).

The magnetic data set was acquired using two cesium vapor magnetometers in a transverse horizontal gradient configuration. Flightlines were spaced 100 m apart along an east-west strike throughout the study site. The magnetic data was tie line leveled and corrected for IGRF effect. Furthermore, micro-leveling was performed in order to eliminate along-line, non-geologic noise. Information from only one sensor was implemented as current inversion procedures do not allow for the use of gradient data.

Low frequency, long wavelength data can be attributed to deep source input. In order to ensure solutions maintain a focus on local-scale geology the regional field contributions must be removed before any inversions are performed. To remove the regional field input the signal is isolated through upward continuation and grid subtraction. The magnetic and gravity data were upward continued 2 Km above the measuring surface, this very low frequency signal was then removed from the data to obtain the residual datasets of the study site. The observed anomalies within a residual dataset are presumed to be caused by local phenomenon and as such are appropriate candidates for inverse modelling.

An unavoidable characteristic of any geophysical data set is the presence of noise. Factors contributing to this noise include aspects such as environmental effects, systematic and device oriented error as well as measurement uncertainty. Any solution delivered through an inversion cannot then be truly correct as it must replicate the geology and the noise perfectly. In order to account for this, data uncertainty must be specified for data input for a UBC inversion. This controls to what degree of accuracy the inversion predicts the observed data. Noise within any geophysical dataset is assumed to possess a Gaussian distribution with the uncertainties within the data being the standard deviation of the Gaussian noise (Williams, 2008).

It is crucial that appropriate standard deviations be assigned to the data to be inverted. A higher standard deviation will result in more simplified outcomes while very low standard deviations will almost certainly provide solutions for non-geologic signal. For a gravity survey this will be input as a constant which should be ideally one to two percent of the data range (Williams, 2008). Higher standard deviations should be applied in circumstances where known interference or cultural influence may affect the data. In situations like this or where data confidence is very high, a lower uncertainty level may be supplied. For older surveys with less accurate measuring equipment or when noisy conditions are suspected, a greater level of uncertainty should be input (Williams, 2008). When working with any magnetic data set where greater dynamic ranges are encountered, a higher degree of uncertainty (5%) should be allotted (Williams, 2008). There is no perfect guideline for assigning the correct level of uncertainty in any data set however.

After the removal of the regional field the range in the residual data is 8.2mgal so an uncertainty of 0.082 (1%) was specified. The constant error should be dictated by the measurement accuracy of the device used. It is recommended that data be upward continued to the same distance as the cell size used in the inversion. By doing so you eliminate the high frequency noise that only small cells can replicate (Williams, 2008).The station spacing of the gravity survey was 25m. Although the earth should in reality be represented as a series of infinitesimally diminutive cells, Nyquist's law dictates that our resolution is limited to twice that of our survey spacing. Willams (2008) recommends grid cell sizes be set at no more than the average station spacing as a best-practice procedure. Due to irregular station spacing and in order to decrease inversion computational time, the inversions were performed using 75m cells.

After defining the uncertainty in the data and then comparing the difference between the observed and predicted data, a data misfit factor is calculated:

$$\emptyset_d = \left\|\mathrm{W}_d\left(\mathrm{Gm} - \mathrm{d}^{obs}\right)\right\|^2$$

(Williams, 2008)

$$\mathrm{W}_d = diag\left(\frac{1}{\sigma_i}\right)$$

The predicted geophysical response of the recovered model is Gm while σ_i is the standard deviation of noise at the i^{th} data point. This becomes a significant component in the optimization problem associated in recovering an appropriate model. An appropriate model will be recovered in the situation where balance is achieved between a small model objective function, Φ_m, and a target data misfit, Φ_d (Williams, 2008). The target data misfit will be equal to the number of observations, N, assuming Gaussian noise with a zero mean.

Geologic and Geophysical Constraints

Until recently most inversions were carried out with little or no prior constraints, or bounds. Theoretically viable physical property distributions were derived by applying mathematical algorithms which sought to find an optimum match between observed and calculated geophysical data sets. Stemming from the fact that potential field data contain no inherent depth information, early recovered models often resulted in a geometry known as the "surface plate" effect where predicted signals were hypothetically generated by only the thin upper surficial portion of any given model. In order to combat this, implementation of a depth weighting function has been included into the smooth and small model algorithms developed by Li and Oldenburg (1996; 1998). This however leads to yet another fundamental problem associated with inversions known as the "smoothed blob". In this instance the observed signal is fully reproduced by the hypothetical model but again the output model contains no real geologic information. The smoothed blob simply reproduces the observed signal by very minor variations in density which do not allow for the depiction of any structure (Williams, 2008). The geologically meaningless solutions associated with these simple inversions reveal the necessity of a constrained

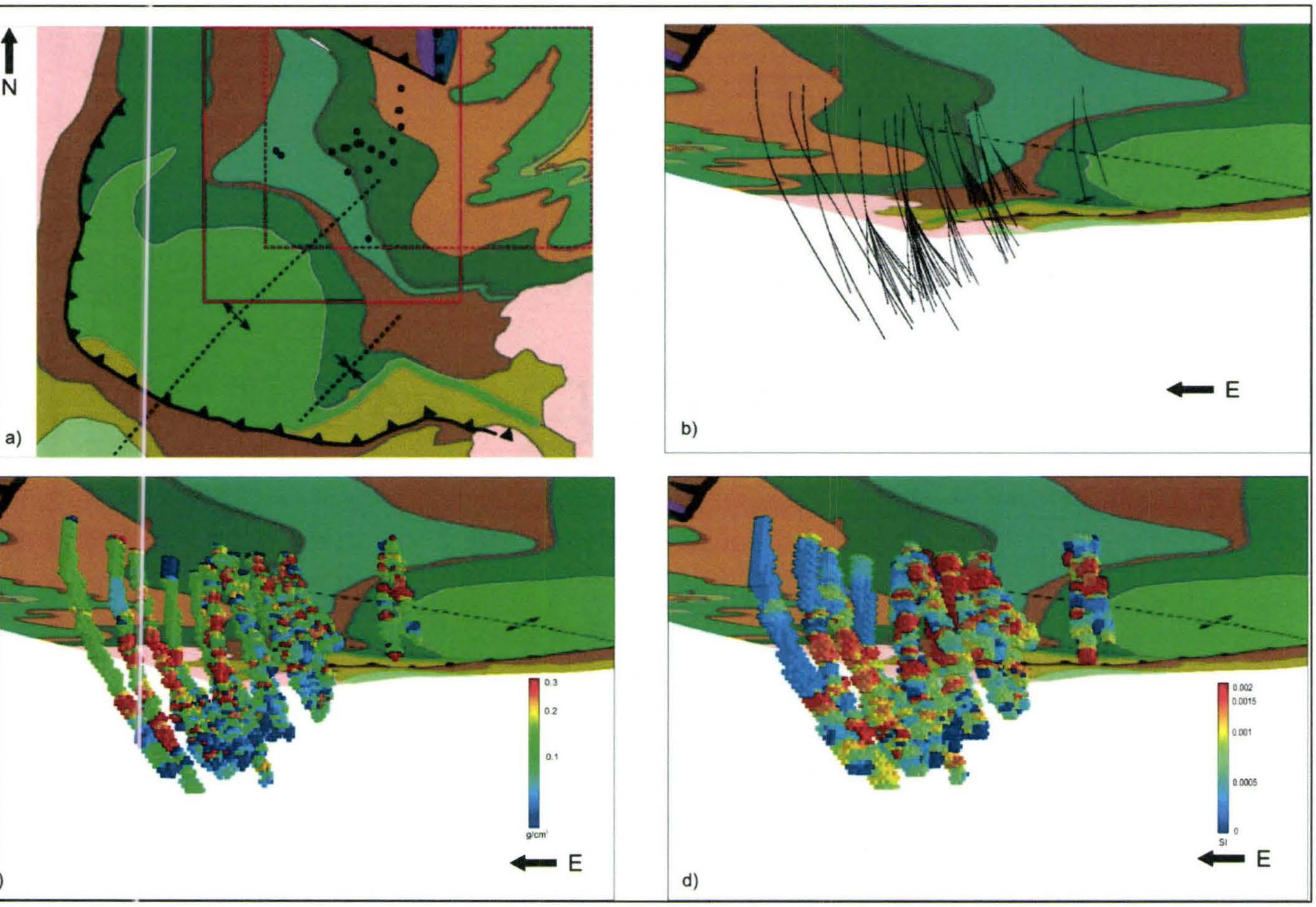
N
a)
b)
E
0.3
0.2
0.1
g/cm³
E
0.002
0.0015
0.001
0.0005
0
SI
E
d)

Figure 4-2 - a) Study site within the Pacquet Harbour Group. Gravity inversions are contained within the sold red while magnetic inversions are within the dotted red box. Borehole locations are marked by black circles. b) Subsurface distribution of boreholes. c) 3D voxel model of borehole density with 200m elliptical buffer. Values are relative to a 2.67 g/cm^3 datum. D) 3D voxel model of borehole susceptibility measurements with a 500m buffer.

approach. This leads to the next stage where priori geological constraints are introduced into the inversion process.

Voxel Models

In order to incorporate previous geologic constraints it is necessary to develop a reference model which includes known bounds. This model, which can be considered as a starting point for the inversion, supplies a best estimate reference for initial computations of physical property distributions. Information which can be exploited in a reference model includes surface geological maps, drill-hole logs, and surface as well as down-hole physical property measurements. While down-hole and surface measurements provide the most reliable constraints, the drill logs and surface mapping will more likely allow the spatial constraints desired within any given inversion. In order to establish the reliability of one source of data over another a smallness factor can be supplied in order to further constrain the inversions in regard to each component of the reference model (Williams, 2008).

Physical property measurements including density and magnetic susceptibility were obtained on 17 boreholes throughout the Rambler and area (Spicer et al., 2010, unpublished). Density was measured by means of a standard Archimedes Principle submersion approach while magnetic susceptibility was recorded using a Bartington Instruments MS2 magnetic susceptibility meter. The boreholes varied in depth, the deepest being 1200 m and the most shallow merely 200 m. The average properties (Table 1) were assigned to each corresponding unit in holes where no physical properties were recorded yet geologic logging was performed.

The subsurface mesh volume for the gravity inversion was constructed using voxels with 75m x, y dimensions with the sides of the voxel being aligned to geographic N-S. In agreement with the UBC-GIF model procedures the z dimension of the voxel mesh was systematically increased with depth. Incrementing the spatial extent of the voxels with increasing depth attempts to maintain the same influence of deeper sources in the model on the outcome of the inversion. Physical property measurements on the bore-core were taken approximately every meter. After computing the trajectory of each borehole from a series of drillhole dip and azimuth measurements it is possible to locate each physical property measurement in three dimensional space. Upper and lower bounds of physical property variations were assigned as the value of the measurement point +/- one standard deviation. Incorporating this prior knowledge as a constraint into the initial reference model required three dimensional gridding of the data.

Two continuously variable meshes of density and susceptibility were created by implementing the inverse distance gridding algorithm provided within Encom's Profile Analyst (PA) (Fig 2). Using this method the distance from voxel epicenter to all source data points is calculated based on specific weighting parameters. Since the z dimension of a voxel is increased with depth shallower voxels incorporate fewer measurements than the larger deeper voxels of the final reference model (Fig 3). Values associated with the shallower sources therefore more closely approximate the observed data. Taking advantage of known geologic strike and dip trends, an elliptical buffer was applied to extenuate the lateral continuity of the borehole gridding. The use of a buffer allows for an expansion of the subsurface reference model along expected trends. The buffer was constrained to 200 m for gravity borehole grids and 500 m for the equivalent magnetics grids. Additional constraint was deemed necessary for magnetics as no surficial references would be used. This decision was based on the occurrence of highly varying susceptibility values within a given mapped geologic unit. From figure 2 we

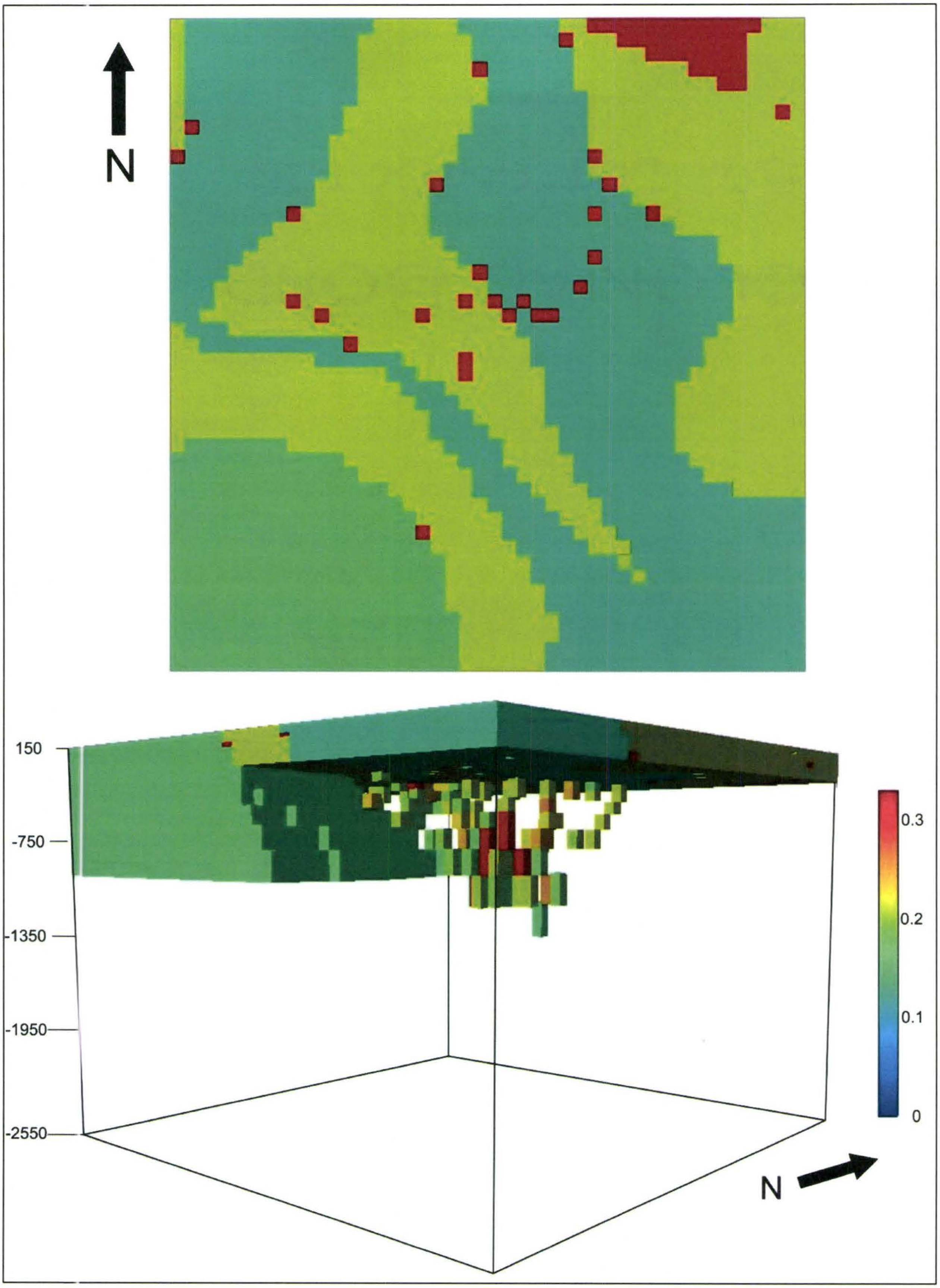
N
150
-750
-1350
-1950
-2550
0.3
0.2
0.1
0
N

Figure 4-3 - Reference model of density values within the rambler property. A plan view displays lateral constraints derived from geological mapping and boreholes (left) while in three dimensions (right) constraints are imposed at depth. The Rambler rhyolite is continued 1 km into the subsurface plunging 40 degrees to the northeast. The size of cells within the reference model increases by a factor of 1.25 with depth.

can see the occurrence of the Rambler rhyolite at depth within the density voxel models as a relative low to the surroundings. This feature is not obviously apparent within the magnetic grids however. The gabbroic dykes though, which appear as density highs, also have high magnetic susceptibilities and are easily distinguished within both voxel models.

The primary spatial constraint for lithological contact surfaces in x,y space of the reference model were based on a 1: 20 000 scale geologic map (modified after Skulski, et al. 2010; Fig 1). Average properties from a simplified geologic code (Table 1) were assigned to map derived components based on rock type. The surface geological boundary constraints were only extended to a depth of 300 m to minimize their influence at greater depth where map trends may dissipate. The Rambler rhyolite however has been extended to a depth of 1 km along the known surface trend, plunging 40 degrees to the northeast as its presence is strongly supported at these depths within borehole logs. Since magnetic susceptibility is known to vary to a much larger degree than density within these units, no surface map constraints were included in the construction of the magnetic susceptibility reference model.

Spatial constraint in three dimensions was derived from individual drillhole logs and a 3D geologic model of lithological surfaces constructed from drillcore logs supplied by Rambler Mining and Metals PLC (Fig. 2). Since physical property measurements were produced as an average of each unit encountered in the map and model, the value of any given voxel within a reference model produced from these cannot be established to the same confidence as our measured drill holes. Also it should be noted that as the geologic characteristic of a single unit will vary in space, so too will its physical properties. Knowing this it is important that less reliability be assigned to a reference model component spanning a large lateral proportion. Such is the case with surface constraints derived from geologic maps. Within figure 3 it can be observed that the physical properties of the drill cores are readily distinguishable from those of the map constraints. These borehole values are much higher and likely represent occurrence of higher density intrusive dykes within the lower density tuffs and sediments. While the presence of these dykes is known, mapping of their spatial extent is limited by the poor outcrop control.

Ideally in order to accommodate the less constrained data, lower smallness values should be input for their portion of the reference model. This lowers the ratio of smallness to smoothness within the model objective function and in effect drives the model to a more smoothed outcome. Higher smallness values should be input for the areas where measured drill holes were incorporated, increasing the ratio of smallness to smoothness and introducing more structure (Williams, 2008). Unfortunately, as the current UBC-GIF GUI does not support separate smallness values within inversions and instead imposes a common value for an entire model, this was not possible. Instead, an approach varying the degree of restriction within the bounds files was enforced to take into account the more irregular physical properties of different input sources. Tighter bounds of 0.5 the unit standard deviations were placed on the drill core measurements in order to provide more constraint on reliable values. Conversely 1.5 the unit standard deviations were assigned to components of the reference model derived from surficial geologic maps.

Code	Description	Average Density (g/cm^3)	Standard Deviation	n	Average Susceptibility (S.I.)	Standard Deviation	n
B	Mafic Volcanic Rocks	2.87	0.12	482	0.0002	0.0004	730
F	Felsic Volcanic Rocks	2.79	0.16	61	0.0002	0.0006	494
Mgb	Gabbro-diorite Dykes	2.93	0.10	207	0.002	0.003	609
S	Sedimentary Rocks	2.79	0.06	12	0.0005	0.001	32
Vms	Sulphide (Stringer)	3.32	0.29	5	0.001	0.002	41

Table 4-1- Average physical properties of units throughout rambler property according to provided drill core logs. No massive sulphides were available for sampling. Sulphides sampled were either disseminated or stringer type mineralization.

Results and Discussion

An inherent component controlling the outcome of any inversion is the specific type of data being used. While maps depicting potential field measurements can appear visually appealing and are considered to depict the spatial extent of lithological structures quite accurately, it is important that we keep in mind what is being presented. Gravity maps display changes in the gravitational field which, after proper reduction, are the result of density contrasts. Magnetic maps, be they total field or gradient, display changes in the magnetic field as proscribed by magnetic susceptibility distributions. Knowing this, it becomes imperative that our expectations of an inversion are clear. It would be futile to expect the output of a magnetic inversion to provide insight into the nature of a non-magnetic body; while conversely resolving that same body is not possible through means of a gravity dataset if there is no associated density contrast to that of its surroundings. Only when the limits of the data are properly understood can the tool of inversion be effectively exploited.

Density Distribution

The distribution of density throughout the Rambler area has been mapped by a new high resolution gravity survey collected by MAGGIC. Whereas previous geophysical investigations within the area were limited to regional data (Miller, H.G. and Deutsch 1975; Miller and Wiseman 1994), this was the first high resolution gravitational work performed on the BVP. The target of this inversion was the Rambler rhyolite. It was anticipated that this dataset would provide the most insight into this feature as the lower density felsic volcanic rocks comprising this structure represent a strong density contrast to the surrounding high density ocean-floor derived mafic volcanic rocks. Depiction of the Rambler rhyolite at depth is critical as the major ore deposits in the area are known to be associated with the upper margin of the felsic volcanic rocks (Skulski et al., 2010). Through use of a detailed reference model derived from borehole constraints and a 1:20,000 scale geologic map the 3D geometry of the Rambler rhyolite has been revealed (Fig 4). The geophysical signature of the inversion results is essentially identical to that of the observed data (Fig 5).

While the initial intention of the inversion was to reveal the extent of the VMS-hosting felsic volcanic sequence laterally as well as at depth, limitations arising from the surficial distribution of observation points dictate a focus towards the behaviour at depth within the known VMS producing area. The vicinity of inversion was designed to contain as much data as possible while maintaining the dimensional constrained imposed by the x,y nature of the mesh. As such, not all of the data points collected could be used. From the results of the inversion the lithological surface is depicted plunging to the northeast roughly at 40 degrees. The dip of the structure appears to increase in the lower portions however this may be related to a combination of voxel cell size variation and signal attenuation with depth. The cells which comprise the structure range in density values of 2.71-2.75 g/cm^3. From table 1 we see that this value is within one standard deviation of the average density value calculated for the logged felsic volcanic rocks.

The Rambler rhyolite appears to only occupy a minor portion of the investigatory area in the south-west within the upper portions of the mesh. The results of this inversion however depict a considerable extent of the study site occupied by the structure, primarily in the subsurface. Incorporating the current model of ore reserves in to the same image space as the gravity inversion model demonstrates a strong linkage between the two (Fig 4b). The ore bodies dip nearly parallel to the

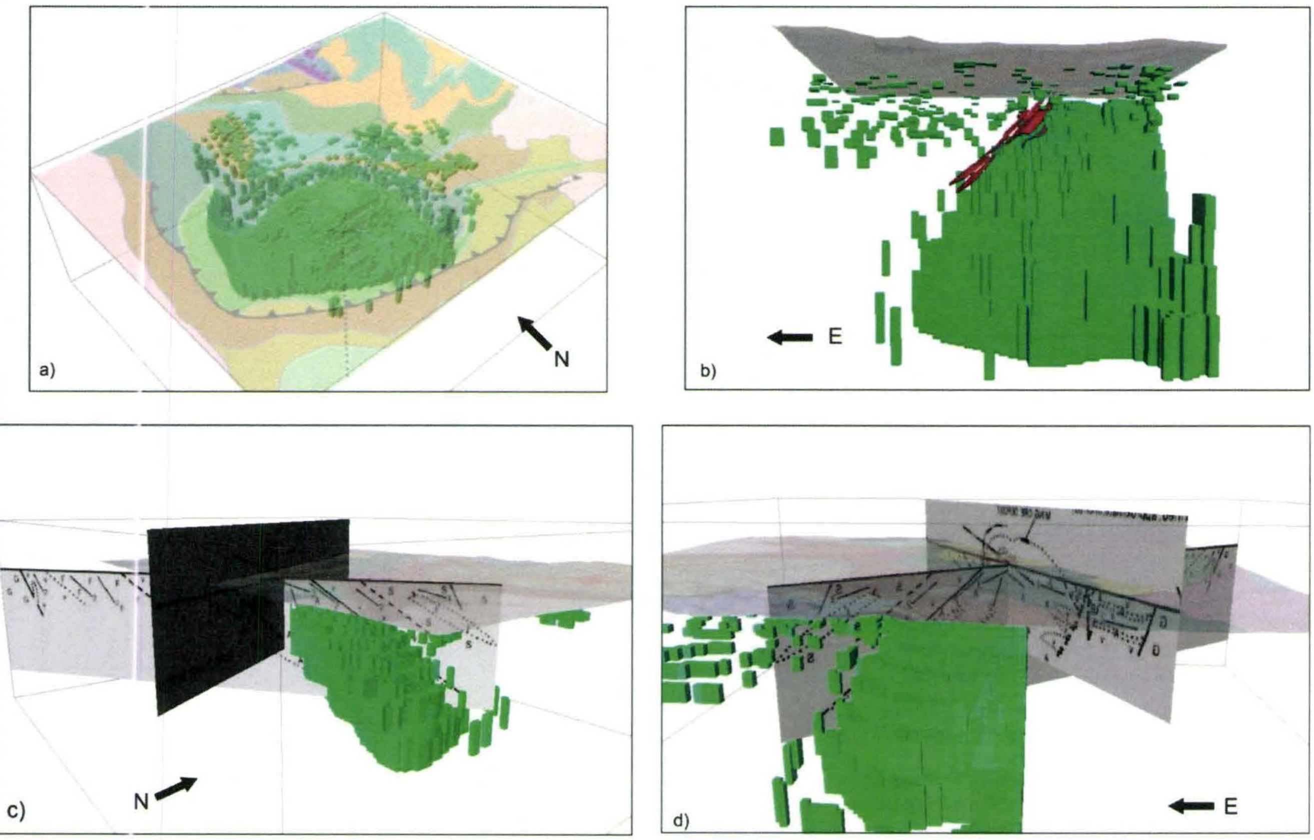
a)
N
b)
E
c)
N
d)
E

Figure 4-4 - Gravity inversion result isolated within a density range of 2.71 to 2.75 g/cm^3. a) Plan view of a transparent geologic map displays the lateral extent of the inversion result. b) Known ore distributions are displayed (red) flanking and in close association to the inversion results depicting the rhyolite (green). c) and d) comparison of transparent inversion results with local cross sections developed by Tuach and Kennedy (1978).

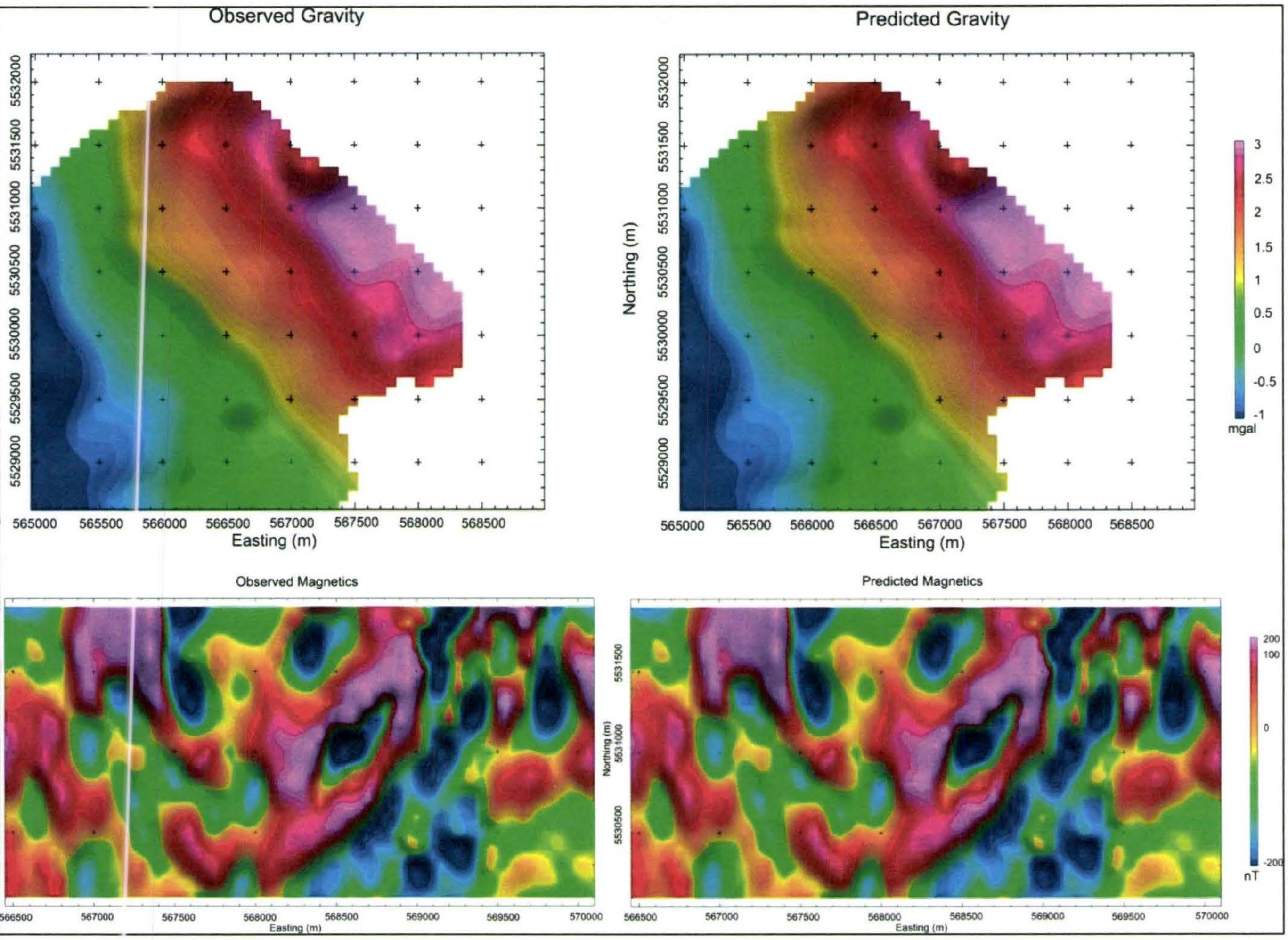
Observed Gravity
Predicted Gravity
Northing (m)
Easting (m)
mgal
Observed Magnetics
Predicted Magnetics
Easting (m)
Northing (m)
nT

Figure 5-5 – Gravity (above) and magnetic data (below) input for 3D inversion. Observed signatures (left) are displayed next to the near identical inversion model response (right).

structure near the surface and begin to diverge at depth. Again, this may be a function of signal attenuation, however this also suggests ore potential at greater depths than previously considered. When compared to geologic cross sections contrasted by Tuach and Kennedy (1978) the morphology of the structure is in agreement with lateral and near surface trends (Fig 4 c,d). The cross sections have been georectified in three dimensions and displayed alongside a semi-transparent inversion model. This allows for the comparison of the rambler footwall contact (displayed as a thick black line plunging in a similar fashion as the rhyolite) as perceived by Tuach and Kennedy on the basis of geological inferences to the results of the geophysical data. Deviations from these trends are encountered at depth where the structure veers from surface projection. However, for the most part the geophysical data is in agreement with the work of Tuach and Kennedy (1978).

Magnetic Susceptibility Distribution

While the gravity inversions were successful in capturing the rhyolite body at depth the magnetic data proved incapable of providing any information regarding the Structure at all. Although the Rambler Rhyolite is host to several VMS deposits, it was recognized that as a whole, this body of felsic volcanics is rather non-magnetic (Table 1). However, cross-cutting the stratigraphy and scattered throughout the study site are a highly magnetic suite of gabbroic dykes are observed. These mafic bodies are assumed to represent a 'feeder' system to the overlying volcanic tuff and flow units. Important information regarding local deformation can be extracted from these dykes. Examination of high resolution magnetic maps of the property suggests the presence of a large scale open fold (Fig 6). The axis of this fold is oriented north-northeasterly, correlating to the late upright folding reported in past geologic mapping (D_3 of Castonguay et al. 2009, D_4 in Tuach and Kennedy 1978, D_L in Hibbard 1983). Figure 6b displays the magnetic tilt angle derivative, a ratio between first vertical and horizontal derivatives of the magnetic field (Millerand Singh 1994; Salem et al. 2008), as a three dimensional surface with sun-shading extenuating the grid peaks. Ranging from +/- 90 degrees, magnetic source bodies are outlined at 0 degrees.

The mesh for the gravity inversion was designed to optimize coverage across the rhyolite. Williams (2008) maintains that while performing inversions with multiple data sources, in this case magnetics and gravity, it is preferable to use a common mesh. This is suggested in order to allow confirmation and correlations between results. However, lacking sufficient susceptibility contrasts though, the magnetic inversions using the same survey design as the gravity mesh provided little information. To take advantage of a densely sampled magnetic dataset, a new mesh with 50m voxels was crafted for magnetics on the Rambler area. This new mesh covers an area north-east of that of the gravity mesh (Fig 2). The magnetic signature of this area has more texture as it contains a greater concentration of magnetic dykes.

The results of the magnetic inversions depict the behaviour of the mafic dykes in the subsurface (Fig 6). Inversion results indicate these features are upright to slightly inclined, dipping to the northeast with a magnetic susceptibility range of 0.02 to 0.009 SI units. The lower end of this susceptibility range is within the upper bounds of our measured physical property database (Table 1). It should be noted that these measurements however are derived from bore-core drilled in the less magnetic areas of the Rambler area. In this case inversions were applied in the more magnetic zones. It is possible that the upper extent of the susceptibility range reported here is valid; however, the physical property database should be updated, sampling the mafic dykes in the area where the inversion is contained. As indicated

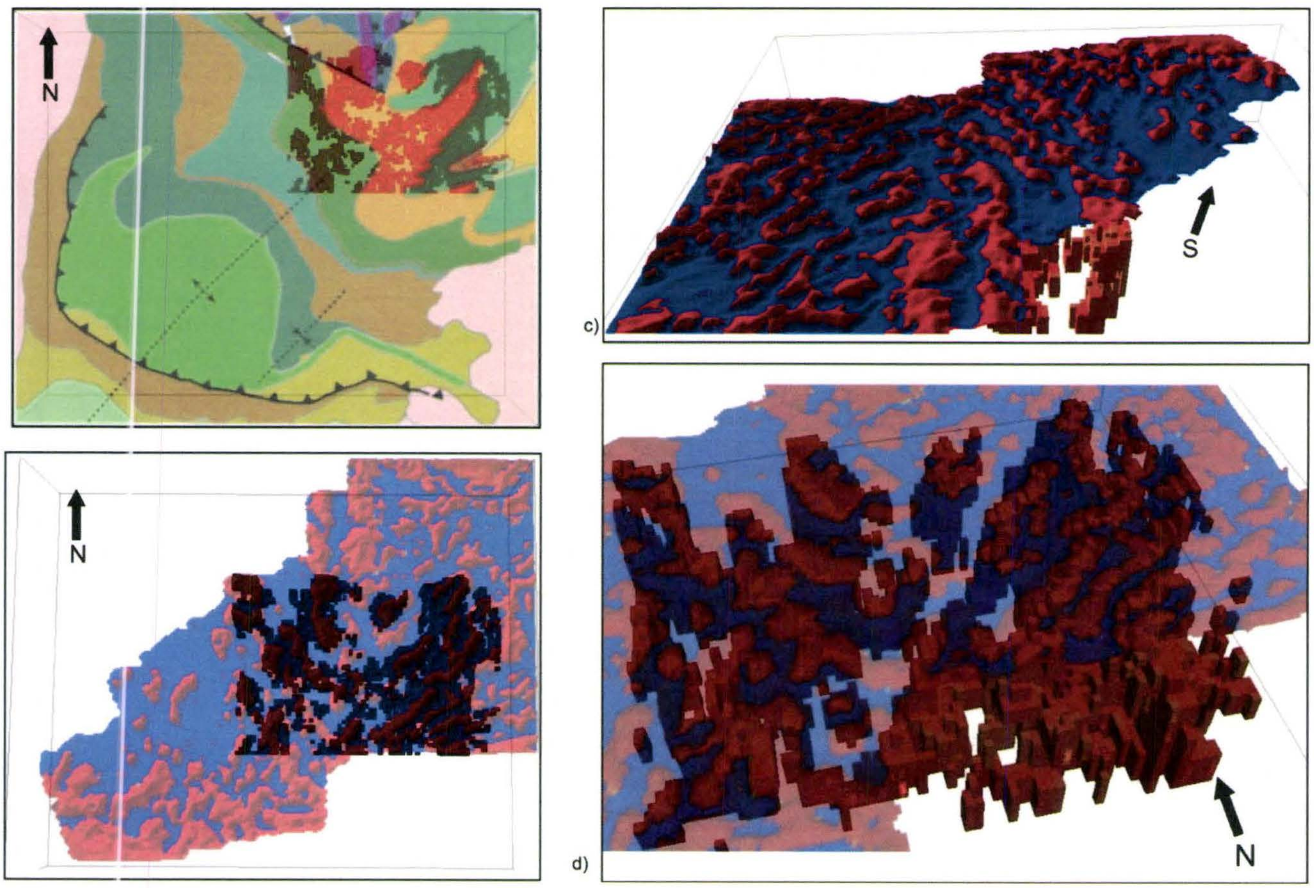
N
N
c)
S
d)
N

Figure 4-6 - Magnetic inversion results isolated within a magnetic susceptibility range of 0.02-0.009 S.I. units. a) Plan view geometry and location of magnetic 3D inversion within the PHG. b) Plan view of the magnetic tilt angle grid and the location of the magnetic inversion results. Positive tilt angles representing source bodies are red while non magnetic sources are blue. These are in agreement with the trends of the bodies produced by the magnetic inversion of the residual TMI data. c) View of the magnetic tilt angle grid from the north accentuates the presence of an open fold. d) Magnetic inversion results depict steeply dipping to vertical source bodies extending downwards from outlines provided by the transparent tilt angle grid.

by two dimensional magnetic grids, the dykes appear to play host to a fold with an axis trending roughly to the northeast.

From Figure 6d it can be noted that in three dimensions the fold is roughly upright. This correlates to D_3 cross-folding which is responsible for the current morphology of the Rambler rhyolite bodyto the southwest (Castonguay et al. 2009). While the more competent gabbroic dykes were likely less affected by the imposing stresses producing these trends as the surrounding sedimentary rocks and volcanogenic tuffs, the dykes appear to host this fold in the subsurface. This area of the property though is also known to host an iron bearing jasperite unit that is strongly magnetic. Although discontinuous in outcrop, it is reportedly as much as 5-10m in thickness at some sites (Skulski et al., 2010). The result of the magnetic inversions, specifically in the easternmost portions may stem from the magnetic contrasts of this unit with surrounding geology.

Conclusions

Following the construction of a detailed physical rock property database a reference mesh model incorporating all available geologic information was established. Once created this reference model outlining known and expected physical property distributions was used to provide the geologic constraints for 3D inverse modeling.

From these inversions, the structure of the Rambler rhyolite has been revealed. From gravity data taken across the extents of the Rambler area, the structure is depicted as a 2.71 to 2.75 g/cm^3 body dipping roughly 40 degrees at the near surface and steepening with depth. This observation has obvious implications for future exploration techniques. Whereas current ore reserves encountered in the subsurface are within the first few hundred meters below the surface flanking the structure down plunge. Deeper drilling will be necessary to follow the dome as it steepens at greater depths. 3D magnetic inverse modeling to the northeast of the structure outlines the geometry of a suite of highly magnetic gabbroic dykes. These features are depicted as roughly upright, elongate bodies with a magnetic susceptibility range of 0.009 to 0.02 S.I. units. The axis to a large scale fold hosted throughout the property and affecting the geometry of the Rambler rhyolite is contained within the magnetic inversion results as well. This upright northeasterly trending fold may be a very favourable exploration target for future drilling.

The inversions performed in this study have taken all available geologic and geophysical information into consideration. While geophysical inversion models are a powerful tool it should be kept in mind that they are indeed only models. The results of inversion should be compared with known geology with an assessment regarding compatibility being made. In order to remain effective and ensure the most accurate results, the physical property database and reference model for inversions should be updated as new information becomes available. This ensures that future inversions will continue to provide increased insight into subsurface physical property distributions and structure.

Acknowledgments

The authors wish to thank Rambler Metals and Mining PLC., specifically Larry Pilgrim, for providing property access, geologic models and drillhole information. In addition to geologic consultation, Dr. Tom Skulski provided geology map files and stratigraphy logs used in the production of reference models and figures. Funding has been provided by the Geologic Survey of Canada's Research Affiliate Program as well as a Natural Science and Engineering Research Council grant.

References

Anderson, S.D. (1998). Structure metamorphism, and U-Pb and $^{40}Ar/^{39}Ar$ geochronology of the Ming's Bight Group, and the Paleozoic tectonic evolution of the Baie Verte Peninsula, Newfoundland. Unpublished Ph.D. thesis, Dalhousie University, Dartmouth, Nova Scotia. 452 p.

Anderson, S.D., R.A. Jamieson, Reynolds, P.H., (2001). Devonian extension in northwestern Newfoundland: 40Ar/39Ar and U/Pb data from the Ming's Bight area, Baie Verte Peninsula. Journal of Geology, **10:** 191-211.

Bosch, M. and McGaughey, J. (2001). Joint inversion of gravity and magnetic data under lithologic constraints. The leading Edge, August: 877-881.

Castonguay, S., Skulski, T., van Staal, C., Currie, M. (2009). New insights on the structural geology of the Pacquet Harbour Group and Point Rousse Complex, Baie Verte Peninsula, Newfoundland: Current Research (2009) Newfoundland and Labrador Department of Natural Resources, Geological Survey, Report 09-1, p. 147-158

Church, W.R., and Stevens, R.K. (1971). Early Paleozoic Ophiolite Complexes of Newfoundland Appalachians as mantle-oceanic crust sequences. Jour. Geophysics. Research, **76**: 1460-1466.

Coates, Howard. (1990). Geology and Mineral Deposits of the Rambler Property; in Metallogenic Framework of Base and Precious Metal Deposits, Central and Western Newfoundland, (Field Trip 1, 8TH IAGOD Symposium). GSC Open File 2156; p. 184-193.

Cook, R. B, and Cochrane, L, B. (2000). Technical Report on the Rambler Property, Baie Verte Peninsula,Newfoundland, Canada – prepared for Rambler Metals and Mining PLC; Report for NI 43-10 Dube, B, Gosselin, P, Hannington, M and Galley, A, 2000, Gold-rich volcanogenic massive sulphide deposits, Geological Survey of Canada

Dias, F., Barbosa, V., Silva, J. (2009). 3D gravity inversion through an adaptive-learning procedure. Geophysics, **74:** I9-I21.

Fergoso, E., Gallardo, L.A. (2009). Cross-gradients joint 3D inversion with applications to gravity and magnetic data. Geophysics, **74:** L31-L42.

Gale, G. H. (1971). An investigation of some sulphide deposits in the Rambler area, Newfoundland. Unpublished PhD Thesis, University of Durham, England. Rambler Metals and Mining PLC, Placing and Admission to Aim. 2005. http://www.ramblermines.com/pdf/RMM_Prospectus.pdf. October, 5th, 2009.

Gale, G.H. (1973). Paleozoic basaltic komatiite and ocean floor type basalts from northeast Newfoundland. Earth and Planentary Science Letters. **18**: 22-28.

Hibbard, J.P. (1983). Geology of the Baie Verte Peninsula, Newfoundland. Newfoundland Department of Mines and Energy. Memoir 2, 279p.

Li, Y. and Oldenburg, D. (1996). 3-D inversion of magnetic data. Geophysics, **61:** 394-408.

Li, Y. and Oldenburg, D. (1998). 3-D inversion of gravity data. Geophysics, **63:** 109-119.

Miller, H.G. and Deutsch E.R. (1975). New gravitational evidence for the subsurface extent of oceanic crust in north-central Newfoundland. Canadian Journal of Earth Science, **13**: 459-469.

Miller, H.G. and Singh, V. (1994). Potential field tilt – a new concept for location of potential field sources. Journal of Applied Geophysics, **32**: 213-217.

Miller, H.G. and Wiseman, R. (1994). Potential field interpretation of the Baie Verte Peninsula, Newfoundland, utilizing constraints from Lithoprobe East seismic line 89-13. Atlantic Geology. **30**: 25-36.

Oldenburg, D.W. (1974). The inversion and interpretation of gravity anomalies. Geophysics. **44:** 730-741.

Piercey, S.J., Jenner, G.A., Wilton, D.h.C. (1997).The Stratigraphy and geochemistry of the southern Pacquet Harbour Group, Baie Verte Peninsula, Newfoundland: implications for mineral exploration. Newfoundland Department of Mines and Energy, Geological Survey, Report **97-1**: 119-139.

Portniaguine, O. and Zhdanov, M. (2002). 3-D magnetic inversion with data compression and image focusing . Geophysics, **67:** 785-796.

Salem, A., Williams, S., Fairhead, D., Smith, R., Ravat, D. (2008). Interpretation of magnetic data using tilt-angle derivatives. Geophysics, **73**: L1-L10.

Skulski, T., Castonguay, S., van Staal, C.R., McNicoll, V.J., Piercey, S., Slavinski, H. (2007). Geology of the Baie Verte Peninsula revisited; stratigraphy and structure of the Pacquet Harbour Group. Proceedings, Geological Society of America, Northeastern Section, 42nd annual meeting, Durham, New Hampshire., pp. 49-50.

Skulski, T., Castonguay, S., McNicoll, V., Rogers, N., van Staal, C., Morris, W, Ugalde, H., Slavinski, H., Spicer, W., Moussallam, Y., Kerr, I. 2010. Tectonostratigraphy of the Baie Verte Oceanic Tract and its Ophiolite Cover Sequence, Baie Verte Peninsula, Newfoundland and Labrador. *In* Current Research. Newfoundland and Labrador Department of Natural Resources, Geological Survey, Report 10-1, pages 315-335.

Spicer, B., Tschirhart, V., Skulski, T., Morris, W.A., (2010). Rambler bore-core petrophysicaldataset. Geological Survey of Canada, Open File report.

Tuach, J.T. (1976). Structural and stratigraphic setting of the Ming and other sulphide deposits in the Rambler area, Newfoundland. M.Sc. thesis, Memorial University of Newfoundland. 128 p.

Tuach, J.T., Kennedy, M.J. (1978). The geological setting of the Ming and other sulphide deposits, Consolidated Rambler Mines, northwest Newfoundland. Economic Geology, **73**: 192-206.

van Staal, C.R., Whalen, J.B., McNicoll, V.J., Pehrsson, S., Lissenberg, C.J., Zagorevski, A., van Breemen, O., Jenner, G.A. (2007). The Notre Dame arc and the Taconic orogeny in Newfoundland. Frame work of Continental Crust: The Geological Society of America, Memoir 200, pp. 511-552.

Williams, N.C. (2008).Geologically constrained UBC-GIF gravity and magnetic inversions with examples from the Agnew-Wiluna greenstone belt, Western Australia. PhD thesis. University of British Columbia, Vancouver, BC. 509 p.

Zeyen, H. and Pous, J.(1993). 3-D joint inversion of magnetic and gravimetric data with priori information. Geophysical Journal International. **112:** 244-256.

Chapter Five

3D Regional Geophysical Modeling of the Baie Verte Peninsula, Newfoundland

B. Spicer[1], B. Morris[1], H. Ugalde[1] and Cees van Staal[2]

MAGGIC, School of Geography & Earth Sciences, McMaster University, 1280 Main Street W., Hamilton, ON L8S 4K1. Canada

Geological Survey of Canada, 625 Robson St. Vancouver, British Columbia, V6B 5J3

Abstract

The Baie Verte Peninsula records closure of the Iapetus Ocean and the periods of orogenic activity that were responsible for the creation of the Appalachian mountain belt. Bisected by the Baie Verte Line, a northeasterly trending composite fault zone, the Baie Verte Peninsula is divided into two major lithic terranes. West of this line, the Humber Zone represents the margin of ancient continental Laurentia. To the east, Ordovician ophiolitic and island arc lithologies of the Baie Verte Oceanic Tract, vestiges of the narrow Humber seaway ocean floor, have been accreted and subsequently intruded by a surge of Silurian volcanism. Past geophysical and geologic studies have interpreted continental margin below the BVOT as a ramp or wedged structure with a slope dipping to the east. This study presents a series of 2D forward profile based models of gravity and magnetics with intersections between individual profiles to enable a geophysically supported geologic framework for the Baie Verte Peninsula. Independent full 3D magnetic inversions provide additional support for some of the interpreted structures. Results of this study indicate that basement morphology mirrors many surficial trends. In some instances such as at Ming's Bight significant faulting has lead to exposure of the continental basement at surface. A similar phenomenon may explain near surface exhumation of ophiolite near Betts Cove below the surface cover formed by the Silurian Cape Brule Porphyry. Geophysically the Snooks Arm and Pacquet Harbour groups are similar; these lithologies may exist below the Cape Brule Porphyry hosting an antiform within the vicinity of the Baie Verte Flexure. On a regional scale the Cape St. John volcano sedimentary continental cover series comprises a series of overturned anticlines and synclines where late stage faulting may propagate fold limbs into their core. Finally, 3D magnetic inversions depict the Baie Verte Line as a near vertical conjugate fault zone which may have been dissected by late stages extensional faulting supported in many cross cutting west dipping structures.

Introduction

The Baie Verte Peninsula (BVP) of north-central Newfoundland represents the northernmost termination of the Appalachian mountain belt on land. With a rich history of copper, gold, asbestos and other mineral resources, the BVP is one of Newfoundland's most prospective sites for mineral exploration. In addition to having important economic significance, the stratigraphy and structure of BVP has also been the site for many academic studies concerning the role of plate tectonics in orogenic events. It is the association of specific types of mineral deposits with allochthonous ocean crust lithologies, regional scale structures formed during obduction of oceanic tracts over the adjacent continental margin sequence and orogenesis related to subsequent collisions with outboard terranes (van Staal et al., 2009), that forms the linkage between the academic and economic interest in the rocks of the BVP.

Academic interest in the BVP increased along with the development of our understanding of the geochemical, structural and mineralogical significance of plate tectonic processes. Many of the early papers discussed topics such as; the ocean floor provenance of specific rock units (Church and Stevens, 1971; Dewey and Bird, 1971; Bird et al. 1971; Kennedy and Philips, 1971; Upadhyay et al. 1971); the sense of motion on hypothesized Paleozoic age subduction zones (Miller and Deutsch, 1976; Haworth et al. 1978); and the timing of the emplacement of ocean floor sequences over the cratonic margin (Waldron et al. 1998; van Staal et al. 2007). While there have been numerous other studies describing specific aspects of the Baie Verte geology, the last geological map compilation for the BVP was published by Hibbard in 1983. Economic exploitation of mineral resources present on the Baie Verte Peninsula has experienced a similar periodic advance and subsequent decline. Volcanogenic massive sulphide deposits present on the BVP have been mined since the early 1860's and gold deposits often related to regional scale tectonic structures have been exploited since 1905. In most instances these mines extracted resources which had surface expression, or could be inferred from nearby showings. A fundamental tenet of many mineral exploration programs is that the highest probability of locating new mineral resources lies within existing and abandoned mining camps. Central to this hypothesis is the belief that through the integration of multiple geoscience datasets, all available geological maps, and mineral deposit models, it should be possible to locate zones of additional resource potential. An increasingly detailed understanding of the surface geological distributions, structural and tectono-stratigraphic relationships (Castonguay et al., 2009; Skulski et al., 2010) on the BVP has been an integral component of the Targeted Geosciences Initiative Program (TGI3) of the Geological Survey of Canada (GSC). TGI3 aims to strengthen interest, and reduce risk in base-metal, exploration on the BVP by providing a well supported geological framework for predictive purposes.

Geological outcrop on the BVP is highly variable. While the coast is often formed of tall cliffs with clear exposure, inland outcrop is generally less than 1% of the total area, thus making it difficult to construct meaningful geological maps solely on the basis of outcrops. Like many other areas with limited outcrop geologists have used remotely sensed geophysical data to provide a framework for local geological interpretations. Recognizing the limitations of the previous aeromagnetic and gravity coverage of the Baie Verte Peninsula, the Geological Survey of Canada sponsored the acquisition of new geophysical data as part of the TGI3 program. These new geophysical data sets have outlined structures and lithologic bodies that were not detected by previous surveys.

The magnetic and gravitational response at any point above the earth's surface represents a summation of all contributing anomalous source body concentrations within a given distance of the sensor. Geophysical map images therefore contain information about the contacts exposed at the earth's surface and the morphology of any source bodies located in the subsurface. Prior attempts to model the subsurface geometry of the Baie Verte Peninsula using geophysical data were mostly 2D block models linked to profiles based on a small number of observation points (Miller and Deutsch, 1976; Haworth et al. 1978). These data sets and model studies, which represented state-of-the –art level contributions at the time were severely limited by the limited computational capabilities then available. This study offers a new insight on regional-scale subsurface relationships between lithological units of the complex BVP geology through the integration of geological, geophysical and petrophysical data. The models developed in this study have the benefit of new gravity and magnetic data sets for the BVP, a comprehensive physical rock property database, and the use of new geophysical modeling routines. Two approaches have been used to construct interpretive models of the 3D distribution of geological structure from the observed geological outcrops and the geophysical data. The first approach emphasizes the inputs provided by recently completed geological maps of the BVP (Castonguay et al., 2009; Skulski et al. 2010). In this approach a series of 2D gravity and magnetic profiles were forward modeled using constraints based on known petrophysical values, mapped surficial geological contacts, and the interpreted geometry of the contact as projected on the profile. Linking subsurface contact information from a series of intersecting 2D profiles it is possible construct an estimation of the 3D geological structure. It must be remembered that bounds identified in the geophysical data are also often used as a primary resource for constructing the geological contact map. The second approach at estimating subsurface geological morphology emphasizes the geophysical data, specifically the new aeromagnetic data, as this is based on 3D numerically optimized inversions. These 3D inversions, which are less geologically constrained than the 2D forward models, provide additional mathematical confidence in the outcome of the final 3D geological framework. Specific geologic features addressed by this study include: the Baie Verte Lineament; the Cape St John fold and thrust belt, the Ming's Bight outlier and the Cape Brule pluton.

Geologic Setting

The BVP (Fig. 1) is located in north-central Newfoundland and is divided by the north-east trending, composite fault zone known as the Baie Verte Line (BVL) (Hibbard, 1983). The BVP chronicles the Taconic obduction and accretion of ophiolite and related island arc complexes of the Baie Verte Oceanic Tract (BVOT) (Waldron and van Staal, 2001; van Staal et al., 2007) along the Cambro-Ordovician Laurentian continental margin during the closure of the narrow Humber Seaway between 480 and 470 Ma (Waldron and van Staal, 2001). The complex and protracted BVL juxtaposed metasedimentary rocks of the eastern Humber zone with ophiolitic rocks and their subsequent volcanic cover sequence of the western Dunnage zone (=Notre Dame subzone Williams et al., 1988).

Ophiolite sequences on the BVP have been dated at circa 490 Ma (Dunning and Krogh, 1985; Skulski et al., 2010). These consist of the Betts Cove (Upadhyay, 1973; Bédard et al. 2000; Spicer et al. 2010), the lower Pacquet Harbour Group (Hibbard, 1983; Piercey et al., 1997), the Point Rousse (Norman and Strong, 1975; Kidd et al., 1978), and the Advocate Complexes (Kenney, 1975). Each sequence also includes a respective syn-obduction volcano-sedimentary cover series. While separated and scattered throughout the BVP, Ordovician ophiolites and their associated cover series are considered by some to be correlative to one another (Skulski, et al. 2010).

Subsequent to the Ordovician Taconic accretion of the BVOT, a phase of intense Silurian Salinic tectonism ensued (Cawood et al. 1993, 1994, 1995). Prompted by the accretion of the peri-Gondwanan terrane, Ganderia, to Laurentia (van Staal and de Roo, 1995; van Staal et al., 2009), the Salinic orogeny generated volcano-sedimentary rocks of the Cape St. John Group (Neale et al. 1975) on the eastern side of the BVP. These volcano-sedimentary packages were accompanied by the intrusion of large granitoid bodies (Cawood et al. 1993) which now cover and mask much of the BVOT (Hibbard, 1983). A tectonic window of Humber zone metasedimentary rocks, bordered by Devonian extensional shear zones, is juxtaposed next to mafic volcanic rocks of the Baie Verte oceanic tract within the central portion of the BVP east of the BVL (Anderson, 1998; Anderson et al. 2001). This group of semi-pelitic to psammitic schists make up the Ming's Bight Group and has been correlated to the Late Proterozoic to Early Paleozoic Fleur de Lys Supergroup of the Humber Zone (Hibbard, 1983).

Recognition of Humber Zone components east of the BVL supports the hypothesis of an allochthonous Dunnage Zone structurally overlying a wide segment of the ancient Laurentian margin at depth (Hibbard, 1983). A significant divergence in regional structural trends encountered near the contact with the Mings Bight Group (Anderson, 1998) is marked by a change from north-northeasterly towards east-west structural fabric. This divergence in structural trend is generally thought to have arisen from a pre-existing morphology in the ancient continental margin, referred to as the Baie Verte flexure (Hibbard, 1982).

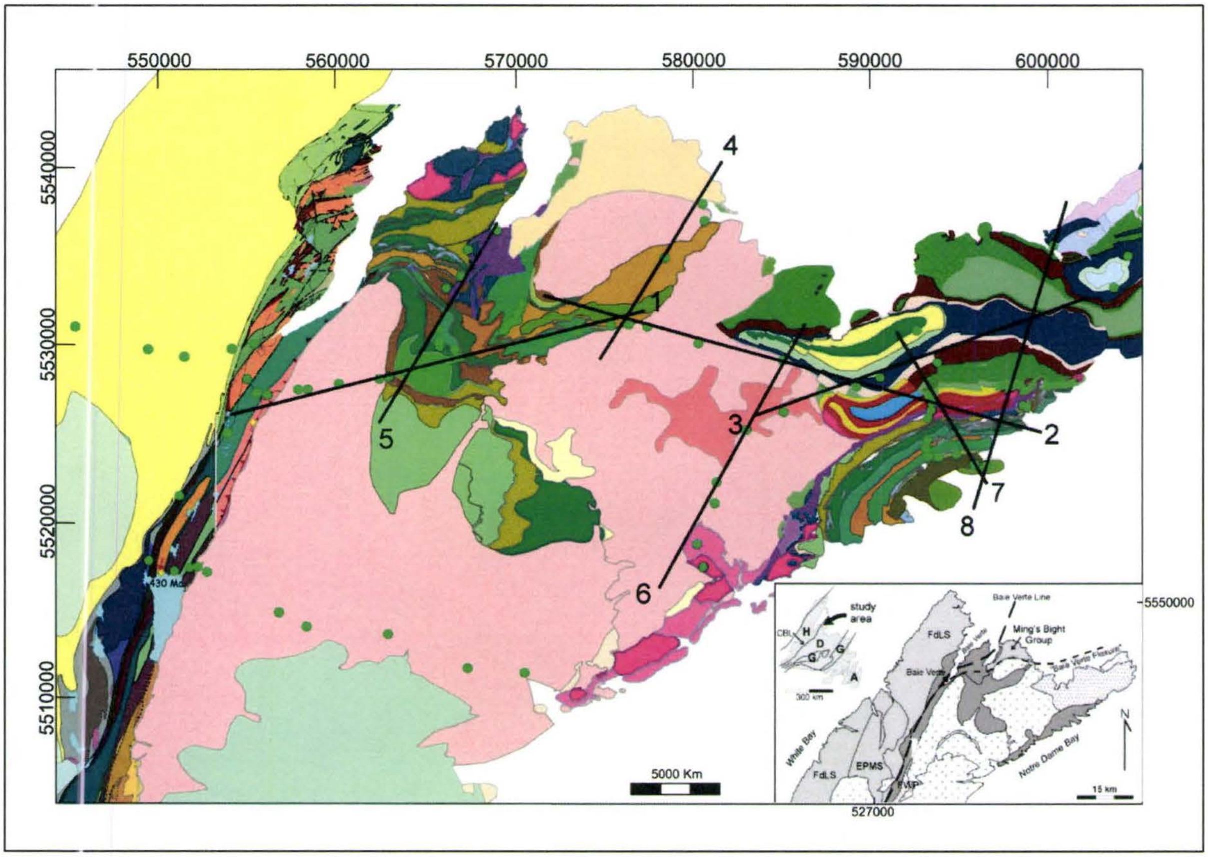
550000
560000
570000
580000
590000
600000
5540000
5530000
5520000
5510000
4
1
5
3
2
7
8
6
430 Ma
5000 Km
5550000
527000
study area
CBL
H
D
G
G
A
300 km
Baie Verte Line
FdLS
Ming's Bight Group
Baie Verte
Baie Verte Flexure
White Bay
FdLS
EPMS
Notre Dame Bay
15 km
N

Figure 5-1 - The Baie Verte Peninsula. Model profiles are displayed (black lines) and samples sites for physical rock property specimens have been included (green dots). Detailed geology from Skulski et al. (2010) and inset from Anderson et al. (2001).

The BVP underwent a complex polyphase structural history (D1-D4) with deformation starting in the Ordovician related to ophiolite (BVOT) obduction and accretion of the Notre Dame arc (van Staal et al. 2007). Little evidence of this deformation has been preserved in the BVOT and most deformation present in these rocks is due to subsequent Silurian to Devonian oblique accretion of outboard terranes. Orogenesis terminated with Carboniferous deformation accompanying the collision between Laurentia and Gondwana. The various structures formed during these events have been summarized by Hibbard, (1983) and Castonguay et al. (2009).

Geophysical Setting

Magnetic and gravity maps (Fig. 2) of the BVP are significantly influenced by the distribution of the ophiolite and volcano-sedimentary cover packages. These geologic units simultaneously possess high density and high magnetic susceptibility which leads to increased gravitational and magnetic signals relative to surrounding lithologies. Recognizing this, several geophysical studies (Miller and Deutsch, 1975, 1976; Haworth et al. 1978; Haworth and Miller, 1982; Spicer et al. 2010) have been implemented on the BVP including Canada's National Lithoprobe Geoscience Project (Miller and Wiseman, 1994, Waldron et al. 1998).

Previous geophysical studies on, or near, the BVP have attempted to provide subsurface insight along limited profiles (Miller and Deutsch, 1976; Waldron et al. 1998). Although some depth and physical property information have been revealed through these reports, the three dimensional distribution of geology on the BVP was never fully investigated. This stems from the fact that most of these studies were limited to under-sampled, low-resolution surveys (Haworth and Miller, 1978; Miller and Wiseman, 1994) or were designed to address issues of a larger scale in which the BVP encompassed only a minor component (Miller and Deutsch, 1975).

The occurrence of oceanic crust at depth along the eastern portions of the BVP was suggested by Miller and Deutsch (1976) on the basis of forward models along two profiles of regional gravity data with a mean station spacing of 2.5km. Further examination of gravity by Jacobi and Kristoffersen (1976) also showed the gravity highs to be confined within the margins of Notre Dame Bay. Haworth and Miller (1978) presented regional scale interpretations of magnetic and gravity data for offshore BVP within Notre Dame Bay. Limited to the easternmost extent of the BVP, they reported a consistent seaward (east) dip for all ophiolitic units along the Western margin of Notre Dame Bay. They provided a maximum depth extent of 7km for ultramafic ophiolitic rocks within Notre Dame Bay; however no information regarding the onshore extent of these bodies at depth was examined for the BVP in this study.

Miller and Wiseman (1994) adopted a more geological perspective in their work, moving from simplified single-slab models (Miller and Deutsch, 1976) to recognizable geologic cross sections with interpreted lithologic packages and major faults. Two east-west oriented magnetic and gravity transects were modeled. The more easterly profile of Miller and Wiseman (1994) attempted to model the subsurface geology on the eastern margin of the BVP. In their model Miller and Wiseman (fig 10, 1994) propose that the eastern side of the BVP is underlain by a Grenvillian terrane. The Cape Brule porphyry is modeled as directly overlying the Grenville. To model the increased magnetic and gravity signature seen along the eastern coast of the BVP Miller and Wiseman (1994) proposed a steep easterly dipping sequence that comprised the Snooks Arm Group and the Betts Cove Complex overlaying the younger Cape St John Group. All of these units are modeled as overlying a deeper more shallowly dipping dense and magnetic unit which was hypothesized as being part of a much larger fragmented ophiolite imbricate thrust sequence. Recent geological mapping as part of the TGI3 program has supplanted many of the surface constraints used in this

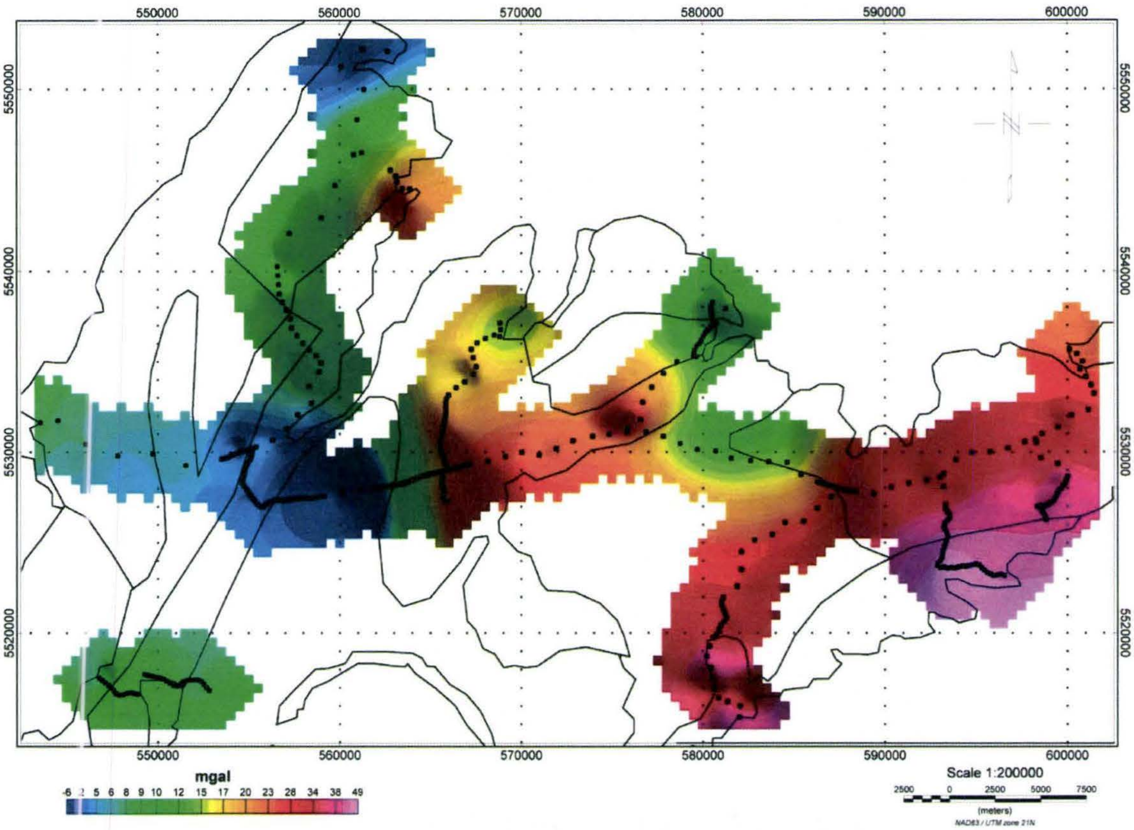
550000
560000
570000
580000
590000
600000
5550000
5540000
5530000
5520000
mgal
-6 2 5 6 8 9 10 12 15 17 20 23 28 34 38 49
Scale 1:200000
2500 0 2500 5000 7500
(meters)

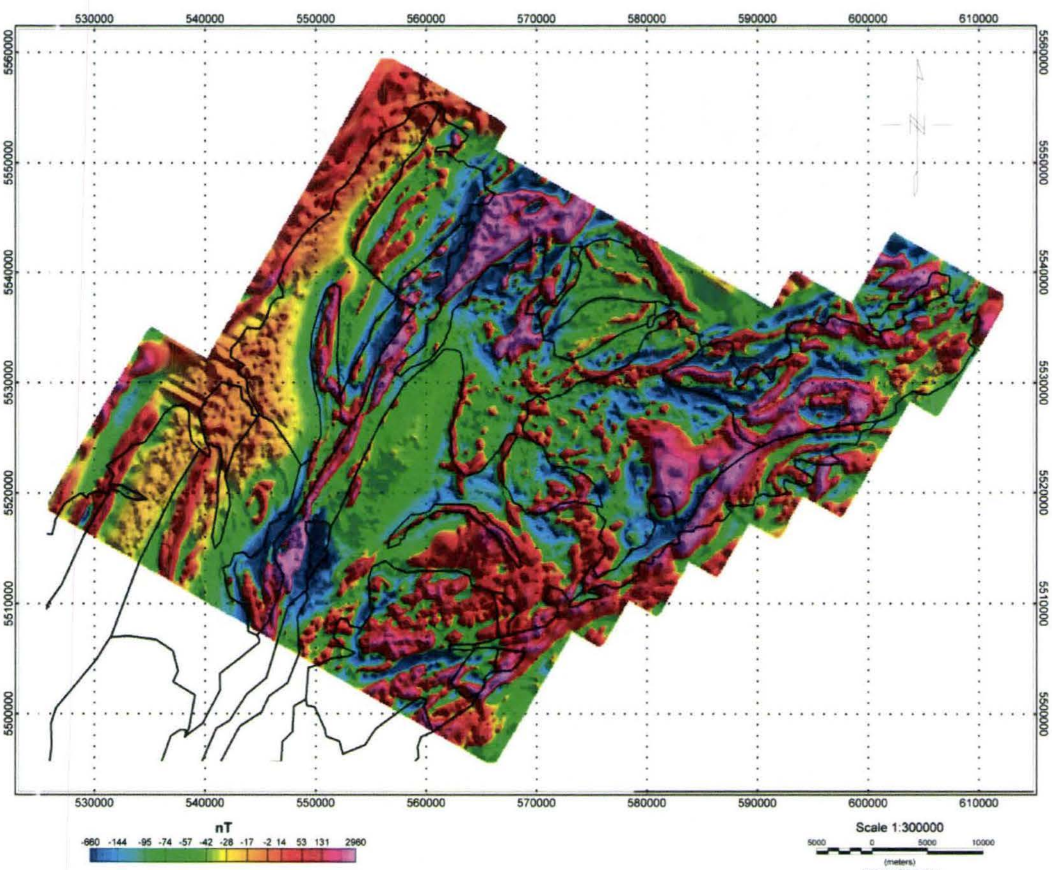
530000
540000
550000
560000
570000
580000
590000
600000
610000
5560000
5550000
5540000
5530000
5520000
5510000
5500000
nT
-660 -144 -95 -74 -57 -42 -28 -17 -2 14 53 131 2960
Scale 1:300000
5000 0 5000 10000
(meters)

Figure 5-2 - Geophysical data utilized for modeling. Generalized geologic elements have been overlain. Gravity (above) stations are displayed as black dots while magnetic (below) flight lines are not presented. Areas of simultaneous gravity and residual magnetics highs represent the occurrence of ophiolitic bodies.

profile. More recent detailed geophysical modeling of the Betts Cove Complex (Spicer et al., 2010) has suggested that the original model of Miller and Wiseman (1994) is incomplete.

The more westerly profile modeled by Miller and Wiseman (1994) focused on the subsurface structure associated with the BVL. Unlike the other profile this one incorporated depth and lithological contact constraints provided by Lithoprobe Seismic Line 89-13. While the general form of the interpretation does not differ from previous models (Miller and Deutsch 1976; Haworth and Miller, 1982), the later model included a westward dipping reflector which was thought to be cut by an east dipping listric BVL. Miller and Wiseman (1994) model the area east of the BVL as comprising an ophiolite sheet overlaying Grenvillian basement which in turn is overlain by a thin cover of Burlington Granodiorite. To accommodate the reduced magnetic signal adjacent to the BVL, Miller and Wiseman (1994) invoked a gradual thinning of the ophiolite sheet accompanied by a dramatic reduction in magnetic susceptibility. Using the same seismic line data Waldron et al., (1998) incorporated an additional near surface, vertical to slightly westward dipping zone of reflectors that were thought to represent boundaries to the Advocate Complex ophiolite suite. These features were not incorporated into the potential field models of Miller and Wiseman (1994). As noted above the BVL has had a long and complex displacement history which includes periods of lateral, and both and upward and downward displacement. So any profile attempt to model the form of the BVL can only describe the geometry as seen at one locale. Its true form can only be partially realized through a 3D investigation which can unravel some of the variations that exist along its length.

Geophysical Data

Grids

Data utilized within this study includes a detailed aeromagnetic survey acquired by the GSC (Coyle and Onescnuk, 2008) and a regional gravity survey (Spicer, 2008). These datasets are all sampled at a much higher resolution than any previous study implemented on the BVP and supplemented by new 1:20,000 scaled geologic maps and structural data (Skulski, et al. 2010).

Gravity data (Fig. 2) was collected along major roadways of the BVP with variable sample spacing ranging from 2 km to 200 m, depending on the vicinity to mapped contacts (Spicer, 2008). This data was reduced to the Bouguer anomaly (Telford, 1976) using a Bouguer slab density of 2.67 g/cm^3 and was gridded with 500m cells and a blanking distance of 1.5 km. This blanking distance was adopted as a compromise between sampling distribution and grid extent. A small blanking distance ensures true values are displayed at their proper geographic location. A larger blanking distance will increase the extent of the grid based on trends within the data extrapolating beyond the confines of, in this instance, restrictive roadside profiles. A high resolution DEM was down-sampled to match the gravity sampling rate for modeling purposes.

The high resolution aeromagnetic survey (Fig. 2) collected along flight-lines spaced 250m was utilized for this work. The flight direction within this survey was along a 300 degree bearing in order to optimize signal coupling between the regional geologic strike and the magnetic survey, a component lacking within the previous regional airborne survey. The data from this survey was IGRF corrected, micro-leveled to remove along line corrugations related to non-geologic input, then reduced to the pole to avoid geographic related asymmetries (Telford et al. 1976). This data was also implemented in the use of 3D magnetic inverse modeling as well. 3D magnetic inversions were performed to a depth of 10km using a mesh of 250m voxels. The methodologies involved in implementation of inverse modeling are presented in Spicer et al. (2010b).

Code	Density (g/cm^3)	SD	Susceptibility K (* 10^-6 SI)	SD	n	Type	Description
NPF	2.72	0.03	71.71	124.04	4	Humber	
OBBD	2.83		15.55		1	Epiclastic	Debrite
OBBf	2.80	0.02	3.28	3.23	2	Felsic Volcanic	Rhyolite
OBBs	2.64	0.02	458.45	642.10	2	Epiclastic	Grapolitic siltstone/shale
OBCe	2.76	0.02	17.44	9.24	3	Epiclastic	wacke, siltstone, shale
OBCf	2.68	0.02	13.97	9.87	3	Felsic volcanic	felsic tuff, lapilli tuff
OBCma	2.81	0.01	26.16	0.57	2	Mafic Volcanic	Andesite
OBCm	2.96	0.03	9.10	1.77	3	Mafic Volcanic	Massive gabbro cut by gabbroic dykes
OBHb	2.92	0.05	19.43	6.63	2	Mafic Volcanic	boninite, pillowed flow
OBHf	2.79		1.38		1	Felsic Volcanic	Rhyolite
OBHm	2.92	0.06	10.02	2.81	4	Mafic Volcanic	Massive and layered gabbro; intermediate TiO2 boninite affinity
OMMm	2.93		11.37		1	Mafic Volcanic	pillow basalt; BABB
OMS	2.95	0.06	359.80	695.85	4	Serpentinite	Altered ultramafics
ORHm	2.96	0.09	1478.62	2058.24	2	Mafic Volcanic	pillow basalt; tholeiitic BABB
OSAg	2.99	0.09	379.01	647.82	4	Mafic Volcanic	Gabbro dykes/sills
OSPm	2.97	0.08	8.00	4.34	4	Mafic Volcanic	pillow basalt; BABB, LREE-depleted BABB
OSPv	2.95	0.00	9.29	6.21	2	Mafic Volcanic	volcaniclastics
OVBm	2.94	0.05	74.28	157.50	7	Mafic Volcanic	pillow basalt; BABB
SAPl	2.82		2846.43		1	Felsic Volcanic	black lapilli tuff
SBGd	2.72	0.04	66.25	112.70	9	Felsic Intrusive	Burlington granodiorite
SBPb	2.85		4753.89		1	Mafic Volcanic	magnetic volcanic breccia
SCB	2.68	0.06	155.03	248.04	6	Felsic Intrusive	Cape Brule Porphyry (Granodiorite)
SCBi	2.68	0.01	22.42	29.75	2	Intermediate Intrusive	Cape Brule Porphyry (intermediate, quartz-diorite)
SCPr	2.84		522.09		1	Felsic Volcanic	Rhyolite (magnetite bearing)
SCSJu	2.84		522.09		1	Felsic Volcanic	Rhyolite (magnetite bearing)
SDGr	2.65		268.68		1	Felsic Intrusive	Dunamonon Granite
SGPb	2.81	0.08	4308.50	950.09	2	Mafic Volcanic	heterolithioc volcanic breccia, strongly magnetic, dark mafic matrix
SGPw	2.61		6.82		1	Felsic Volcanic	Felsic Tuff
SLPm	2.87	0.03	6.33	0.41	2	Mafic Volcanic	massive amygdaloidal, continental tholeiitic basalt
SMBm	2.99		144.12		1	Mafic Volcanic	upper massive amygdaloidal basalt
SML	2.68	0.07	9.31	8.53	3	Mic mac	
SRCPb	2.60	0.12	1.19	0.27	2	Felsic Volcanic	felsic tuff breccia xmas unit
SSIB	2.67		270.38		1	Felsic Intrusive	syenite
SWPr	2.64	0.02	394.20	50.71	2	Felsic Volcanic	aphyric flow banded rhyolite

Table 5-1 - Physical rock property database used for modeling across the Baie Verte Peninsula.

Petrophysics

Knowledge of physical rock properties is an essential component to any geophysical model. Physical property variations are the causative driving force behind observed geophysical signal anomalies. It is uniformly acknowledged that any computed potential field models represent a non-unique mathematically constrained best fit approach to explaining the observed geophysical signature. Since one of the variables in potential field model computation involves the physical property of the rock unit including a known value for a particular rock unit serves to reduce the degree of possible variation. For the gravitational signal which is related to the mass of an object, this requires that density, p, measurements should be taken. The magnetic signal recorded in a magnetic survey is dictated by the magnetic mineralogy of the geology. The physical property in this case is known as the magnetic susceptibility, *k*, or ease of magnetization. Measurements *k* of are taken as a ratio between the magnetic polarization, I, of a material to an external magnetic field, H (Telford et al. 1976).

Rock samples used in this work were collected during previous studies on the BVP (Slavinski, 2007; Spicer, 2008; Spicer et al. 2010). Magnetic susceptibility was measured using a Bartington Instruments MS2 magnetic susceptibility meter. Density values were calculated employing a standard Archimedes Principle specific gravity ratio relative to water. The corresponding lithologic codes assigned to sample specimens were based on recorded GPS positions and the most current geologic maps (Skulski et al. 2010). Additional physical property values not previously reported have been summarized in Table 1. Petrophysics values from Spicer et al. 2010 were implemented exclusively in the Betts Cove area. Values for geologic formations not sampled yet included in models to satisfy known geology were assigned based on rock types (Daly, 1935) then altered as required by the geophysical signal.

Results and Discussions

Models

Geophysical modeling of magnetics and gravity was executed along eight profiles across the BVP (Fig. 1). While cross-sections are more easily produced when created perpendicular to geologic strike, the nature of the regional gravity survey (Fig. 2) dictated that profiles be measured along the major roads which do not necessarily follow such criteria. All cross-sections contain at least, but are not confined to, one intersection with another profile (Fig.3). This principle, absent in previous geophysical investigations of the BVP, ensures continuity in depth and distribution of modeled structures and lithologies. Geologic, or structural trends defined on the topographic surface were honored, but were modified in the subsurface to accord geological continuity with the geology on an intersecting profile. A stronger degree of confidence was assigned to constraints for profiles oriented perpendicular to mapped geology. Apparent dip angles were calculated for each profile taking true dip, dip direction and the cross sectional bearings into account using the Rock Ware's Geotrig software. The Models presented here assume a basement of uniform density and magnetization except in specific instances where mapped geology and physical properties require furthered explanations. The depth to basement is roughly 6-7km on the eastern portions and near 3-5km in the west. This is in agreement with previous studies documenting an eastward dipping subduction zone below the BVP. Additional constraint was provided using models from 3D inversions implementing UBC-GIF code. While unconstrained inversions are inherently non-unique they can provide information regarding possible values and more importantly structural dip directions. All modeled responses include a magnetic and gravity signal. Profiles were limited by the extent of the regional gravity coverage. Each profile uses a consistent lithology colour coding. Figure 4 displays the legend implemented for all profiles.

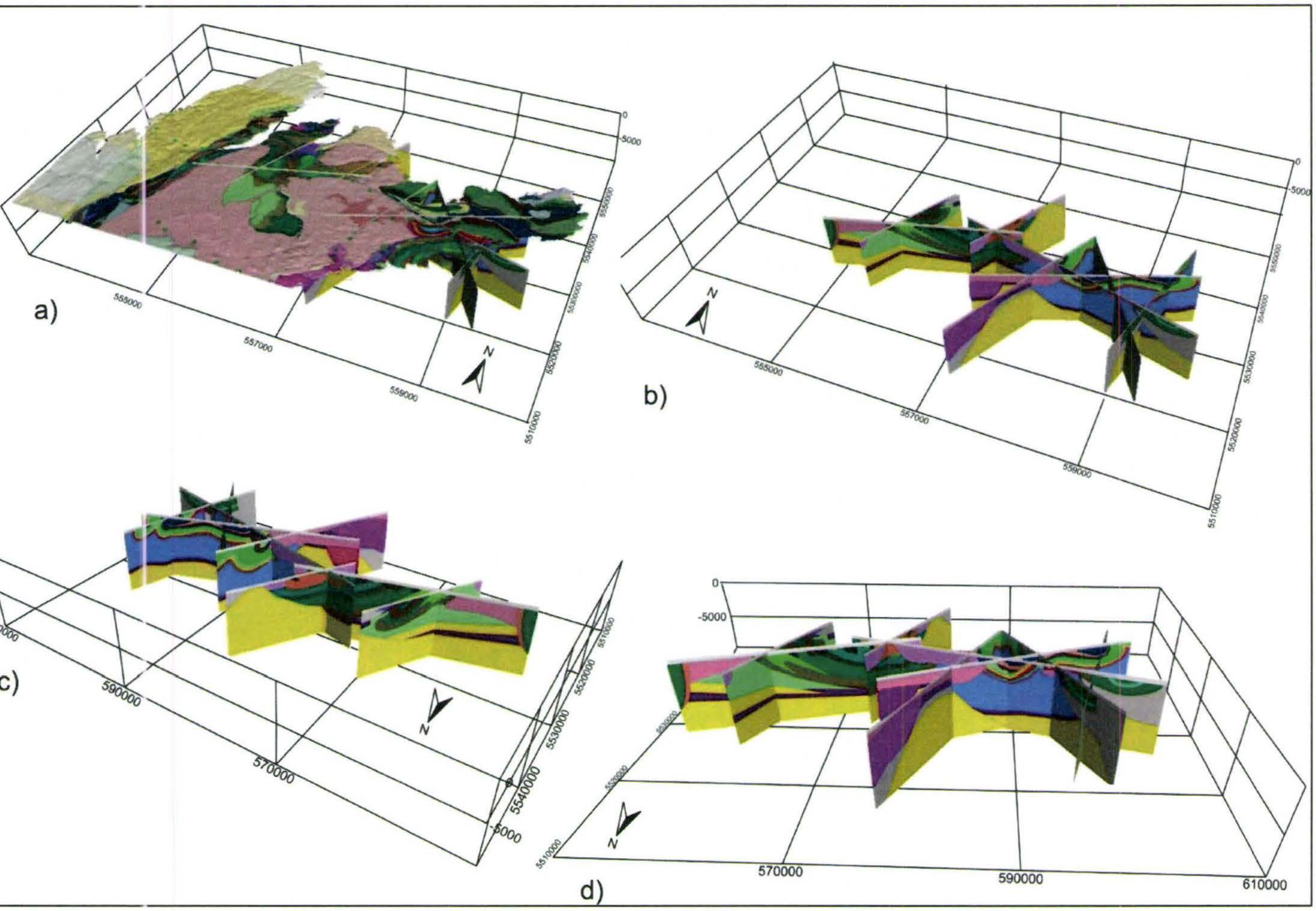
a)
b)
c)
d)
570000
590000
610000
-5000
0

Figure 5-3 - 2D geophysical profiles in 3D space demonstrates the intersection points and the continuities across each section. Regional views with (a) and without geology (b). Close up view towards the south (c) and north (d).

Profile 1

This section begins in the Flatwater Pond Group, a series of mafic and felsic volcaniclastic rocks with some lesser associated conglomerate and finer grained silicilastic sedimentary rocks (Fig. 5). These rocks have a complex history of strike and dip slip movement along the fault zone that marks the Baie Verte Line. These units are juxtaposed against the Burlington Granodiorite (BG) along a steeply inclined, slightly westward dipping fault. The exact form of the fault surface is poorly constrained by the geophysical data. Evidence of the BG is clear within the regional gravity profile where a large negative anomaly represents the presence of a granite body surrounded by ophiolitic rocks. The base of the BG is modeled to a maximum depth of 2 Km along peripheral contacts and its core has folded to form an anticline. This has been included based on observations within the geologic map where units directly along the northern terminus of the BG display an antiformal map pattern.

To the east, units of the Pacquet Harbour Group continue along the limb of this anticline, plunging roughly 40 degrees at surface. The core of the Rambler Rhyolite, which previously had been considered a dome, has been reinterpreted as a fold interference pattern based on new mapping (Fig. 1). Castonguay et al. (2009) and Skulski et al. (2010) suggested that the Ming and Rambler deposits occur along the same stratigraphic horizon, situated along the contact between the rhyolite and basaltic rocks. This fold interpretation has significant economic implications, because it requires that the ore bearing horizon should reoccur along the southern contacts of the Rambler rhyolite, which have been much less explored in the past. This area of the Rambler structure is thus a highly prospective exploration target. However, this part of the fold has been highly attenuated and modified by the Rambler Brook thrust.

The synformal core of a tight to isoclinal, upright fold is hosted within the pillow lavas of the Round Harbor formation at the edge of the geophysical profile. However continuation of the fold at depth below the adjacent Cape Brule Porphyry is poorly known. This geophysical response of the model is discontinued near the axis of the fold, however 3D magnetic inversions support the notion that that some fold limb dips to the west (Fig.6). To the east of the CBP the Cape St. John group must be encountered. The nature of this contact between the PHG and the CSJG is unknown at the present (See Profile 6) however a sharp transition of regional geologic trends suggests that some unconformity or tectonic contact may be in place.

Throughout the PHG gabbroic intrusions into the volcanic pile seem to dominate the magnetic signal. This resembles the responses observed in the equivalent Snooks Arm cover rocks above the Betts Cove ophiolite (see profile 7 and 8) where magnetic peaks are often associated with the mafic sills and dykes. These units commonly have sub vertical orientations. On a regional scale these dykes can be grouped in larger pods throughout the PHG a more detailed interpretation of their extent is presented in Spicer et al., (2010b).

Profile 2

Profiles covering a larger area can provide greater insight into the overall geometry and hence fundamental structural relationships between the major units, particularly where they are masked at surface by intrusions. An example is provided by profile 2. Here the 487 -470 Ma (V. McNicoll, unpublished data, 2009) Pacquet Harbor Group (PHG) is exposed in the west while the 426 Ma (V. McNicoll, unpublished data 2008) CSJG is present in the east, both separated by the CPB

Regionally the profile (Fig. 5) documents the occurrence of two mapped synclines separated by a Silurian granitoid. In the middle where the Cape Brule Porphyry intrudes, an antiform is interpreted. This area is difficult to interpret as it is associated with a significant change in regional structural trends yet is covered by an intrusive sheet; however the gravity is permissive of a limited degree of antiformal curvature within the CBP. While the Snooks Arm and Pacquet Harbour Groups may be correlatable (Castonguay et al., 2009; Skulski et al., (2010) the nature of the transition between the two is difficult to define and geophysically these two units are indistinguishable. The pillow basalts and mafic volcanics of the Lower Pacquet Harbor Group yielded densities of 2.87-2.9 g/cm^3 (Table 1) while the SAG is here simplified (Fig.4) as a large body in the subsurface with a density of 2.86-2.88 g/cm^3 which is based on an overall average of the package. The PHG is continued to the base of the CPB along the surface trends, however it is more probable that units refold within the interpreted anticline and carry on below the CSJG as the SAG.

After this transition there is an abrupt change to lithologies of the CSJG. While there appears to be no evidence of significant faulting at this depth, an unconformity surface may provide the necessary mechanism for such a shift (see profile 6). A fault surface in tectonic contact with the CBP gives an apparent normal sense as the upper CSJ are juxtaposed to lower units. This however is a case of an early F2 fold limb being propagated towards its core during late stage faulting. This fault 'scoop' has been affected by later extensional faulting (see profile 3). Moving east a granitic intrusion is encountered near the surface. This is a geophysical rather than mapped requirement. Very tight folds are modeled to explain map patterns of the lower CSJG near the contact with the Betts Cove Ophiolite Complex. Here the Betts Cove Ophiolite Complex is a synclinal feature with only portions of the SAG present. Serpentinized ultramafics border the structure and below, high density and strongly magnetic mantle peridodite is interpreted to complete the stratigraphic column and satisfy the geophysics. The maximum depth to the basement contact here is only 5km, suggesting the basement has been uplifted during Salinic thrusting (see profile 7) of the BCO over its cover. Further offshore ophiolite is predicted up to depths of 10 Km (see profiles 7 and 8).

Profile 3

This profile is a large section constructed obliquely to the regional geologic strike (Fig.7). Surface contacts were honored however the depths of lithologies and structures presented within this model are the results of intersection constraints from four sections more perpendicular to strike.

Beginning in the west, this profile consists of the Cape Brule Porphyry overlying the Snooks Arm Group, some portion of altered ultramafics, and a basement which is trending towards the surface. The slope observed in the basement may be the consequence of some preexisting morphology, or later fault controlled tilting. A deep-seated northeast dipping fault has been included based on the requirement of uplift in this area within profile 6. The faulting within these profiles is a hypothesis formulated as a consequence of the large magnetic anomaly within the center of the CBP. Some deep seated northeastern dipping structures are also revealed within the magnetic inversions (Fig.8). Based on position, amplitude strength and its broad coverage this anomaly is likely to represent a piece of near surface ophiolite. Some mechanism is required; faulting seems the most likely to explain such an offset. This may be related to the original obduction thrust which is the current understanding for the position of the Betts Cove Ophiolite, however extensional collapse as encountered at Ming's Bight may also be a potential source of explanation.

Further east, the contact between the CBP and the CSJG is encountered. This is non-tectonic and dips steeply to the southwest unlike in other sections where south directed thrusts have created a northeast dipping contact. Adjacent to the contact, a thrust surface hosts the core to a syncline. The full nature of this thrust remains unclear as the geophysical signature is not well matched. Based on evidence presented in other profiles however, the magnetic signal associated with this fault cannot be explained based on the current geologic map (see profile 7). This thrust also consists of a dismembered portion with normal faults dipping to the west, presumably formed some during late stage extensional stress.

Cape St. John Group
Continental Cover

SBCl	Brents Cove Formation - Pumice bearing lapilli tuff	SSPm	Sisters Pond Formation - Massive amygdaloidal basalt
SCPr	Carolina Point - Formation- Magnetite-bearing rhyolite	SBPt	Bench Pond Formation - Fine grained felsic tuff
SGCr	Grand Cove Formation - White massive rhyolite	SGPb	Goss Pond Formation - Strongly magnetic mafic volcanic breccia
SWPr	Welsh's Pond Formation - Aphyric flow banded rhyolite	SRCPb	Red Cliff Pond Formation - Felsic tuff breccia
SlCl	Little Caplin Cove Formation - Beige lapilli tuff	SGPw	Goat Pond Formation - Welded tuff
SAPi	Armchair Pond Formation - Black lapilli tuff	SLPm	Loon Pond Formation- Massive amygdaloidal, tholeiitic basalt

Snooks Arm/Pacquet Harbor Group
Syn-obduction ophiolite cover

SAG	Snooks Arm Group - Lumping	OVBm	Venam's Bight Formation - Pillow basalt
ORHm	Round Harbor Formation- Tholeiitic pillow basalt	OBCe	Bobby Cove Formation - Wacke, siltstone, shale
OBBd	Balsam Bud Cove Formation - Debrite	OBCm	Bobby Cove Formation - Pillow basalt, andesite (calc-alkaline)
OBBs	Balsam Bud Cove Formation - Graptolitic shale, siltstone	OSPv	Scrape Point Formation - Tholeiitic pillow/flow basalt
OBBf	Balsam Bud Cove Formation - felsic lapilli tuff	OSAm	Late mafic sills and gabbroic dykes

Baie Verte Oceanic Tract
Ordovician ophiolite complexes

OMMf	Mt. Misery Formation - Boninitic rhyolite/rhyodacite	OBHr	Pillow Basalts, Sheeted Dykes and Gabbro
OMMm	Mt. Misery Formation - Pillow tholeiitic basalt	Oms	Serpentinite and altered ultramafic cummulates
OBHb	Bett's Head Formation - Boninite, pillowed flows		Mantle ultramafics

Granite
Silurian intrusions and the Laurentian continental margin

	Granite, Granodiorite, qz-feld porphyry		Basement

Figure 5-4 - Legend for lithologies contained within geophysical profiles.

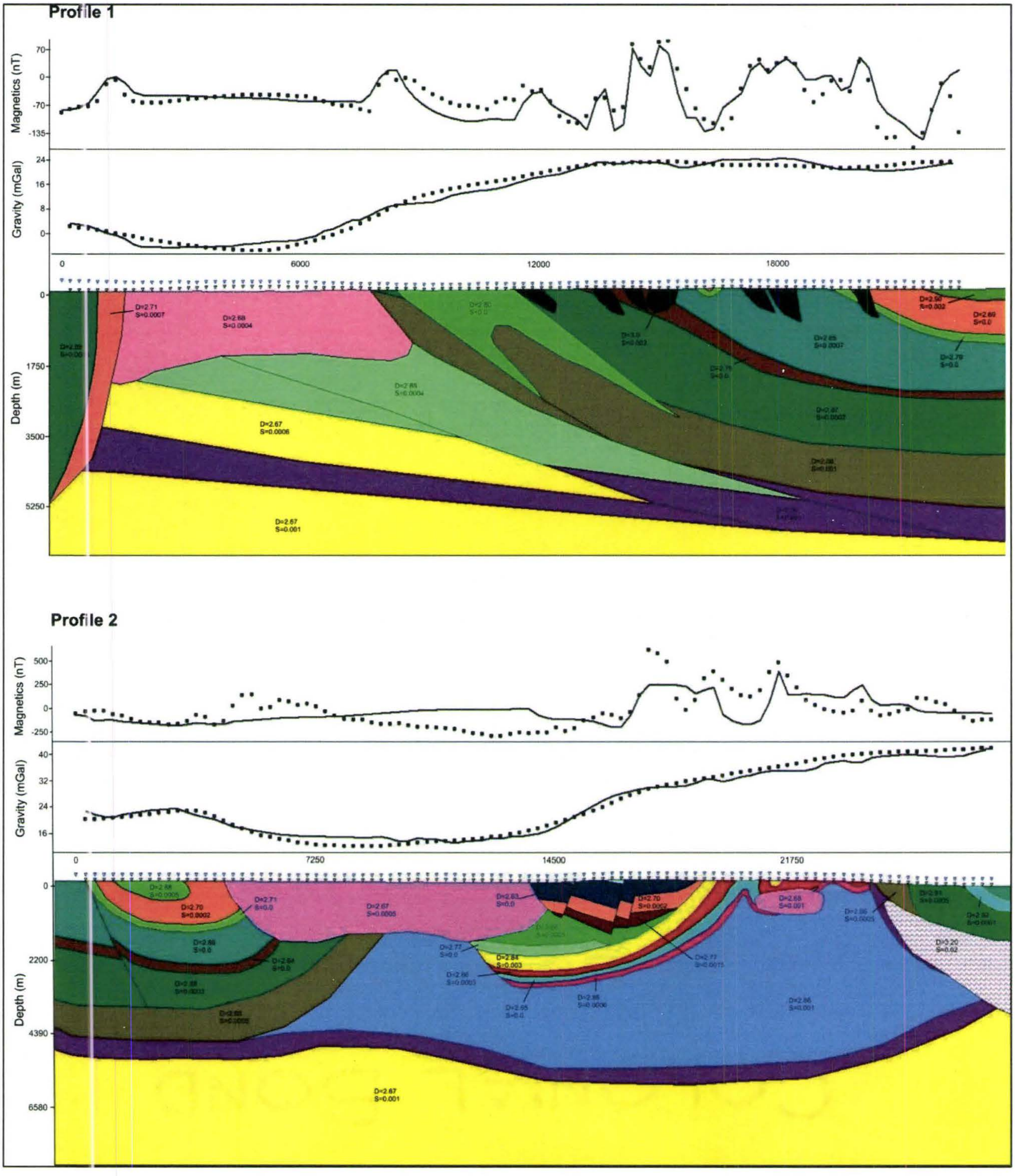
Profile 1
Magnetics (nT)
70
0
-70
-135
Gravity (mGal)
24
16
8
0
0
6000
12000
18000
Depth (m)
0
1750
3500
5250
Profile 2
Magnetics (nT)
500
250
0
-250
Gravity (mGal)
40
32
24
16
0
7250
14500
21750
Depth (m)
0
2200
4390
6580

Figure5- 5 - Geophysical forward models of profiles 1 (above) and 2 (below). Observed magnetics and gravity signals (black dots) and forward model response (solid black) are shown.

An anticline and syncline are encountered next while moving to the east. These host the north south trending axis and represent F_3 cross folding. This suggests folds within the CSJG are also doubly plunging, similar to the nearby Betts Cove Ophilite (Spicer et al. 2010). The modeled gravitational response of the anticline is larger than he observed signal while the synclines gravity appears too low. Constraints from this side are derived from profile 8 where the depth of the syncline core is well supported within by gravity.

Overall, the modeled response of this section does not match the measured signal as tightly as others. This is the result of a complicated map pattern and the restrictions imposed by other profiles. Further complicating matters, the geologic map within this area appears to require some revisions. While this is beyond the scope of this investigation, altering the surface contacts of the map within problematic areas of this profile would significantly alter the map pattern.

Profile 4

Profile 4 (Fig.7) is an important transect across the BVP as it includes the Ming's Bight outlier. Originally the interpretation of the BVP was rather simplified; Ordovician ophiolites were obducted over the continental margin moving along an eastward dipping subduction zone (Hibbard, 1983). However the recognition of a Fleur Des Lys type geologic assemblage east of the BVL at Ming's Bight required some new form of explanation. Hibbard (1982) initially described the effect of some pre-existing continental morphology which he termed the 'Baie Verte Flexure' as a means to achieve this map pattern. Later work though would reveal a late Devonian to early Carboniferous dextral transtensional regime across the BVP (Anderson, 1998; Waldron et al. 1998). Bound by normal faults dipping to the southeast and southwest (Anderson et al. 2001) the Ming's Bight Group was hypothesized to be a horst-like structure and is in fact a tectonic window of basement.

This is the first geophysical model to explore the Ming's Bight area and highlights some issues with previously reported models. The gravity profile across this transect begins higher and decreases towards the shore where the basement window is exposed. Relative to the rest of the BVP though, this entire profile is a gravity low. Lithologies of the surfaceare almost exclusively low density material. Two Silurian intrusions, the Cape Brule Porphyry and the Dunamagon Granite (DG) flank an extensive body of siltstones and shales. The gravity profile increases slightly at the contact between the DG and the MBG. Sampling in the area is low, the DG and MBG have only one representative while the sediments only two (Table 1). All density values are within the lowest allowable range. Based on gravity the DG is a shallow structure. This can also be witnessed within the 3D magnetic inversion (Fig.6).

While the basement throughout the Peninsula has been modeled at 2.67 g/cm^3 in accordance with the average continental crust value and a high magnetic susceptibility based on the regional magnetic signal, the interbedded metasediments sampled of the MBG at surface had a density of 2.72 g/cm^3 and were non-magnetic. A block with these sampled parameters was included until a depth where the interpreted basement was encountered based on intersection points and trends within the other profiles. Even using this higher density, the gravity response across the MBG does not compute well enough and remains lower than observed. Inclusion of any higher density material below this area would be unwarranted based on current knowledge of the local geology and tectonics. Offshore regions may contain near surface ultramafics, the proximal Pointe Rousse Ophiolite complex (see profile 5) has been exhumed by D_2 southward directed thrust (Castonguay, et al. 2009). Inclusion of a large ophiolitic block in the Atlantic Ocean north of this profile allows for only a minor improvement in the overall model though and is still very speculative. A magnetic anomaly over the MBG suggests some form of alteration or the presence of finer scaled magnetic lithologies.

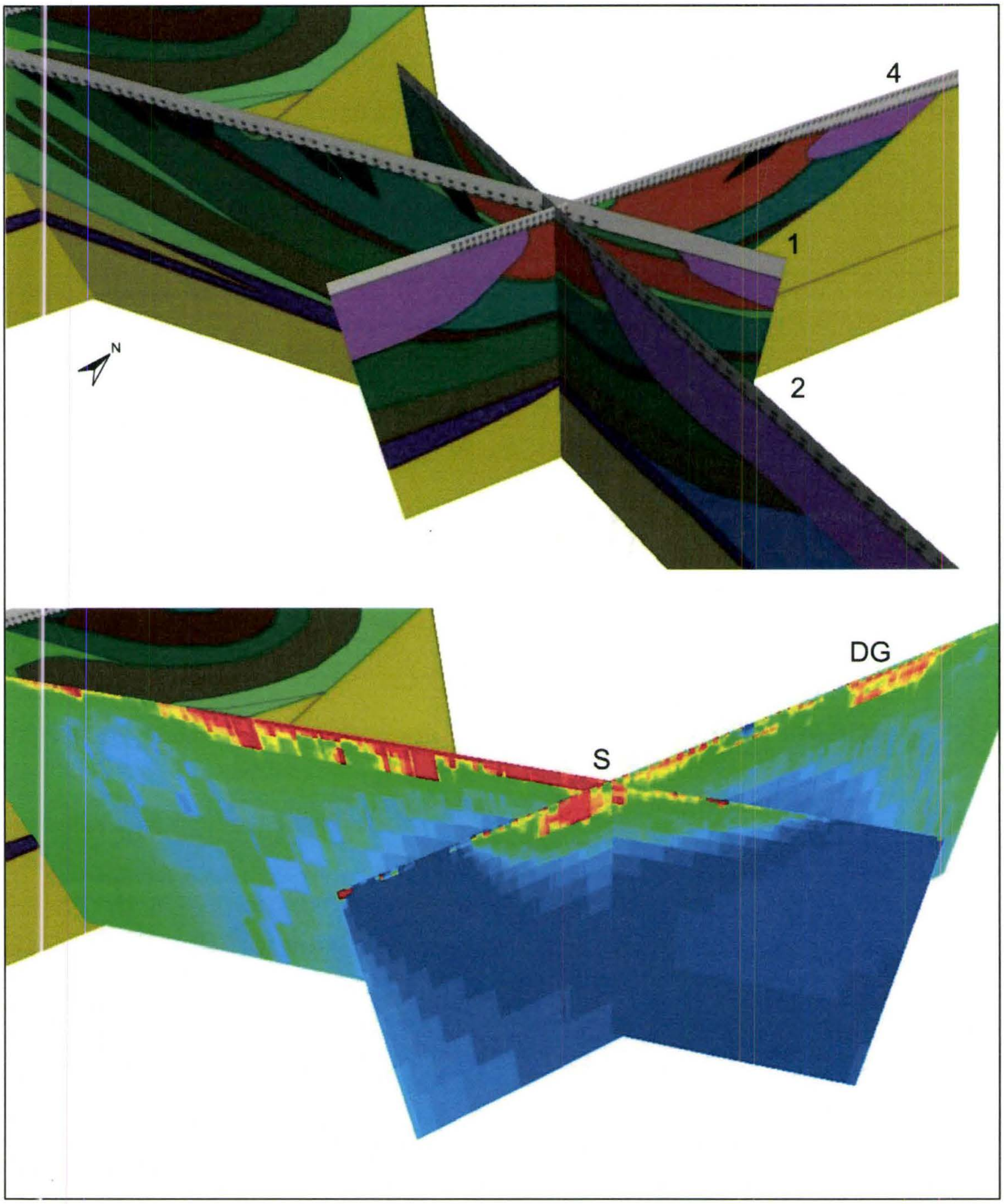
4
1
2
N
DG
S

Figure 5-6 - Intersecting 2D forward models (above) display the presence of a synclinal structure intruded by the Cape Brule Porphyry (pink). 3D magnetic inversions sliced along the azimuths of profiles 1 and 4 supports for the presence of such a structure (S). Further north, the Dunamagon Granite body (DG) can be seen as a sallow relatively magnetic body.

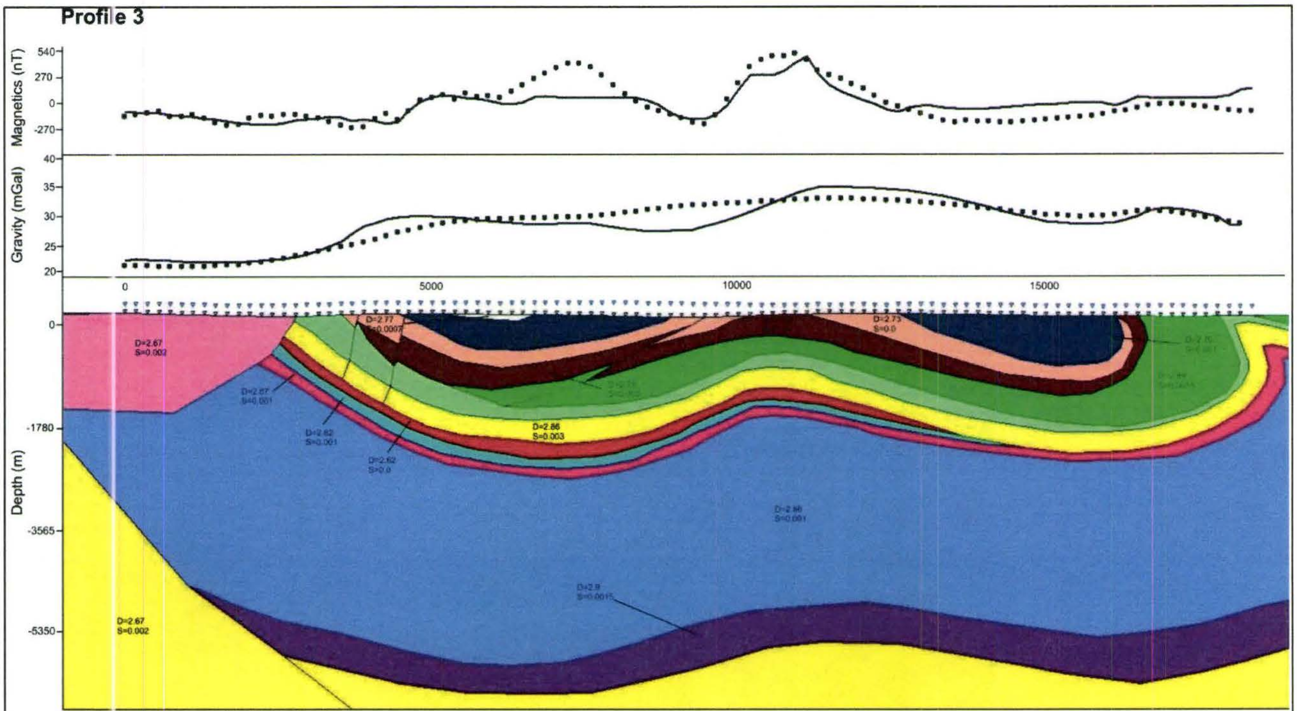
Profile 3
Magnetics (nT)
540
270
0
-270
Gravity (mGal)
40
35
30
25
20
0
5000
10000
15000
Depth (m)
0
-1780
-3565
-5350
D=2.67
S=0.002
D=2.77
D=2.73
S=0.0
D=2.86
S=0.003
D=2.67
S=0.002

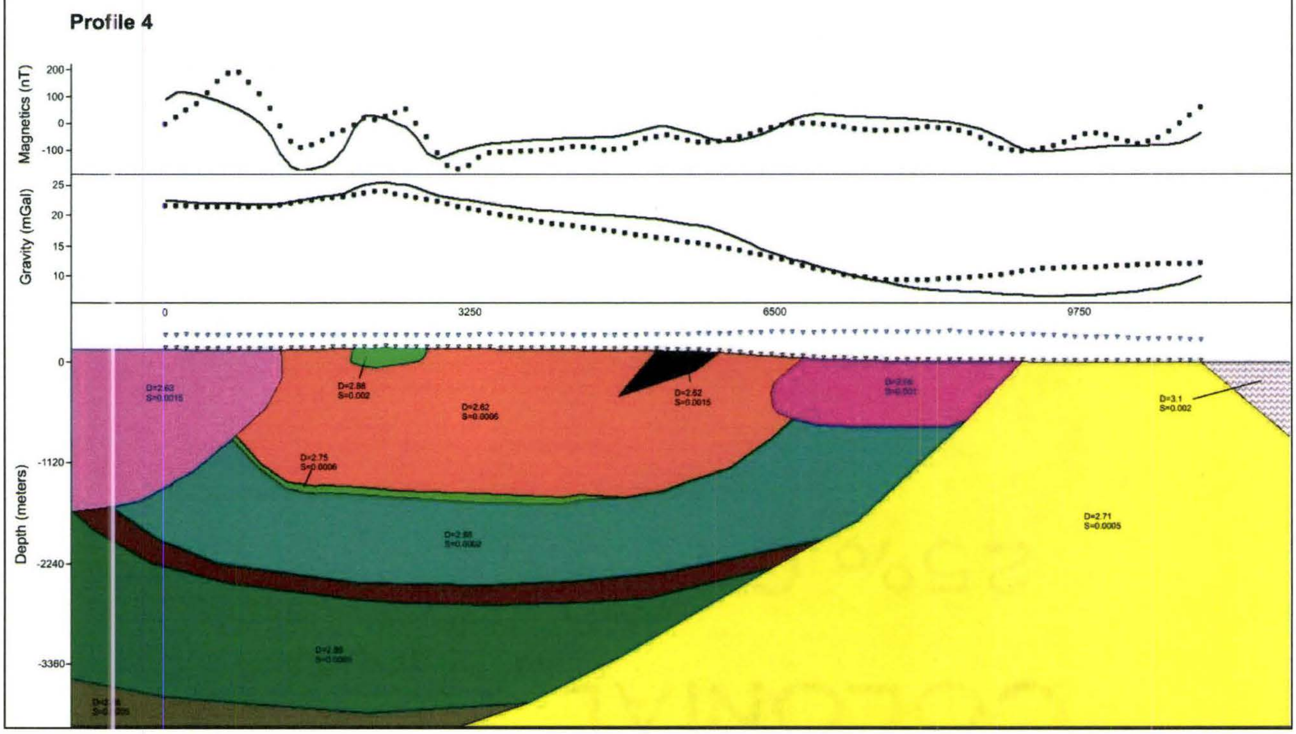
Profile 4
Magnetics (nT)
200
100
0
-100
Gravity (mGal)
25
20
15
10
0
3250
6500
9750
Depth (meters)
0
-1120
-2240
-3360
D=2.88
S=0.002
D=2.62
S=0.0006
D=2.62
S=0.0015
D=3.1
S=0.002
D=2.75
S=0.0006
D=2.71
S=0.0005

Figure 5-7 - Geophysical forward models of profiles 3 (above) and 4 (below). Observed magnetics and gravity signals (black dots) and forward model response (solid black) are shown.

Fine grained sedimentary rocks are modeled to a depth of roughly 1.5 Km. A lesser depth could be obtained if a larger sampling population revealed a lower density. The axis to a regional syncline is hosted within the magnetic pillow lavas correlated to the Round Harbor Group. As at Betts Cove, these rocks are very magnetic. A magnetic anomaly within the sediments may be explained by the presence of gabbroic dykes observed within the Pacquet Harbour Group (PHG), however the gravity does not support this. Below surface the lower portions of the upper PHG are in tectonic contact with the MBG.

Profile 5

This transect (Fig.9) cuts across the Rambler property. In the south a large portion of the Lower PHG is displaced by the Rambler-Brook fault across the upper PHG comprised of the Rambler rhyolite and other mafic pillow basalts and mafic rocks. To the north the Point Rousse Ophiolite complex is thrust above the Scrape Thrust. Interpreted at depth, the contact with the MBG occurs along a normal listric fault. This profile is plagued by significant edge effects. To the south a significant amount of bonitic pillows are indicated on the geologic map. Including these known geologic units though produces a very high gravity signal. This survey was performed on the main La Scie highway where the presence of significant overburden thickness may be having an effect on the observed gravity signal. Combined with the lateral proximity to the low values associated with the Burlington Granodiorite profiles extracted from the gravity grid are likely much lower than in actuality at this location. To the north the model shows more problems. The magnetic signal is dominated by the occurrence of the Point Rousse Ophiolite complex. The geology of this area is very complex, based mapping inconsistencies is appears the exact form of the geology in the subsurface remains unclear. The Point Rousse complex is heavily faulted. Three zones have been modeled, the first two are the serpentinized ultramafic and ultramafic cumulates from the map. The last, which extends seaward, has the characteristics of deep seated mantle in an attempt to strengthen the input of gravity. The edge effects of this profile remain rather severe though.

Profile 6

Profile 6 (Fig.9) permits the least degree of surficial constraint for modeling however gaining insight into the subsurface properties of this area will be critical to understanding the regional geologic framework of the BVP. Here, regional structural trends shift from northeasterly to primarily east-west along the 'Baie Verte Flexure' (Hibbard, 1982). The Cape Brule Porphyry, a late stage Silurian felsic intrusion covers most of this area preventing any analysis of primary structures by conventional geological mapping. However, a window of basalt and gabbro to the south implies that ophiolitic components are likely encountered at depth. The gravity profile across the area also suggests that a significant amount of high density material must be present within the subsurface of this area. The presence of ophiolite within this area is again supported when considering the residual magnetics. A broad, high amplitude anomaly present within the confines of the Cape Brule Porphyry requires a large zone of alteration which is undocumented, or some highly magnetic material below the intrusive. 3D UBC-GIF magnetic inversions across this site indicate similar results (Fig 8). Based on a location directly adjacent to the Betts Cove Ophiolite, this area of high density and increased magnetic susceptibility most likely represents the near surface occurrence of ophiolites. When considering the entire BVP, only ophiolites exhibit such a high magnetic signature over such a broad area. In order for this to be achieved, the ophiolite portion would have been thrust upwards, most likely during the same obduction stage as the other ophiolites on the peninsula.

On profile 6 a portion of altered ophiolite rests above a section of uplifted basement. This material exists 500 m below the Cape Brule Porphyry (CBP) and is more magnetic than any ophiolite elsewhere on the Peninsula. The structure presented is very similar to the horst-like model of the Ming's Bight Group on profile 4, presumably related to extensional stress during a late Devonian dextral transtensional regime

(Anderson et al., 2001; Waldron et al., 1998). The pattern of the magnetic anomaly suggests that this feature plays host to two fold axes (Fig 8). One trending to the northeast belongs to an anticline present within the modeled horst structure while the second which is east-west trending is likely related to folds documented within the Lower Pacquet Harbour Group to the near west (Skulski et al. 2010). Together these folds produce a dome feature. A large near surface occurrence of ophiolite within 2.5 Km of the Betts Cove mines should represent significant mineral potential.

In this profile, as well as others in sections 7 and 8, the presence of a highly magnetic basement is required. While a single fault has been modeled dipping to the south, a series of normal faults occurring along reactivated imbricate thrust sheets is a likely scenario to explain this morphology as well. To further complicate interpretation, the proximity of this structure to the Green Bay Fault implies that a complex history of stress and deformation must have occurred. Regardless, a thick sequence of high density material presented here as a mixture of pillow basalts and gabbro must be in place. In the northern sections of the profile a tectonic contact is proposed between the CBP and the CSJG. While current mapping of this area would support the presence of a thrust, insight provided in this model indicates that some late stage normal movement may also be possible. The Snooks Arm Group (SAG) and a layer of altered ultramafics rest below situated above the basement. Within these models as well as other works (Castonguay et al. 2009, Skulski et al. 2010) the SAG and the Pacquet Harbour Group (PHG) are considered contemporaneous. Near Betts Cove an unconformity relationship is observed between the SAG and the CSJ. Previous workers have debated the relationship between the CSJ and the PHG. Hibbard (1983) along with Neal and Kennedy (1967) believe that some unconformity, or tectonic contact, must be in present while others (Church, 1969; DeGrace et al. 1976) propose a conformable stratigraphy. In truth however, the contact is buried below the cover of a large Silurian intrusion. A detailed model of such a contact would be difficult to prove, or disprove, and is beyond the scope of this paper. The units within this profile however have been terminated abruptly along a surface which may be considered unconformable to the CSJ to satisfy geophysics and map patterns.

Profile 7

Profile 7 (Fig. 10) begins in the north within the Cape St. John Group and moves south where it cuts through the Betts Cove Ophiolite into Notre Dame Bay. While gravity stations do not extend past the shoreline, the model has been continued offshore to combat edge effects and to maintain faults trends from profile 6. Since full coverage of the BCO was beyond the means of the ground gravity survey implemented for this study, aspects of offshore components to this model are somewhat speculative. Using results from a marine magnetic survey, Spicer et al. (2010) provide evidence the BCO exhibits a significant reduction in magnetization a few kilometers offshore. This decrease in magnetization was explained in terms of significant faulting with the BCO lying under up to 2km of non-magnetic cover. This has many similarities to the Carboniferous cover sequence observed within the Deer Lake Basin (Cabot 2001). A mid Devonian to Carboniferous dextral transtensional regime (Waldron et al. 1998) responsible for the exhumation of the Ming's Bight outlier and another similar feature observed on profile 6 along the western margin of Notre Dame Bay may be responsible for an offshore absence of the BCO. With up to 30 km of dextral movement is documented along the Green Bay Fault (Marten, 1971) which trends to the northeast and is interpreted to extend only a few Km's to the shore of the Betts Cove Area, the offshore portions the BCO may be kilometers to the south. Miller and Deutsch (1976) however maintain that rocks of density 3.0-3.1 g/cm^3 exist to depths of 7-10 Km below Notre Dame Bay. This has been included within these profiles to maintain consistencies within the literature and to combat edge effects within the gravity profiles.

The magnetics of profile 7 are not adequately explained using surface patterns, there is an extra anomaly at the northernmost section not explained in the mapped geology (Fig.10). The "brown armchair pond" unit

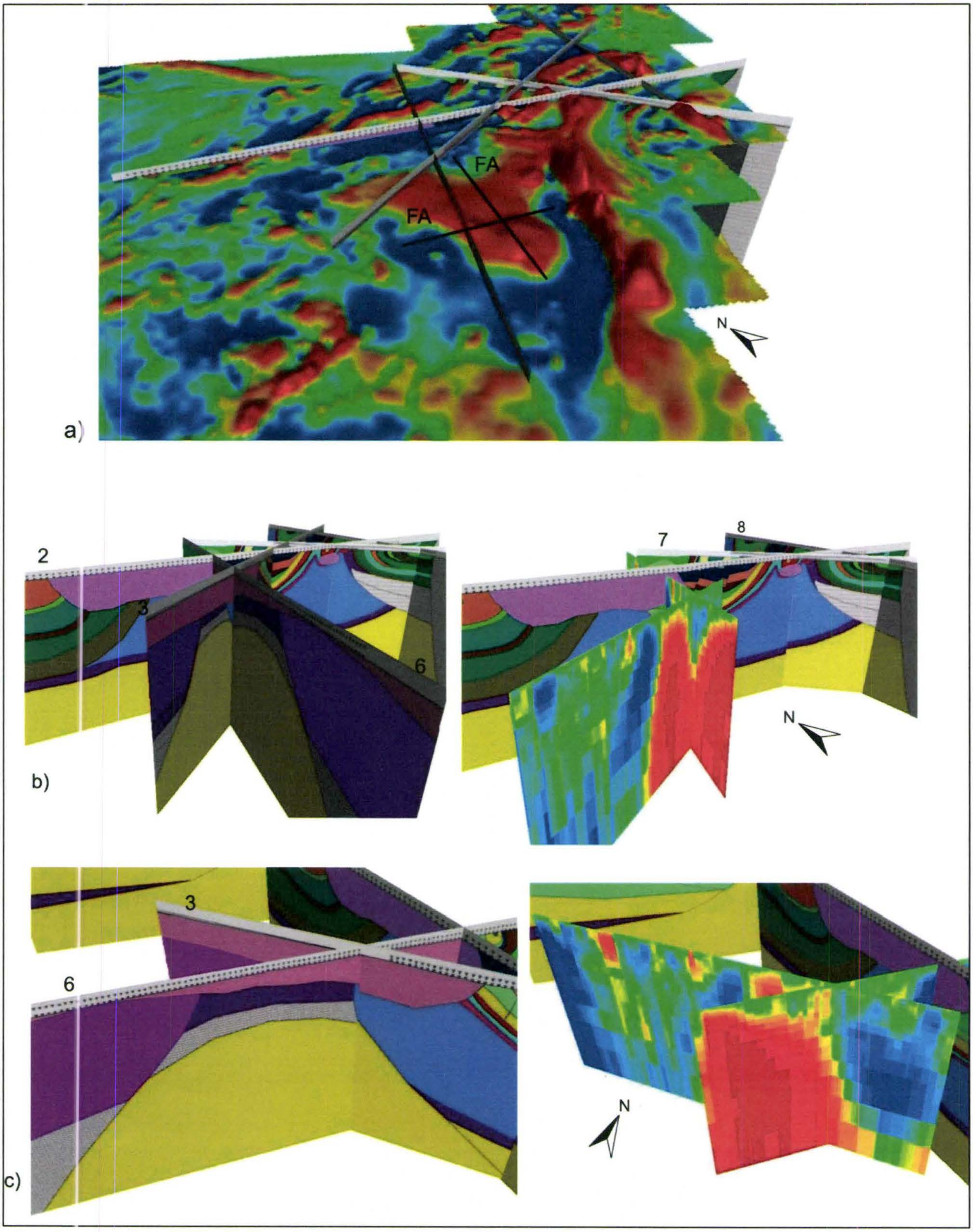
FA
FA
N
a)
2
3
6
7
8
N
b)
3
6
N
c)

Figure 5-8 - a) 3D magnetic grid displaying a potential near surface ophiolite body with two fold axis (FA) interpreted. b) And c) Ophiolite uplift structure from 2D forward models (left) juxtaposed 3D magnetic inversions (right) sliced along identical azimuths.

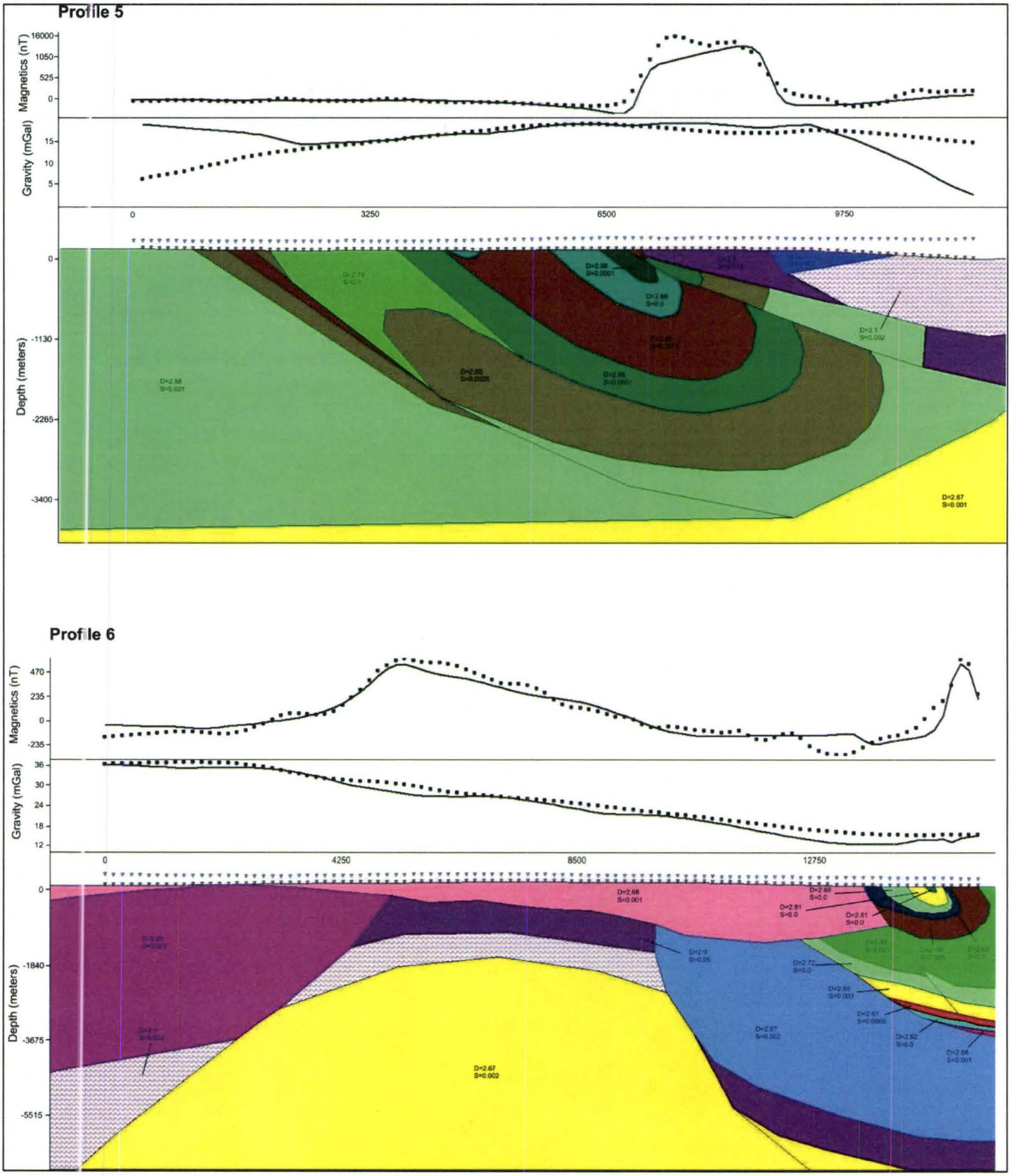
Profile 5
Magnetics (nT)
16000
1050
525
0
Gravity (mGal)
15
10
5
0
3250
6500
9750
Depth (meters)
0
-1130
-2265
-3400
D=2.67
S=0.001
Profile 6
Magnetics (nT)
470
235
0
-235
Gravity (mGal)
36
30
24
18
12
0
4250
8500
12750
Depth (meters)
0
-1840
-3675
-5515
D=2.68
S=0.001
D=2.67
S=0.002

Figure 5-9 - Geophysical forward models of profiles 5 (above) and 6 (below). Observed magnetics and gravity signals (black dots) and forward model response (solid black) are shown.

(Table 1, SAPi) unit is very magnetic. Two alternative models have been presented to explain this. One is a fault controlled model with north dipping reverse faults presumably related to the same south directed stress acting on the Cape St. John Group throughout the eastern BVP causing the east west folding (Fig.10). This model assumes a degree of previous folding as observed in the map, however in order to bring the more magnetic Armchair Pond black lapilli tuff unit to the surface as indicated on the magnetics, a later system of faults are required. Assumed thrust surfaces have also be included near this area in the most recent maps produced by Skulski et al. (2010). A second possible explanation for the magnetic anomaly pattern may be increased fold activity (Fig.11). Situating a fold axis where the fault from the previous model existed, it is also possible to bring the Armchair Point formation to surface. Both of these models satisfy the magnetics to a greater degree with the faulted model more supported by the gravity. If these are corrected however, the surficial distributions of the current maps would require some significant revision. A near surface granitic intrusion has been included in order to satisfy the gravity. While no evidence of such occurrences in this area is documented, felsic intrusions are indeed within the CSJG to the north, informally referred to as the La Scie Igneous Suite (DeGrace et al. 1976, Hibbard, 1983). The presence of this intrusion is also supported within profile 2.

Along this profile where the CSJG and Betts Cove Ophiolite complex meet, a non-conformity is observed. The amygdaloidal tholeitic basalts of the Loon Pond formation within the CSJG overlie the talc-serpentinite schists of the BCO. This was first documented by Neale et al. (1975) and later by DeGrace et al. (1976). Opposite to earlier understanding, this placed the CSJG as a post obduction formation. This unconformity is supported along this profile by both the gravity and magnetics. Parasitic folds here are also present in profile 8 down strike of this location and are required to explain current geologic maps. What Neale et al. (1975) failed to mention however, and something dismissed in all other previous studies are the implications of such an unconformity for the timing of deformation at the BCO. While current interpretations place the BCO as a Salinic structure (Bédard et al. 2000, Spicer et al. 2010), this unconformity requires deeper portions of the BCO must have already been exposed prior to the onset of Silurian volcanism. Although folding of the BCO likely continued during the Salinic, the initial structure present when the unconformity occurred must have begun formation during the Taconic.

Profile 8

The transect across profile 8 (Fig. 11) is similar to profile 7, beginning in the north with the Cape St. John Group (CSJG) and moving south into the Baie Verte Peninsula. These two models were produced perpendicular to the geologic strike of units on the eastern portion of the BVP, making the procedure less complicated. Beginning in the north a series of anticlines and synclines are observed. These large scale folds are overturned with axial planes dipping to the north. Parasitic folding has been included to explain areas where mapped unit thicknesses increase near the contact with the Betts Cove Ophiolite. The axes to these folds are vertical and are contained within an overall synform. The obduction surface boundary encountered between the CSJ and the BCO is steeply dipping and overturned to the north near the surface. This is in agreement with work presented by Spicer et al. (2010) and is a requirement of the magnetics and gravity. Here as also observed in profile 7, significant edge effects plague the interpretation offshore of the BCO. The forward model responses recorded of these profiles are primarily affected by material directly underneath the measurement point. While geologic trends have been continued, the full effect of their contribution to the geophysical signal is minimal.

The Baie Verte Line

There have been multiple geophysical investigations across the Baie Verte Line. Early work depicted this composite fault zone as a vertical structure extending infinitely at depth. Jacobi and Kristofferson noted the high magnetic anomaly associated with this feature while Miller and Deutsch (1976) showed that the gravity throughout the Peninsula increased after crossing this boundary. Initially Miller and Wiseman (1994) incorporated the Lithoprobe seismic results into their forward model of the gravity and magnetic signature of the BVL. Later Waldron et al. (1998) used the same seismic data yet produced quite different geological reconstructions. While this paper has focused on forward models across the entire BVP using 3D magnetic inversions as support, here we wish to address the previous BVL models using this new technology.

The profiles from the abovementioned studies were georectified in 3D and compared to one another then contrasts or similarities were made in relation to magnetic inversions (Fig. 12). While Miller and Wiseman (1994) provide depths within their forward models that are correlated to structures within the seismic data, Waldron et al. (1998) linked geology to travel times only. The depths used in the profiles reported in this study are linked to the depth information as used by Miller and Wiseman (1994)

Interpreting structure from an unconstrained inversion can lead to many problems. These are the result of a mathematical procedure which takes very little geologic input into consideration. In the case of the BVL, the only constraint implemented was an upper bound of 0.01 SI. And although negative susceptibility values are not geological meaningful, UBC-GIF inversions will generate such values, regardless of the bounds imposed on the inversion. While structural information can still be gained, values from this model should simply be considered as relative. The maximum depth of the computed inversion model was limited to a depth of 5 Km. Previous artificial model experiments have shown that results of unconstrained inversions produced blurred images of the truth at depth, providing little useful information. When compared to the model of Miller and Wiseman (1994) many aspects are repeated. A strong eastward dipping feature is present which was interpreted to represent the base of the obducted ophiolite sequence.

In their model Miller and Wiseman (1994) extend this surface to increased depth but this is beyond the resolution of an unconstrained inversion to evaluate. A shallow horizontal structure is also present within the magnetic inversion which agrees with the interpretations made by Miller and Wiseman (1994) for a base of the Burlington Granodiorite. Reflectors interpreted in the Miller and Wiseman (1994) model as being representative of the base of the ophiolite sequence were thought to represent the base of the Burlington Granodiorite (BG) by Waldron et al. (1998). This would place the BG at 5 Km depth which does not agree with the forward models presented within this study or others before and is likely too deep. Waldron et al. (1998) does pick out a reflector at a more appropriate depth, placing the King's Point Ring Dyke Complex where the base of the BG is more likely to occur (Fig 12).

The notion that the BVL represents a near vertical to steeply westward dipping zone is a well documented geological interpretation (Hibbard, 1983) and geophysically supported by Waldron et al. (1998). This observation is also contained within the result of the magnetic inversion. A zone of high magnetic susceptibility almost certainly represents the location of the Advocate complex. While this unconstrained inversion provides poor depth constraint, Waldron et al. (1998) propose the ultramafic sliver tapers off at approximately 10 Km depth. While the bordering Flatwater Pond Group (FWPG) is shown mirroring the Advocate Complex's behavior in Waldron et al. (1998) the magnetic inversion as originally documented by Miller and Wiseman (1994), are strongly influenced by an east dipping structure within these rocks (Fig. 12).

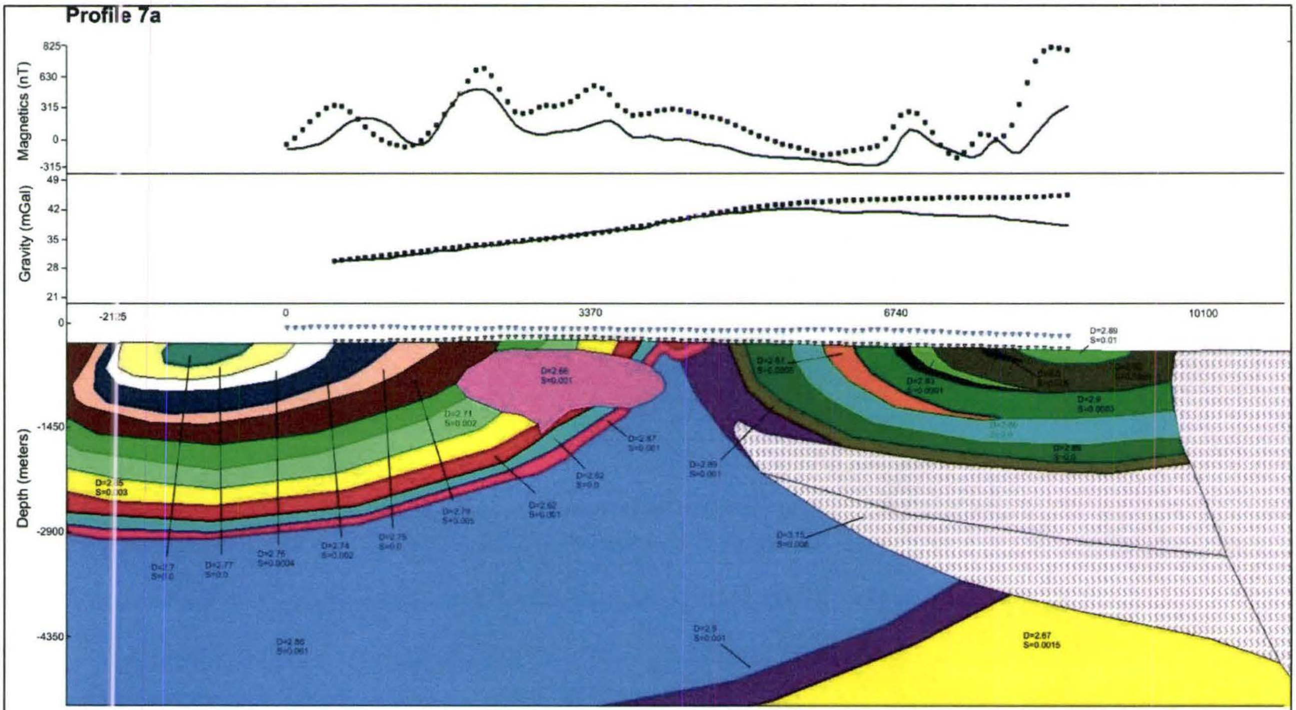

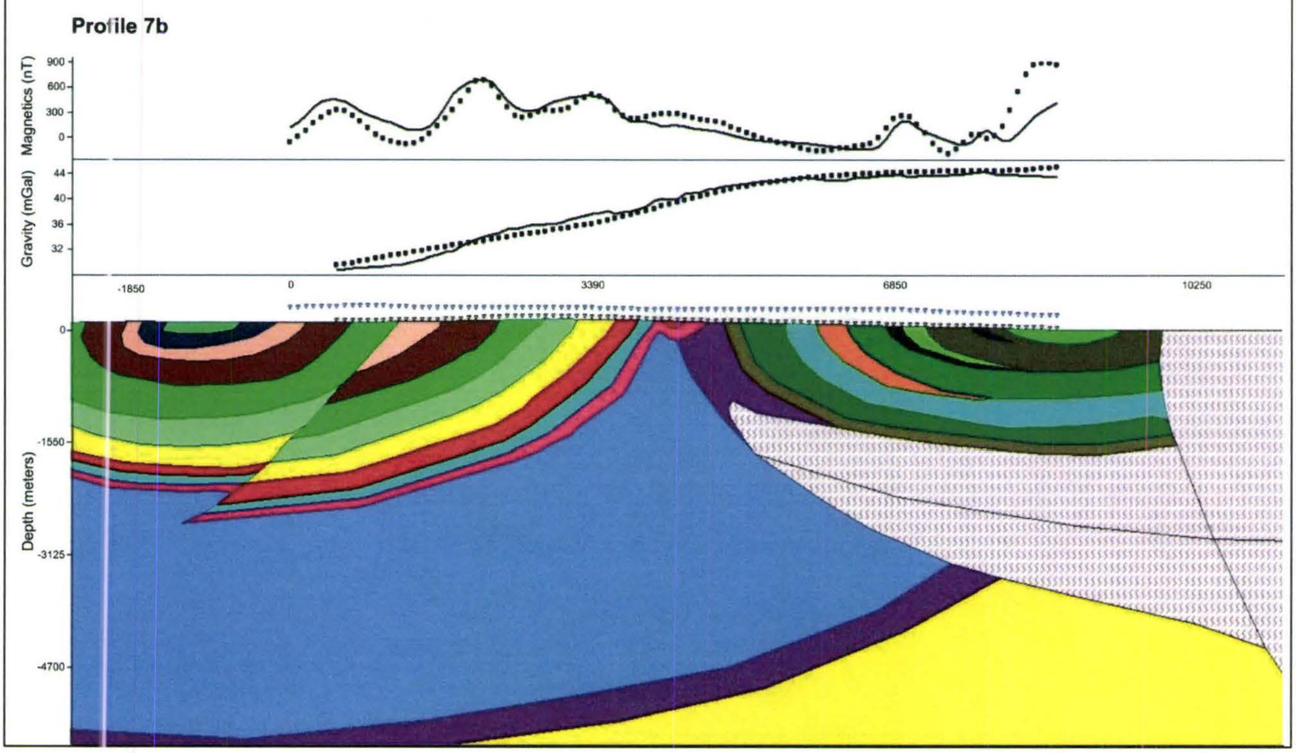

Figure 5-10- Geophysical forward models of profiles 7a (above) and 7b (below). Observed magnetics and gravity signals (black dots) and forward model response (solid black) are shown. Elements within 7a and 7b have identical values.

West dipping structures that are reported in the Waldron et al. (1998) model however are prevalent throughout the magnetic inversion as well. These provide geophysical evidence for late state extensional faulting (Jamieson et al. 1993) along the boundary between the Humber and Dunnage Zones, strengthening the notion that the Advocate may represent some down dropped portion of an overlying ophiolite sheet.

A horizontal structure is also present within the magnetic inversion which agrees with the interpretations made by Miller and Wiseman (1994) for the base of the Burlington Granodiorite. The reflectors used to support the obduction surface of the Miller and Wiseman (1994) model were thought to represent the base of the Burlington Granodiorite (BG) by Waldron et al. (1998). This would place the BG at 5 Km depth which does not agree with the forward models presented within this study or others before and is likely too deep. Waldron et al. (1998) does pick out a reflector at a more appropriate depth, placing the King's Point Ring Dyke Complex where the base of the BG is more likely to occur (Fig 12).

Conclusions

The geology of the Baie Verte Peninsula is exceedingly complex having a history of multiphase volcanism and deformation events brought about during the closure of the Iapetus Ocean and the orogenic building of the Appalachians. This study intended to investigate aspects which for the most part, are generally accepted on a regional scale. And while the geophysical models have provided valuable insight to many of these issues, they have generated nearly as many new questions. The morphology of the basement throughout the BVP is much more complex than previously expected. While the generalized eastward sloping model still holds, the work presented here suggests that a significant degree of folding must be present at depth. In the Ming's Bight area there is support that a tectonic window of basement is exposed and bound by normal listric faulting. Model discrepancies throughout this area however suggest that certain geologic aspects require further attention. This includes the distance that the Ming's Bight tectonic window extends offshore, and the influence of basement below the Point Rousse Complex. A dense and highly magnetic, near surface component within the Cape Brule Porphyry intuitively suggests the occurrence of ophiolite. Requiring some mechanism to achieve this, basement

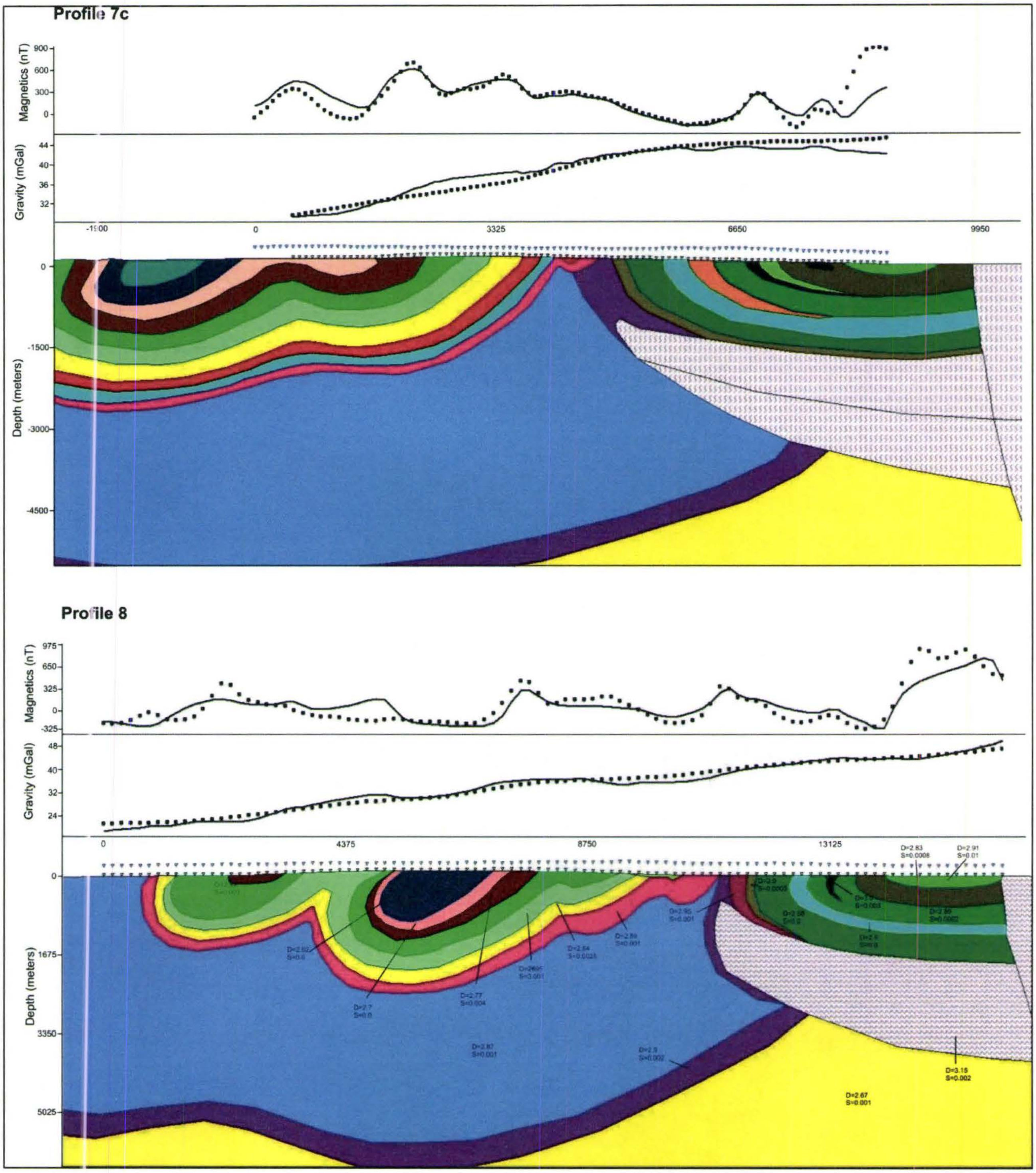
Profile 7c
Magnetics (nT)
900
600
300
0
Gravity (mGal)
44
40
36
32
-1900
0
3325
6650
9950
Depth (meters)
0
-1500
-3000
-4500
Profile 8
Magnetics (nT)
975
650
325
0
-325
Gravity (mGal)
48
40
32
24
0
4375
8750
13125
Depth (meters)
0
1675
3350
5025
D=3.15
S=0.002
D=2.67
S=0.001

Figure 5-11- Geophysical forward models of profiles 7c (above) and 8 (below). Observed magnetics and gravity signals (black dots) and forward model response (solid black) are shown. Elements within 7a and 7c have identical values.

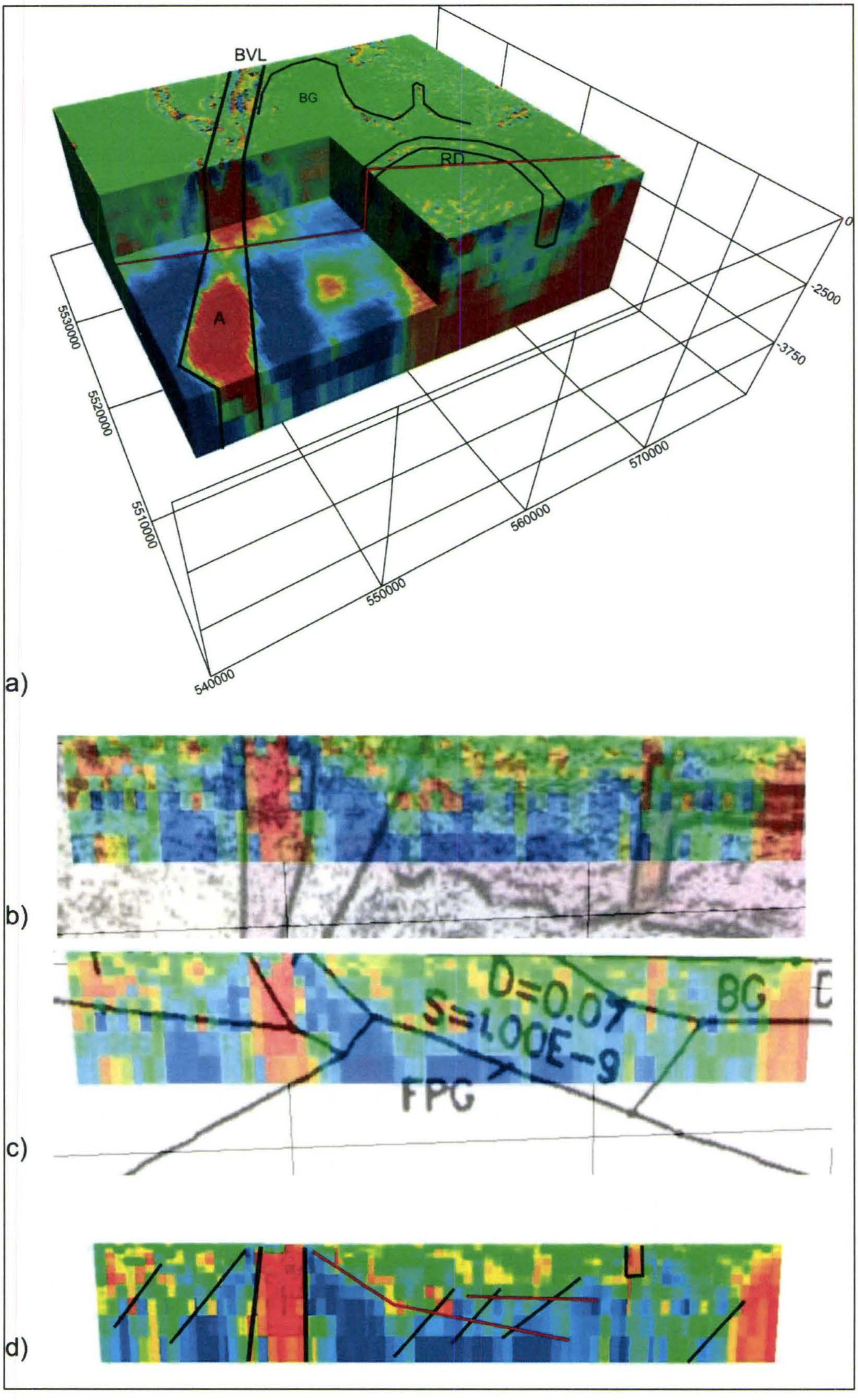
BVL
BG
RD
A
0
-2500
-3750
5530000
5520000
5510000
570000
560000
550000
540000
a)
b)
D=0.07
S=1.00E-9
BG
FPG
c)
d)

Figure 5-12 - a) 3D magnetic inversion across the BVL with interpreted structures (black) and sismic profile location (red). A-advocate complex, BVL – Baie Verte Line, RD – Ring Dyke, GR- Burlington Granodiorite. b) Inversion results with transparent seismic model presented by Waldron et al. (1998). c) Inversion results with transparent seismic constrained potential field model presented by Miller and Wiseman (1994). d) Magnetic profile slice with structures interpreted to coincide with Waldron et al. (1998) (black) and Miller and Wiseman (red).

morphology similar to the window observed at Ming's Bight may be present below the Silurian cover. Folding of the Rambler rhyolite may indicate ore horizons in areas not previously considered.

The extensive Silurian intrusive cover throughout the Peninsula presents a challenge for developing a complete subsurface framework. While certain inferences have been made, the ability to test these hypotheses is difficult as no physical evidence may be acquired for at least 1.5 Km for the most part. The CPB is thickest in the middle and thins to as little as 500 m depth towards it edges. A sheet of high density and magnetic material is required to be present below the CBP. On a regional scale it is possible to model this feature as being associated with the transition of the Snooks Arm Group to the analogous Pacquet Harbour Group. A thin layer of altered ultramafics, likely occurring below this sheet is probably comprised of several imbricate thrusts which are beyond the resolution of this investigation. A near surface ophiolite-like body below the CBP, close to the previous Betts Cove mine is supported by modeling and represents a significant exploration target.

The Cape St. John Group is hosted within an east-west trending fold belt where folds are overturned and plunging to the north. Cross folds can be seen throughout, producing doubly plunging folds. A strong magnetic anomaly, inconsistent with current map patterns suggests the occurrence of very tight folding, or later faulting propagating the lower fold limb towards its core. The non-conformity between the Betts Cove Ophiolite and the CSJ suggests that the BCO is a pre-Salinic structure. While the contact between the CSJ and PHG below the CBP has been modeled as a sharp discontinuity, whether or not this represents an unconformity or is fault related, remains unclear.

Finally, the Baie Verte Lineament was assessed. This is a complex, near vertical, to slightly westward dipping zone. East dipping structures are present within the Flatwater Pond Group at depth which may be related to the original obduction surface. The westward dipping structures present throughout the magnetic inversions provide additional support that the Advocate Complex represents a down dropped ultramafic block. And lastly The Cape Brule Porphyry is likely no deeper than 1-2 Km near the BVL.

Several exploration targets have been identified and a generalized 3D geologic frame work has been established. The results of this study show that while our understanding of the Baie Verte Peninsula is geophysically supported in a regional sense, many imperfections to this model remain on a finer scale. Further investigations with geologic and geophysical methods working in unison will be the only way in which an acceptable framework of this complex area may be achieved.

References

Anderson, S.D. (1998). Structure metamorphism, and U-Pb and $^{40}Ar/^{39}Ar$ geochronology of the Ming's Bight Group, and the Paleozoic tectonic evolution of the Baie Verte Peninsula, Newfoundland. Unpublished Ph.D. thesis, Dalhousie University, Dartmouth, Nova Scotia. 452 p.

Anderson, S.D., R.A. Jamieson, Reynolds, P.H., (2001). Devonian extension in northwestern Newfoundland: 40Ar/39Ar and U/Pb data from the Ming's Bight area, Baie Verte Peninsula. Journal of Geology, **10:** 191-211.

Bird, J.M., Dewey, J.F., Kidd, W.S.F., (1971). Proto-Atlantic oceanic crust and mantle; Appalachian Caledonian ophiolites. Nature, Physical Science, V. 231, p. 28-31.

Cawood, P.A. and Dunning, G.R. (1993). Silurian age for movement on the Baie Verte Line: Implications for accretionary tectonics in the northern Appalachians. Geological Society of America, Abstracts with Programs, V. 25, 6, A422.

Cawood, P.A., Dunning, G.R., Lux, D., van Gool, J.A.M. (1994). Timing of peak metamorphism and deformation along the Appalachian margin of Laurentia in Newfoundland: Silurian not Ordovician. Geology, v. 22, p. 399-402.

Cawood, P.A., Dunning, G.R., van Gool, J.A.M. (1995). Collisional tectonics along the Laurentian Margin of the Newfoundland Appalachians, in Hibbard, J.P; van Staal, C.R.; and Cawood, P.A., eds., Current perspectives in the Appalachian-Caledonian orogeny: Geol. Ass. Canada Spec. Paper 41, p. 283-301.

Castonguay, S., Skulski, T., van Staal, C., Currie, M. (2009). New insights on the structural geology of the Pacquet Harbour Group and Point Rousse Complex, Baie Verte Peninsula, Newfoundland: Current Research (2009) Newfoundland and Labrador Department of Natural Resources, Geological Survey, Report 09-1, p. 147-158

Church, W.R. and Stevens, R.K., (1971). Early Paleozoic ophiolite complexes of the Newfoundland Appalachians as mantle-oceanic crust sequences. Journal of Geophysical Research, v. 76.5, p. 1460-1466.

Coyle, M. and Oneschuk, D., (2008). Residual total magnetic field, Baie Verte aeromagnetic survey, Nipper Harbour, NTS 2 E/13 and part of 2 E/14: Newfoundland and Labrador Geological Survey of Canada, Open File 5633, 1 sheet.

Daly, R.A., 1935. Densities of Rocks calculated from their chemical analysis. Geology. Vol.21. p.657-663.

Dunning, G.R., and Krough, T.E., (1985). Geochronology of ophiolites of the Newfoundland Appalachians. Canadian Journal of Earth Sci. V. 22, p. 1659-1670.

Dewey, J.F. and Bird, J.M., (1971). Origin and emplacement of the ophiolite suite. Appalachian ophiolites in Newfoundland. Journal of Geophysical Research, v. 76.14, p. 3179-3206.

Haworth, R. T., and Miller, H.G. (1982). The Structure of Paleozoic Oceanic Rocks beneath Notre Dame Bay, Newfoundland: Major Structural Zones and Faults of the Northern Appalachians, Geological Association of Canada, Special Paper 24

Haworth, R.T., Lefort, J.P., Miller, H.G., (1978). Geophysical evidence for an east-dipping Appalachian subsuction zone beneath Newfoundland. Geology, v. 6, p. 522-526.

Hibbard, J.P. (1982). Significance of the Baie Verte Flexure, Newfoundland. Geol. Soc. America Bull., v. 93, p. 790-797.

Hibbard, J.P. (1983). Geology of the Baie Verte Peninsula, Newfoundland. Newfoundland Department of Mines and Energy. Memoir 2, 279p.

Jacobi, R., and Kristoffersen, Y. (1976). Geophysical and Geological Trends on the Continental shelf off northeastern Newfoundland. Canada Jour. Earth Sci, **13**: 1560-1570.

Jamieson, R.A., Anderson, S., MacDonald, I., Goodwin, L.B., (1993). Silurian extension along the Humber-Dunnage boundary zone, Baie Verte Peninsula, Newfoundland. Abstracts volume, Late Orogenic extension in mountain belts, Montpellier, France, Document du BRGM no 219.

Kennedy, M.J. (1975). Repetitive Orogeny in the northeastern Appalachians – New plate models based upon Appalachian examples. Tectonophysics, V. 28, p. 39-87.

Kennedy, M.J. and Phillips, W.E., (1971). Ultramafic rocks of the Burlington Peninsula, Newfoundland. Geological Association of Canada, Proceedings, V. 24, P. 35-46.

Kidd, W.S.F. (1974). The evolution of the Baie Verte lineament, Burlington Peninsula, Newfoundland. Unpublished Ph.D. thesis, University of Cambridge, Cambridge, England, 294 p.

Kidd, W.S.F., Dewey, J.F., and Bird, J.M. (1978). The Ming's Bight ophiolite Complex, Newfoundland: Appalachian oceanic crust and mantle. Canadian Journal of Earth Sciences, v. 15, p. 781-804.

Miller, H.G. and Deutsch E.R. (1975). New gravitational evidence for the subsurface extent of oceanic crust in north-central Newfoundland. Canadian Journal of Earth Science, **13**: 459-469.

Miller, H.G. and Deutsch E.R. (1976). A Gravity Survey of Eastern Notre Dame Bay, Newfoundland. Earth Science Symposium on Offshore Eastern Canada: Geol. Survey Canada Paper 71-23. pp.495-499.

Miller, H.G. and Wiseman, R. (1994). Potential field interpretation of the Baie Verte Peninsula, Newfoundland, utilizing constraints from Lithoprobe East seismic line 89-13. Atlantic Geology. **30**: 25-36

Neale, R.E., Kean, B.F. and Upadhyay, H.D. (1975). Post-ophiolite unconformity, Tilt Cove-Betts Cove area, Newfoundland. Canadian Journal of Earth Sciences, v. 12, p.880-886.

Norman, R.E. and Strong, D.F. (1975). The geology and geochemistry of ophiolitic rocks exposed at Ming's Bight, Newfoundland. Canadian Journal of Earth Sciences, V. 12, P. 777-797.

Piercey, S.J., Jenner, G.A., Wilton, D.H.C. (1997).The Stratigraphy and geochemistry of the southern Pacquet Harbour Group, Baie Verte Peninsula, Newfoundland: implications for mineral exploration. Newfoundland Department of Mines and Energy, Geological Survey, Report **97-1**: 119-139.

Skulski, T., Castonguay, S., McNicoll, V., Rogers, N., van Staal, C., Morris, W, Ugalde, H., Slavinski, H., Spicer, W., Moussallam, Y., Kerr, I. (2010). Tectonostratigraphy of the Baie Verte Oceanic Tract and its Ophiolite Cover Sequence, Baie Verte Peninsula, Newfoundland and Labrador. *In* Current Research. Newfoundland and Labrador Department of Natural Resources, Geological Survey, Report 10-1, pages 315-335.

Slavinksi, H. A., (2007). The integration of geophysical, lithological and remote sensing data for geological mapping. Unpublished M.Sc. thesis, McMaster University. Hamilton, Ontario. 120p.

Spicer, B. Morris, W.A., Ugalde, H., Slavinski, H., Skulski, T. (2010). Structure of the Betts Cove Ophiolite Complex beneath the western margin of Notre Dame Bay, Newfoundland. Candian journal of Earth Sciences. 47. 2, p.181-198.

Spicer, B., Morris, W.A., Ugalde, H. (2010b).The structure of the Rambler rhyolite, Baie Verte Peninsula, Newfoundland: inversions using UBC-GIF Grav 3D and Mag 3D. Unpublished M.Sc. thesis. McMaster University, Hamilton, Ontario, Canada.

Telford, W.M., Geldart, L.P., Sheriff, R.E., Keys, D.A., (1976). Applied Geophysics. Cambridge University Press, Trumpington Street, Cambridge, United Kingdom. 860 p.

Upadhyay, H.D., Dewy, J.F., Neale, E.R.W., (1971). The Betts Cove ophiolite complex, Newfoundland Appalachian oceanic crust and mantle. Geological Association of Canada, Proceedings, v. 24, p. 27-34.

Upadhyay, H.D. (1973). The Betts Cove ophiolite and related rocks of the Snooks Arm Group, Newfoundland. Unpublished Ph.D thesis. Memorial University of Newfoundland, St. John's, 224 pages.

Van Staa , C.R., and de Roo, J.A. (1995). Mid-paleozoic tectonic evolution of the Appalachian Central Mobile Belt in northern New Brunswick, Canada: collision, extensional collapse and dextral transpression. In Current perspectives in the Appalachian-Caledonian Orogen. Edited by J.P. Hibbard, et al. Geological Association of Canada Special Paper 41, p. 367-389.

Waldron, W.F., Anderson, S.C., Cawood, P.A., Goodwin, L.B., Hall, J., Jamieson, R.A., Palmer, S.E., Stockmal, G.S., Williams, P.F., (1998). Evolution of the Appalachian Laurentian margin: Lithoprobe results in western Newfoundland. Can. J. Earth Sci. 35: 1271-1287.

Williams, H. (1979). Appalachian Orogen in Canada. Canadian Journal of Earth Sciences, 14: 987-1003.

Chapter Six - Conclusions

B. Spicer

MAGGIC, School of Geography & Earth Sciences, McMaster University, 1280 Main Street W., Hamilton, ON L8S 4K1. Canada

From the beginning of its implementation, geophysical modeling has established itself as an invaluable tool providing vital information in areas where traditional means of exploration cannot or have not reached. With continued technological advances coupled by a global trend towards improved survey coverage and resolution, the practicality and necessity for geophysical modeling increases. An understanding of the target is essential to the modeling process. All models have some predefined expectations, or goal. The quality and reliability of a geophysical model can be improved through the inclusion of constraints that ensure some meaningful bounds are imposed on the resulting output models. Integration of priori information such as physical rock properties, boreholes, geologic maps and sections, ensures a model satisfies preexisting knowledge and maintains geologic integrity. The case studies presented in this thesis have demonstrated the use of both forward and inverse modeling techniques in building a 3D geologic framework of the Baie Verte Peninsula in Newfoundland. Geologic structure, tecnonstratigraphic relationships, depth to basement were revealed through the modeling of potential fields.

Chapter Summary

Chapter one was a brief introduction to the overall concept of this thesis and the study site which it concerns. The Baie Verte Peninsula is an area of socioeconomic and academic importance, hosting mines of volcanogenic massive sulphides, asbestos, and epithermal gold while also having played a pivotal role in the development of the plate tectonic pardigm. Geophysical data sources modeled in this study were established and the concept of a non-unique potential filed was presented. Both approaches to modeling, forward and inverse were introduced and the importance of geologic constraint alongside a physical rock property database was stressed.

The Betts Cove area of the Baie Verte Peninsula is presented in Chapter 2. In this section the subsurface morphology of the Betts Cove Ophiolite (BCO) and the syn-obduction Snooks Arm volcano-sedimentary cover series were investigated through modeling high resolution magnetics. The BCO was deemed a prospective candidate for magnetic modeling as this feature, comprised of serpentinites ultramafic cumulates, sheeted dykes, gabbroic intrusions and several basaltic lithologies, possesses a characteristically strong magnetic signature. While incomplete airborne coverage prevented previous studies from performing a full geophysical investigation, a marine magnetic survey was implemented to provide an additional 10 Km of information. Through micro-leveling, upward continuation and the subsequent extraction of a residual signal, the surficial geophysical signature of the BCO was revealed. From physical rock property analysis it has been determined that signals observed at the Betts Cove area arise mainly through induced magnetization. A late Ordovician remenance magnetization direction present within some ophiolitic horizons is likely the result of thermal overprinting brought about during obduction above the Laurentian continental margin. 2D magnetic forward modeling constrained by petrophysical and geologic measurements reveals that the BCO and its cover comprise a doubly plunging syncline. The core to the syncline is located within the pillow basalts of the Round Harbour Formation and fold nose closures bound the BCO at its northern and southernmost extremities. This study has also revealed the presence of significant faulting throughout the BCO. To satisfy the magnetics the onshore perimeter of the BCO, interpreted as the original obduction surface, has been overturned by southward directed thrust. This implies ophiolites north of the north of this thrust may exist near surface under cover of the Silurian Cape Brule Porphyry. With all ore deposits on the BVP associated with ophiolites, and the proximity of the fault to the historic Betts Cove and Tilt Cove ore deposits, a prospective exploration target has been identified. A significant amplitude decrease combined with a large wavelength increase of the magnetic profile is observed to the south. Maintaining sampled rock properties, an increased depth to source is required. Thus offshore, the BCO must be affected by some late stage extensional faulting. These southward dipping faults are listric at depth and when compared to documented northward dipping faults on the eastern margins of Notre Dame Bay, combine to produce a carboniferous basin. The end result of this study is a 3D geologic model of the BCO and its cover. Utilizing new information and technology a more thorough understanding has been achieved of this type locality source for ophiolites on the BVP.

Chapter three of this thesis delivers an alternative approach to collecting density measurements utilizing gamma radiation. The intent of this study was to produce a portable device capable of rapid density measurements that could function in variable environments and operate on multiple borecore calipers. This was achieved through minor modifications of a Berthold Technologies LB444 industrial gauge intended for consumer goods. While the method intuitively seems quite straightforward this study touched upon many underlying aspects governing gamma-gamma density estimates which need to be taken into consideration. The foremost component controlling the absorption of gamma particles begins at the atomic level with the Mass Attenuation Coefficient. Based on the ratio between atomic mass and number, this value is quite common for many of the elements comprising most silicate based lithologies. However, when working in a primarily mafic to ultramafic geological setting such as the BVP, absorption coefficient inconsistencies can result in significant miscalculations in density. Although absorption coefficients have been well determined of most elements for varying energies, relatively little information is available concerning specific minerals let alone rocks as a whole. A calibration curve can be established in lieu of this, however the medium used in constructing such a curve should be similar to the rocks to be studied. Density standards crafted from metal alloys were ineffective in producing reliable curves for the rocks of the BVP. This stemmed from the effect of dissimilar absorption coefficients. Using a one-to-one gamma density versus standard specific gravity measurement technique, an empirical calculation was determined providing a relationship between the two. After applying this correction, the density values provided by the LB444 density gauge were within ± 0.2 g/cm^3 of values from the SG method. Another factor which must be regarded when implementing this technique relates to core diameter. It was determined that the range of error reported within this study may be accounted for by core diameter variations on the mm scale. This method of measurement rapidly provides density information, conducive of the large sampling populations required of quality physical rock property databases. Combined with a magnetic susceptibility logging system, down hole petrophysics can provide insight into lithologic distributions and alteration patterns while at the same time collecting constraints required for geophysical inversion of magnetics and gravity data. Although the potential for this system is high, current results fall short of an accuracy required for inversion constraint. Future studies will entail a precise bore core diameter variations and rock-like density standards before true potential is realized.

In the fourth chapter, 3D inversions of magnetics and gravity are performed implementing University of British Columbia Geophysical Inversions Facility (UBC-GIF) code. This section demonstrates the necessity for including geologic constraint within the mathematical realm of inversion. A detailed physical rock property database was constructed from lithologies throughout the Rambler area. Integrating petrophysics, borehole logging, geologic maps and sections, magnetics, and gravity, a reference model of known physical property values and distributions at the Rambler area was established. Performing inversions while including a detailed reference model, restrictions are emplaced in order to limit model outcomes and contest the effects of a non-unique potential field. Ore deposits mined on the Rambler property are encountered along the upper contact of a local rhyolite body that is surrounded by mafic volcanic rocks. In the absence of sufficient outcrop, the form of the rhyolite body has yet to been fully interpreted and as such, the subsurface extent remains unclear. Physical rock properties collected show the Rambler rhyolite to have a lower density than its surroundings. The structure of the Rambler rhyolite was revealed upon the inversion of a high resolution gravity survey collected for this study constrained by the reference model. Depicted as a body with density ranging from 2.71-2.75 g/cm^3, the Rambler rhyolite dips roughly 40 degrees near surface with the plunge apparently steepening with increased depth. Results agree with known ore distributions and surficial geologic projections predicting the extent of the rhyolite. While current ore is encountered at shallower depths along surface trends, this study suggests that deeper drilling will be required than previously suspected to encounter ore down plunge. It is also possible to derive geologic information on the Rambler property using magnetic inversions. The 3D extent of many magnetic gabbro intrusives was been established, outlining the presence of a large scale fold. These bodies are upright to steeply inclined and posses a high magnetic susceptibility. This axis to this fold is correlatable to regional D_3 cross-folding. This fold axis may also represent a favorable exploration target. While including geologic constraint within an inversion has been an important recognition within the geophysical community, it is rarely performed in practice. Although UBC-GIF inversions include a procedure that permits the introduction of pre-inversion geological constraints, the means to construct such models are not readily available. A customized and multi-software approach was implemented in order to produce a reference model. The procedure used for building the inversion reference model is outlined appendix A. While initial implementation may be time consuming, this study demonstrates that subsurface distributions can be more precisely predicted when including all available sources of information within the inversion process.

Chapter five is an investigation which aims to provide regional scale insight into the geologic framework of the Baie Verte Peninsula. Similar to the local scale case studies, this work focuses on geophysical modeling supplemented with geologic constraint. While chapters two and four make use of only one of either two modeling techniques, this study combines aspects of each. The objective of this study was to address regional issues include the Baie Verte Lineament; the Cape St John fold and thrust belt, and the Cape Brule problem. 2D forward models are constructed across the Peninsula, constrained based on geologic mapping and a regional physical rock property database. A gravitational and magnetic model response is recorded simultaneously to ensure increased continuity throughout models. The profiles all intersect at least one other section in order reinforce continuities. Veracity of the 2D to 3D compilation can be assessed by performing full 3D magnetic inversions, specifically this has served confirm the presence of structural dip directions and some information regarding the depth to the tops of sources. Information provided within these models proves that the peninsula is underlain by a uniformly distributed zone of high density material. On a regional scale this implies that Ordovician Ophiolites may have been emplaced along a single sheet, however it remains possible and more geologically probable, that this is in fact some imbricate thrust stack. The Basement of the BVP remains an eastward dipping surface however has a morphology mirroring many surface trends and in some instances is affected by significant faulting. Below the Cape Brule Porphyry the Snooks Arm and Pacquet harbor groups transition, however they are in fact one in the same. The nature of this contact with the overlying Cape St. John Group is sharp, possibly fault controlled or some unconformity. The CSJG was also shown to comprise a zone of doubly plunging fold affected by late state fold thrust propagation. Where structural trends diverge along the 'Baie Verte Flexure' a fold or some fault zone related uplift has been presented. Elements from previous models of the Baie Verte Line were assessed, proving that unconstrained magnetic inversions can still provide relevant information.

Limitations and Modeling Considerations

Geophysical modeling of magnetics and gravity can provide practical insight into geologic problems and aid in predicting subsurface geology. This thesis demonstrates the ability of forward and inverse modeling techniques to vector towards potential exploration targets, providing an outline of stratigraphic and geological distributions at depth. Including geologic constraint within the modeling procedure guides the outcome of a non-unique phenomenon within reasonable bounds and strengthens the overall reliability of a model. While geophysical models can aid in depth estimation and the 3D visualization of geologic phenomena, ignoring or failing to recognize the inherent limitations associated this technique will result in serious problems.

Physical Rock Property Values

Developing physical rock property constraints is essential to the geophysical modeling process. Without knowing the values of properties for units modeling processes operates blindly. In the absence of physical rock property values there is no way to assess whether or not the outcome is an acceptable interpretation, or some random combination of values and orientations which satisfy the non-unique potential field. In forward models this is readily apparent as a modeler observes their ability to fit a signal while adhering to accepted geologic principles. When limited to a finite range of physical property values the modeler begins to recognize the geophysical characteristics of each unit and understands the implications of their distribution. Anomalies are no longer considered the consequence simply of physical property values and distributions, but as the function of some geologic mechanism required to achieve those necessary conditions. In areas where these mechanisms are supported, the geophysical model provides additional support. Where the geologic mechanism to produce a known geophysical signal cannot be explained by current understandings, a modeler must produce their own explanation while adhering to geologic principles. In this situation valuable new insight is provided which may or may not hold truth; however it remains that some problem exists within the original understanding which was identified through the modeling process. In either case supporting or disputing geologic understanding can only be achieved when the known values of the geology are honored.

The construction of a physical rock property database to be used for model constraint is limited by several factors. One of the most prevalent issues relates to sampling. The greater the number of observations, the better a population is represented. Having many samples of a lithology allows for greater determination of the average physical properties. It may however remain impossible to adequately reproduce a geophysical response while remaining faithful to the average recorded property of a rock. Yet population variances permissive within the modeling procedure are better understood when sampling is high as well. These known deviations from an average can be appropriately exploited to better fit a signal. Unfortunately it is often the case that sample populations will be low as the collection procedure can be time consuming and not all lithologies will be easily accessible. This is especially true over a large area where many lithologies are recognized. In these instances it may be that no data exists for a specific rock or physical properties arise from a single sample. With situations such as this, physical property values for constraint become a guideline rather than rule. Knowing that the physical properties of rocks vary in space, it may be unwise to maintain unit specific values from a sampling site far from the modeling area. While physical properties summarized of a lithology are usually based on a sample population which occurs at or near the surface, models are expected to provide insight into much greater depths. It is quite probable that the properties at surface will be in some way altered to that of the rock as a whole as exposure to the elements can degrade magnetic susceptibility and density values. This is another physical rock property issue that should be taken into consideration.

The method of data collection will also cause limitations. Measurements utilizing the specific gravity approach to density estimates are taken as a ratio of dry to wet mass after samples are submersed in some liquid then multiplied by the density of that liquid. Although the value of 1.0 is often the used, rarely is distilled water used in the field. Particulates from rock surfaces will also accumulate in the water column, altering its density further. The level of accuracy is also limited by the precision of the scale. Measurements derived by radiation methods can be plagued by problems relating to mass attenuation coefficients, variable source-sensor distances and calibration errors. Magnetic susceptibility readings can vary similarly with calibration problems and issues originating from poor sample contact. These devices also have model specific precisions. Databases complied from values obtained with multiple susceptibility devices may encounter incongruities caused by factors such as different frequency of ac current in sampling coil, and different coil size.

Forward Models

2D forward models are a convenient form of modeling as they are simple and more straightforward that their inverse counterparts. While controlled by a modeler ideally relating everything to geology, no post process interpretations or speculations are required. That is not to say forward models are lacking of any ambiguities, yet each component has been premeditatedly input by the modeler themselves. There are still however some issues with this method that should be considered. Forward modeling along 2D profiles is limited by a requirement to maintain a single physical property within any model unit. Unlike the continuous variations observed in the natural world the recorded response is that of a uniform object. 2D modeling may be performed on data along a flightline where the signal is primarily acquired in the direction of the section. However, as was the case for many of the models within this thesis, 2D profiles are often extracted from a grid. This allows a greater degree of freedom to the modeling process as sections can be modeled along any direction. However this can cause problems as most of the data along a section extracted from a grid has been interpolated based on trends within the original profile. While the effects of this are minimal in most cases, there are certainly model discrepancies that may arise based on this alone. As this data is based on mathematical algorithm instead of true geology, no real solutions may be achieved. Any issues from the processing stage such as leveling error, non-geologic noise or gridding related discrepancies will be carried into modeled profiles. Another major limitation associated with forward modeling comes about through the attempt to reproduce a signal measured of a three dimensional surface while working in 2D. While some modeling software packages will boast 2.5D or 2.75D capability, with model response including an infinitely extending slab along the non-visible dimension, 2D models cannot account for the full 3D impact of signal input. As the distance from the sensor to sampling surface increases, signal is augmented by sources adjacent to the point directly below the sensor. Any data collected through an airborne method suffer from this problem to some degree. This implies that a 2D forward model of airborne data may never be achieved which correctly explains a geophysical signal. The sampling rate along a profile emplaces strict limitations as well. Oversampling a profile to a point where responses are being calculated where no observed data exists will result in a modeled profile full of spikes. In contrast when profiles are undersampled certain details of a geophysical signal produced by small geologic features are not included within the computed response and result in an overly smooth model.

Inverse Models

The largest limitation within inverse modeling is the difficulty in implementing geologic constraint. With the intricacies involved in this mathematical procedure most inversion algorithms provide little, or no, room for such information. The model objective function is the cornerstone of UBC-GIF inversions and an optimization routine which includes a term dictated by a reference model of physical rock properties. Minimizing the difference between a mathematically probable solution and known geophysical values, the model objective function seeks to explain a geophysical signal within the appropriate geologic context. Unfortunately, even with an algorithm capable of including such constraints, developing a reference model with physical property distributions and values using the same format as the output inversion is difficult. No single graphical user interface based software is available to perform this task in an effective manner. While a computer scientist familiar with more complex code-based software such as Matlab may be able to develop their own model building routines, the average geoscientist will be left to perform their inversions unconstrained. The UBC-GIF routines do include depth weighting factors to combat the occurrence of a thin plate of highly variable physical properties at surface as well as the ability to limit the overall range of possible values. While these unconstrained inversions can incorporater some information such as geological strike directions and relative property contrasts, the truth of the matter will be hidden within a 'smoothed blob' model outcome. Producing a reference model for input is still possible though. To do this a suite of geophysical software packages including Modelvision and Profile Analyst must be in place. Obtaining such resources and developing an effective methodology will initially be costly and time consuming. Inversions are also affected by the same sampling and post-processing issues as forward modeling. 3D inverse models are inverted within a mesh of user defined dimensions; this mesh is a discretization of an infinitely continuous medium. Knowing this the appropriate resolution may never be reached to explain some geologically derived signal. Finally, while voxel sizes increase with depth to account for deep seeded input and avoid surface plate effects, a decrease in subsurface resolution also occurs.

Geology

The geology of an area can impose its own limitations within the modeling process. In the case of the Baie Verte Peninsula, rocks originated from a dominantly ocean-floor spreading center and volcanic island arc regime comprised of igneous and volcano-sedimentary lithologies. As encountered in previous studies, the rocks of the BVP may appear the same in outcrop yet geochemically or geophysically can be exceedingly dissimilar. This arises as a consequence of a complex tectonic history resulting in diverse melt compositions, multiple stages of intrusion as well as comprehensive history of faulting and multi-staged reactivations. Combining these difficulties to the already discontinuous nature of igneous geology in general, makes developing a geophysical model representative of known lithologies difficult. Understanding this, it should be realized that the geologic maps these models are based on may not necessarily correct. As maps are in themselves only models, interpretations made by a geologist across outcrop observation points, surface constraints based on geologic maps can be inherently flawed.

Concluding Statement

Geophysical models present subsurface information in a non-invasive and inexpensive manner. The insight gained from this procedure can be of insurmountable value within the decision making process of geologically based financial or social decisions. While geologic distributions obtained from the geophysical modeling process should be evaluated and thoroughly considered, this method is not intended to replace traditional exploration techniques entirely. In addition to a tool used for testing or confirming existing geologic hypotheses, geophysical models often breed additional tribulations which require some furthered form of address. Prospective areas and potential targets can be identified through geophysical modeling methods however no true answers are provided until some material evidence is acquired. A responsible exploration campaign cannot rely solely on any one technique. The greatest degree of success will be obtained where multiple methods establish a common target. Through integrating an understanding of geophysics and geology a clear representation of subsurface distributions can be achieved in turn this information can be of great use, vectoring towards the most prospective sites for exploration.

Appendix:

Building Reference Models for Geologic Constraint in UBC-GIF Mag3D and Grav3D inversions

Introduction

While inverse theory and its application for revealing the extent of subsurface physical properties is nothing new, the idea of including geologic constraint to these literally endless solution arrays is still in its infancy. Geophysicist's agree that while dealing with a non-unique phenomenon such as a potential filed, some form of constraint needs to be in place in order to establish a degree of control inside the inversion. For geology this means this inclusion of known or expected geologic trends and distributions. And while the proposal of including such information seems rather obvious, the implementation of such is another thing. Many studies stating the requirement of geologic constraint within their inverse models go no further than that. However recognizing a need for constraint is not the same as enforcing it.

The UBC-GIF (University of British Columbia Geophysical Inversion Facility) is the leading advocate for geologically constrained 3D potential field inversions. Their 3D gravity, magnetics and IP inversion codes are currently available for academic purposes, and have been granted to several contributing industry constituents. While results presented by the UBC-GIF implement code within the MATLAB setting where more advanced parameters and inversion restrictions may be employed, a more user friendly graphic user interface (GUI) with a slightly limited range of functions is provided to others. Specifically, the code running on the GUI does not allow the smallness term to differentiate for individual cells. In examples presented in the Williams (2008) Thesis, different levels of data uncertainly were stated depending on the source. The importance of data uncertainty has been explained in terms of data sourcing in regards to 3D inversions by the UBC-GIF (Li and Oldenburg 1996, 1998; Williams 2008). For example, one may wish to assign a large smallness factor to drillhole data when there is high confidence that reliable data is outlining the physical property of at a specific point in space. Conversely, lower smallness values may be more appropriate for physical properties within the same reference model derived from a geologic map as these are an interpretation between outcrops and physical properties of a single unit may vary in space. At the moment the GUI for 3D UBG-GIF inversions allows input of only one smallness value to be assigned to the entire model. A quick way to offset this problem though would be to assign looser bounds on our units of less confidence.

The UBC-GIF inversions require a reference model of known physical property distributions to be input as geologic constraint. This reference is essentially a 3D geologic model which will be discretized into voxels contained within the user defined mesh. Each component to the model is assigned a value describing the physical property of interest. For Magnetics this is susceptibility while for gravity or IP this would imply density and resistivity respectively. The UBC-GIF is in the development stages of a model building software for future installments of the GUI, however at the moment they do not provide any software to implement geologic constraint for their 3D inversions. Currently there are several software packages which allow for the import of UBC-GIF inversion results. Regrettably though, few have included an export function using the same format as UBC-GIF. *Geosoft* 3D gridding can produce voxels models which may be loaded and viewed within the UBC-GIF *Meshtools 3D* model visualizer software. Inclusion of these models as a reference model within the GUI though causes an immediate crash with an error message reporting a corrupt reference model file. Creating a reference model to use within the UBC-GIF GUI is still possible though. The construction of such is best achieved using a combination of Encom Geophysics software packages, *Profile Analyst* (PA) and *Modelvision*. PA is used to grid borehole data for inversions while *Modelvision* quickly converts geologic maps into simple 3D models with assigned physical properties. Exporting to the proper UBC format is also performed in *Modelvision*. A detailed step by step guide to achieving this is outlined as follows:

Step 1: physical rock property database construction (performed in *excel*)

Before the model is built a master physical property database pertaining to all encountered geologic units should be organized. The larger the database with the greater the measurement number the better. This data base will contain all values used to define the reference model used within the inversion.

1. Sort the database according to geologic unit. You should perform a statistical analysis on each unit in order to gain insight into the overall picture of its physical properties. This is important as you may find that you have abundant geologic information in the form of drillhole logs and map/point data of lithology locations, but may find your petrophysical data stems from a few drill holes or scattered rock samples.
2. In this case above assign the average property value for each unit within your reference model, using the average +/- the standard deviation of the sample population as your upper and lower bounds value for each unit. Our lower bound should not be negative. The bounds are used within the inversion to coincide with the misfit factor. An appropriate model is achieved when we find a balance between the data misfit factor and the model objective function (see Williams, 2008).
3. If you prefer to use only use measurements you have taken yourself, use the true values measured for each location in space. This may be preferable if one wishes to remain as faithful to the true data as possible, however it may be that such limited information proves ineffective in imposing any real constrain within the inversion.
4. If a geologic map is our only constraint we simply assign the average property value into our map derived reference model. If we have bore-hole information we should assign this value to each unit.

A	B	C	D	E	F	G	H
Hole ID	From	To	Litho	K	k_avg	lower	upper
C-81-1	924.6	932.8	Fp	6.5	0.00065	0.0001	0.0012
C-81-1	874.5	876.2	Fp	2.75	0.000275	0	0.000825
C-81-1	797.4	832.6	Fvc	2.75	0.000275	0	0.000825
C-81-1	872.4	874.5	Bm	0.5	0.00005	0	0.00064

5. In addition to this information, we will require collars and surveys files if we wish to import our drillhole information for 3D gridding. These are files with information regarding the locations and attitude of each drillhole.

Step 2: Using 3D gridding to produce drillhole Voxel Models (performed in *PA*)

1. In order to use out information in a reference model we must grid our physical properties in 3D space. This is achieved in *PA* using the voxel toolkit. But first we must import our drillhole data. Go to *file/open/downhole/import ASCII downhole.* We import all of our collars and survey data here and also our organized physical property data base as *from-to* type data. It is important we have the same wording for hole ID in every file.
2. Now that we have imported our drillhole data we have a master spreadsheet in one window and a second window with the drill holes displayed as tubes. We can select or deselect which holes we wish to remain active by double clicking the drillhole icon in the workspace window.
3. To grid in 3D we click *voxels/voxeltoolkit/gridding.* From here we choose our method of gridding. Use the continuously variable technique and inverse distance weighting as the method. Kriging is an option as well but is time consuming and does not seem to produce as favorable results as the inverse distance technique. Click *next.*
4. From here make sure the x, y, z field for your drillholes are in the property drop down list, and select the field you wish to grid in the data feilds box. Whichever field we choose will be repeated two more times gridding the lower and upper bounds as well. Click *next.*
5. In *gridding conditioning* we can apply a spatial clip on our data if we wish. Click *next.*
6. *Gridding Size* is where we define the cells of our grid. The cells are defined in the *column, row,* and *plane* spaces. After you choose our dimensions, click *auto/fit to extents*.
7. *Gridding Search* is where we define how we will grid the data. The default search will produce a series of square voxels in x, y, z space. Refer to the *PA* manual for details on each option here. If we wish to apply a buffer and extent our data we can choose the anisotropic search. This is a preferable method where we have geologic strike and dip information and wish to increase the influence of our 3D grids in the subsurface. Parameters selected at this point can be saved and loaded in future gridding. It is key that identical parameters be used when making the other two grids (bounds) as these must occupy the same space.
8. *Gridding method* is where we decide how the influence of our data will fall off in 3D space. Exponential is quite effective in limiting the interference effect of closely neighboring boreholes.
9. Repeat steps 3-8 for the upper and lower bounds.
10. Now we must export our grids so we can include them with into the surface data yet to be constructed in *Modelvison*. Click *voxels/voxeltoolkit/grid management*.
11. Select the 3D grid you wish to export and click on the  icon. Choose the .tkm format. Note: so we can import these voxels to *Modelvision*. When you do this the file is in the correct format however does not get assigned the .tkm extension. Simply open the folder containing the file, click on the file as you would to rename it and add *.tkm* to the end of the file yourself. You will be prompted by *windows* asking whether you want to do this, click *yes*.

Step 3: Reference Model Building (in *Modelvision)*

Before building your reference model, make sure you have the required licensing to export to the UBC format. Click *model/export/export UBC mesh model.* If the last option is not available, contact Encom to order the appropriate licensing.

1. First we must set our modeling parameters. Click *file/project properties*. UBC inversions assume magnetics are submitted in SI units and gravity in mgal. If working with gravity only there is no need to provide an IGRF, however this is vital in a magnetic inversion as our exported observations file requires magnetic field strength, declination and inclination.
2. Now we must import our data. Click *file/import* and then choose corresponding to the data we wish to work with. If we wish to work with grids then we must create synthetic lines as the magnetics observation file for UBC is sampled from survey lines. Geologic maps can most easily be imported as .ers files while Geosoft .grd files are fine for our geophysical data.
3. To view our input data click *view* if we want 2D click *map* for 3D click *perspective*. In map view right click and choose *configuration* to here we can select what we display. The same can be done in the perspective view.
4. To create synthetic lines click *utility/synthetic lines*. Here we can define the area we wish to sample from our grid along lines of a specific azimuth and spacing. I
5. As all files imported have the same naming formatting, we would like to rename our files to remain organized. Click *utility/data maintenance* and then select the type of data we wish to change the name of. This way we can keep track of which lines are magnetics and which are gravity, or we can differentiate between our topography or magnetic grids.
6. Now we can build our surface components to our reference model based on the geologic map. We have two options at this point; we can choose to perform an inversion on a flat surface and using shapes that are completely flat. Click the *create body* icon and choose plunging prism. Here we can digitize the geologic map, defining petrophysical and spatial properties in accordance to our physical property database. This is a favorable approach when we have relatively little topography. We should not extend our bodies more than a few hundred meters into the subsurface. Our subsurface constrains comes in the form of out gridded boreholes. If we wish to include topography we must create our bodies in another manor.
7. If including topography click *model/body operations/3D model generator*. Here we can select our topography grid as the elevation of the top surface. Click *draw boundary* to digitize our geologic map as described above. These bodies are no different however they have a topography included based on a tinning algorithm. Note: When including topography in this manor make an interpolation between data points across a triangular surface. That surface will be down sampled into cubes for inversion. Problems can arise when we down sample, as any point included in the inversion lying above the specified location as described by the original topography grid will result in an inversion crash. It will not work if our voxels disagree with our raw data. This implies that in areas of significant topography we require very fine voxel discretizations in order to avoid this. The size of the voxels however is limited by our sampling though. In instances where we have significant topography we require dense sample in order to avoid aliasing.
8. Note: Introducing a dip to one body will cause it to intersect its neighbor. In this instance the physical property assigned to each is added in the area of intersection. We wither have to keep the same dip for every unit or can open our reference model and edit the raw data with a text editor or software like mat lab. However this is difficult and should only be performed if absolutely necessary.

9. We can now import the voxel models of our boreholes for subsurface constraint. Click *model/import/.tkm file*. Select our files created from PA.
10. Repeat these steps importing the upper and lower bounds files. Adjust our surface constraints to the upper and lower bounds respectfully. Upon completion we will create three different models of upper, lower and average property values.

Step 4: Mesh Design (within *Modelvison)*

UBC inversions are performed within a mesh discretizing a three dimensional space into a series of voxels. The size of the cells chosen is based on a variety of factors, the obvious relating to sampling rates. The voxels should contain at least one data point each, it is imprudent to expect a solution where there is no data. In addition to this we must note the scale of problem to be addressed. Regional scaled geologic features can be inverted within larger voxels whereas localized phenomenon requires smaller voxels for a higher resolution output. A final factor to consider is computational time. Inversions requiring a large number of solutions will also take much longer to compete. A balance should be achieved between the two to optimize the inversion procedure.

1. Click *model/export/export UBC Meshmodel.* This menu will export our reference model within voxels of a user defined dimension.
2. The *mesh* tab is where we defined our mesh in space. For example X1 represents the easternmost while Y1 represents the southernmost extends of our mesh. The *core* is how many units (defined based on original project properties, if UTM then is meters) the mesh is and the *cells* define how many voxels are contained within that distance. The same can be said for Z however there is a multiplication factor we can apply. 1.0 implies no change, but if for instance 1.25, the cells increase by one quarter their previous extent with each successive voxel. The result of this being larger cells at the bottom of our model. This is performed in order to maintain an equal influence in our inversions of deeper voxels in comparison to those near surface, combating signal attenuation and the dreaded 'thin plate' paradox.
3. We can select the *pad* box if we wish to use padding. This is a secondary mesh along the border of our original. This mesh should not be more than a few voxels in x, y space and does not require any z component necessarily. The purpose of padding is to avoid edge effects within our primary mesh, the area of concern.
4. Clicking the *data* tab we can choose which data to include. We must select the gravity data for our gravity model and magnetics for magnetic modeling. Bounds files are currently only available for gravity data. However we can construct our own later.
5. Before we click *create* we need to have folders ready for where the data is to be stored. As soon as we click *create* files will be made regardless of whether we click cancel. Also, file naming formats are invariable so we must also have a well organized system of folders established.
6. The dimensions of the mesh should be identical in our upper, lower and average property reference models.

Step 5: Creating Bounds Files

While model vision will produce a bounds file for our gravity data, it currently does not for magnetics. Implementing a text editor we can solve this problem quite simply. Using the two files *model.sus* in our upper and lower bounds folders we can make one file we will call *bounds.sus.* This file should be stored in the same folder as our final reference model of the average physical properties. The *model.sus* files are formatted as a single column of values representing the physical property of one voxel. The location of that voxel is related to the *mesh.dat* file defining the mesh. The *bounds.sus* files are of the same formatting however there are two columns, the first being our lower and the second our upper bounds. As long as the mesh is identical in all three models these numbers will all correspond to the same space.

1. Open each file in a text editor of choice. Copy and paste the values from the upper bounds file into the lower bounds. They can be tab or space delaminated but they must be in side by side columns. In the *text pad* editing software this means we must work in *block select mode*.
2. Scroll to the bottom of the file (it will be quite large) to make sure both columns end at the same row. If not we either have used different meshes in creating these files, or we did not copy the entire file.
3. When sure our bounds have a lower and upper value for each row save as *bounds.sus* in the folder containing the *model.sus* of our average physical property values.

Step 6: Defining Data Uncertainty (UBC-GIF Data Viewer)

The inversion process provides a physical property distribution model presumably describing geologic elements that produces a geophysical signature matching an input observed signal. Unfortunately, an unavoidable characteristic to any geophysical dataset is the presence of noise. This noise may be caused by a variety of factors ranging from device or human oriented error, environmental effects. Performing data reduction one wishes to remove these noise effects, however no matter the success, some degree signal within a dataset should be considered as a result from non-geologic input. Knowing this it then becomes impossible for any inversion to accurately produce a physical property distribution that precisely describes the observed data. Defining data uncertainly however, we can control the degree to which an inversion is required to match the observed geophysical signal and as such affirm the presence of non-geologic signal. This is achieved by defining a standard deviation at each observation point within our dataset. This is used in the calculation of the matrix *data misfit factor*, ϕ_d (Williams, 2008). An appropriate inversion solution will be achieved when we produce a balance between our *data misfit factor*, ϕ_d and the *model objective function*, ϕ_m (Williams, 2008).

1. Open your observation file in *data viewer*. For gravity this is your obs.grv while your magnetics file will be named obs.mag. the current *Modelvision* installation (8.0) does not write an extension in our observation file however data viewer can still read it.
2. Data viewer displays the data in a crude grid. Below the title, the number of data points and magnetic inclination/declination for the study site are stated. These should match your *Modelvision* settings. Large amounts of data points along synthetic lines created from a grid are unnecessary if they are not required by our voxel sizes. In this case we can down-sample the data in order to speed the inversion process. Click *edit/downsample data*. You may then choose what factor to divide your data by.
3. Next we add noise. Click *view/errors*. This displays a second grid with our error values used in the calculation of the data misfit factor. By default it will be blank unless we chose a data column from our *Modelvision* database to assign as noise.
4. UBC-GIF inversions assume a Gaussian noise with a normalized distribution. This noise is taken as the standard deviation plus an offset value. Click *edit/assign standard deviation*. Although there is no perfect recipe, a generalized rule of thumb as outlined by Williams (2008) is to use 5% of our data range for magnetics while gravity can vary from 1% to 2% depending on the accuracy of survey. Factors to consider here are the age of the gravity survey, the measuring device accuracy. We also must provide a minimum offset value which can be quite low.
5. Save the dataset with a new name so you can recognize it is the edited version.

Step 7: Performing inversions using the UBC-GIF Graphic User Interface (GUI)

Inversions are carried out using the GUI. Before these can be used however we must have the software installed with the provided device specific (check raw file to make sure the Hardware ID matches your computer's) license file in the same folder as our executable files. For an in-depth explanation and background information to the components of the GUI refer to the UBC-GIF 3D inversions workflow: http://www.eos.ubc.ca/ubcgif/iag/workflow/3D-mag/index.htm. While most components to the GUI are self-explanatory one important aspect to note is that output files, as in the reference model construction, are non-unique. Care should be taken to keep the results well organized in appropriately named folders.

1. To check the Hardware ID of your computer click *start/run* then type *cmd* to open the command window. Type *ipconfig/all* to find your hardware ID for your computer, use the license file matching this number.
2. The observation file is the only required data to perform an inversion. If using only this file we perform an 'unconstrained' inversion. Selecting the reference and bounds files, we implement our geologic constraint. When performing additional inversions where we change the parameters only slightly we may wish to select previous inversion solutions as our *initial model.* This speeds the process, however unless we are inverting across a very large area, it is unnecessary.
3. For *depth weighting* we will leave all default parameters. This describes how our source body signal declines with distance. For magnetics this is 3 and gravity it is 2.
4. The two most important parameters to consider are the *mode* and the *alpha/length scales*. The *mode* function determines how the tradeoff parameters between the misfit factor and the model objective function are set. In the *chi fact* mode a tradeoff is achieved using a line search such that a target value, ϕ_d, of data misfit is achieved. Here ϕ_d = *chi fact* x *N*, where *N* is the number of data points. This is a common option if errors on data are assumed to be Gaussian and un-correlated. The *gvc* mode produces a computer calculated tradeoff parameter which implements cross validation analysis on the inversion without positivity. This is computing intensive however often provides favorable initial results.
5. The *alpha/length scales* define our model objective function, ϕ_m. We can define the s,x (e),y (n), and z values or make use the defaults. Conversly, we may wish to use the Length Scales. These implement the same terms in a slightly different manner. Here $L = (A_{x,y\ or z}/A_s)^{0.5}$. There are some generalized rules of thumb when using these. $L_{e,n,z}$ should be less than the total x, y or z extent respectively of the mesh and greater than the extent of a single cell with the mesh.
6. After we have all settigns in place we must save them before we can run our inversion. Afterwards the  icon is active. Click this to begin the inversion.
7. Upon completion we may open the results in either UBC-GIF *meshtools 3D* or *PA* as a voxel model. Use cuttoffs to isolate for specific features or interest and slicing to view whole results at specific areas. While extreme low/high values are an indication that a regional signal remains within the data set, changing the color sceheme max/min is a quick way to isolate for the proeprty value range of interest as well.
8. To test our results in comparison to the original data a forward model of the inversion outcome is nessesary. Within the *meshtools 3D* software click *forward model,* choose the type of data as either magnetics or gravity, then provide the locations of the observations to be forward modelled. This will require selecing the file with extentsion *.loc* created by modelvision at the time of reference model building. Compare the results of the forward model grid to that of the observed grid. If significant deviations occur an appropriate balance between ϕ_d and ϕ_m was not achieved. Revisit the mode selection portion or re-define a tighter SD for the data error.

9. Finally the model should be compared against all know geoogic information. Does the model fit geologic maps or sections? If not is the result still acceptable? What is the level of confidence in our priori information? Addressing such issues as these while updating our physical proerty data bases and inversion models as new informaiton becomes availible is critical to achieve optimum results while using UBC-GIF geologically constraiend 3D inversions.